

Rock Glacier Dynamics
near the Lower Limit of Mountain Permafrost
in the Swiss Alps

Atsushi IKEDA

A dissertation submitted to the Doctoral Program
in Geoscience, the University of Tsukuba
in partial fulfillment of the requirements
for the degree of Doctor of Philosophy in Science

January 2004

Contents

Contents	i
Abstract	iv
List of figures	vii
List of tables	x
Chapter 1 Introduction	1
1.1. Mountain permafrost and rock glaciers	1
1.2. Internal structure and thermal conditions of rock glaciers	2
1.3. Dynamics of rock glaciers	4
1.4. Purpose of this study	6
Chapter 2 Study areas and sites	7
2.1. Upper Engadin and Davos	7
2.2. Büz rock glaciers	9
Chapter 3 Classification of rock glaciers	11
3.1. Classification by surface materials	11
3.2. Classification by activity	11
Chapter 4 Techniques	14
4.1. Mapping and measurements of terrain parameters	14
4.2. Temperature monitoring	15
4.2.1. Ground surface temperature	
4.2.2. Subsurface temperature	
4.3. Geophysical soundings	17
4.3.1. Hammer seismic sounding	
4.3.2. DC resistivity imaging	
4.4. Monitoring mass movements	19

4.4.1. Triangulation survey	
4.4.2. Inclinator measurement	
4.5. Rockfall monitoring	20
Chapter 5 Contemporary dynamics of Büz rock glaciers	21
5.1. Internal structure	21
5.2. Thermal conditions	22
5.2.1. Snow thickness	
5.2.2. Bottom temperature of the winter snow cover	
5.2.3. Mean annual surface temperature	
5.2.4. Subsurface temperature	
5.3. Movement	27
5.3.1. Surface movement of BN rock glacier	
5.3.2. Surface movement of BW rock glacier	
5.3.3. Internal movement of BN rock glacier	
5.4. Rock glacier dynamics in a marginal permafrost condition	32
5.4.1. The origin of rapid permafrost creep	
5.4.2. Temporary acceleration followed by deceleration of permafrost creep	
Chapter 6 Long-term variations in rock glacier dynamics	41
6.1. Parameters relating to climatic conditions	41
6.1.1. Altitude and aspect	
6.1.2. Ground surface temperature	
6.1.3. Active layer thickness	
6.2. Parameters relating to dynamic conditions	46
6.3. Response of rock glaciers to long-term environmental change	47

Chapter 7 Conclusions	51
Acknowledgements	53
References	55
Figures	68
Tables	106

Abstract

Rock glaciers, a mass of frozen debris moving downslope, are the best geomorphological indicator of permafrost in steep mountainous regions. Although recent studies have revealed in detail the distribution, structure, surface movement and thermal conditions of rock glaciers, few have addressed mass balance and internal movement. This study aims at evaluating rock glacier dynamics near the lower limit of mountain permafrost in the light of both thermal conditions and mass balance. For this purpose, two series of field observations were undertaken in the eastern Swiss Alps. The first half addresses the contemporary dynamics of two small rock glaciers located near the lower limit of mountain permafrost. The second half focuses on the difference in activity status of rock glaciers on a regional scale, which may reflect long-term variations in climate and debris supply.

The first series of observations include excavation with portable drills, triangulation survey, inclinometer measurement, seismic and two-dimensional DC resistivity soundings, ground temperature monitoring and rockfall monitoring on two small rock glaciers lying close to the boundary between the permafrost and non-permafrost terrains: BN and BW rock glaciers located on the northeastern slope and western slope of Piz dal Büz, respectively. The two rock glaciers have mean annual surface temperatures (MAST) close to 0°C. A borehole 5.4 m deep dug on the upper part of BN shows permafrost temperatures near the melting point throughout the year. DC resistivity tomograms also display that permafrost layers in these rock glaciers are extremely warm ($\approx 0^\circ\text{C}$) and probably thin (< 20 m). The frontal parts of BN and BW have a thick active layer (> 5 m), resulting from degradation of permafrost. The triangulation survey indicates that BN is active but BW inactive. Subsidence of BW implies ongoing degradation of ice lenses in

permafrost. In contrast, the upper part of BN shows rapid movements (50–150 cm a⁻¹) with a large inter-annual variation, although the lower part moved downslope very slowly. Two inclinometers installed at 4 m and 5 m depth also showed rapid deformation with large seasonal and inter-annual variations in permafrost of the upper BN.

The rapid movement of the upper BN is primarily attributed to creep of the frozen debris close to 0°C, which contains a significant amount of unfrozen water. In addition, the movement is sensitive to seasonal and inter-annual changes in ground thermal conditions, which are mainly controlled by the thickness and duration of snow cover. The quick response of movement to change in ground surface temperature may reflect permeable structure of permafrost, which allows unfrozen water to percolate into the frozen debris. In the light of the mass balance, the rapid movement of the upper BN does not reflect the debris supply, because the observed retreat rate of the rockwall ($3 \times 10^{-5} \text{ m a}^{-1}$) above BN is too small to compensate the large volume lost by the rapid downslope deformation. A model of the deformation based on the geometry and creep properties of the upper BN predicts that the observed rapid movement declines within two decades.

The differences in movement and structure between the upper BN, lower BN and BW suggest a sequence of inactivation of rock glaciers. Warming of a thin permafrost layer to the melting point makes rock glaciers much unstable and sensitive to seasonal and inter-annual variations in ground temperature. Such an unstable condition is temporary and eventually followed by inactivation of the rock glacier because of the insignificant debris input and progressive permafrost melting.

The second series of observations include measurements of the terrain parameters (altitude, aspect, slope angle and size of source rockwalls) on maps, seismic soundings and ground temperature monitoring on a number of active,

inactive and relict rock glaciers. A comparison of thermal conditions and debris supply between active, inactive and relict rock glaciers allowed evaluation of long-term change in dynamics of rock glaciers. The three types of rock glaciers show differences in rockwall size, altitude, aspect, ground surface temperatures and active layer thickness. The results of temperature monitoring and geophysical soundings demonstrate that active rock glaciers have the lowest MASTs and inactive rock glaciers intermediate MASTs. Such a spatial variation in thermal conditions indicates the response of rock glacier dynamics to long-term variations in temperature. The difference in the highest MAST between active and inactive rock glaciers roughly corresponds to the bandwidth of the Holocene climate variations (c. -1°C), implying the present-day inactive rock glaciers were active in the cold periods during the Holocene, such as the Little Ice Age. In addition, the three types are also distinguished by additional parameters: length of source rockwalls (L_{RW}) and slope angle of rock glaciers (α) that control debris supply and slope stability, respectively. A diagram of mean annual air temperature (MAAT) and a parameter in which the size of source rockwalls multiplied by sine of the slope angle ($L_{RW}\sin\alpha$) shows that active rock glaciers have larger $L_{RW}\sin\alpha$ than inactive and relict ones at a same MAAT level. This suggests that a large amount of debris supply is also necessary for the continuous development of rock glaciers through the Holocene near the lower limit of mountain permafrost.

Key words: mountain permafrost, rock glacier, permafrost creep, permafrost degradation, ground temperature, topoclimate, rockwall, Swiss Alps.

List of figures

Figure 1	Typical rock glaciers in the Upper Engadin, Swiss Alps.	68
Figure 2	Location of the study area, shown with distribution of rock glaciers.	69
Figure 3	Distribution of rock glaciers in the Corviglia region.	70
Figure 4	Contour map of Büz rock glaciers.	71
Figure 5	Büz rock glaciers.	72
Figure 6	Bouldery and pebbly rock glaciers.	73
Figure 7	Active, inactive and relict rock glaciers.	74
Figure 8	Definition of morphological parameters discussed in the text.	75
Figure 9	Borehole stratigraphy of the upper lobe of BN rock glacier (BNU).	76
Figure 10	Travel time curves of P-wave velocities for Büz rock glaciers.	77
Figure 11	Electrical DC resistivity tomogram of BN rock glacier.	78
Figure 12	Electrical DC resistivity tomogram of BW2 rock glacier.	79
Figure 13	Five years of ground surface temperatures on BNU, BNL and BW2 rock glaciers.	80
Figure 14	Three years of ground temperatures on BNU.	81
Figure 15	Annual horizontal displacement of boulders on BN rock glacier in 1998–2003.	82
Figure 16	Longitudinal profile of BN rock glacier and talus slope with slope angles in italics.	83
Figure 17	Small ridges (c. 30 cm high) just below the western margin of BNU, indicated by dotted lines.	84
Figure 18	Annual vertical velocity profiles of solifluction movement in	

	BNL and BW2 rock glaciers, measured with flexible probes.	85
Figure 19	Average annual horizontal displacement of boulders on BW2 rock glacier for five years (1998–2003).	86
Figure 20	Vertical displacement and downslope dip of displacement vectors on BW2 rock glacier for five years (1998–2003).	86
Figure 21	Three years of internal deformation in BNU rock glacier, shown by changes in inclination and calculated strain rates.	87
Figure 22	Annual vertical velocity profiles estimated from the observed inclination at the 4 and 5 m depths in BNU rock glacier over three years.	88
Figure 23	Three years of internal deformation (upper) and ground temperatures (lower) of BNU rock glacier.	89
Figure 24	Simulated change in the longitudinal profile of a talus slope.	90
Figure 25	Rock glacier geometry for a numerical simulation discussed in the text.	90
Figure 26	Simulated deformation of BNU rock glacier.	91
Figure 27	The effect of slope aspect on the altitudinal distribution of the terminus of rock glaciers in the Upper Engadin and Davos.	92
Figure 28	Five years of ground surface temperatures on active bouldery rock glaciers.	93
Figure 29	Five years of ground surface temperatures on active pebbly rock glaciers.	94
Figure 30	Five years of ground surface temperatures on inactive bouldery rock glaciers.	95
Figure 31	Five years of ground surface temperatures on inactive and possibly relict pebbly rock glaciers.	96

Figure 32	Five years of ground surface temperatures on relict bouldery rock glaciers.	97
Figure 33	Relationship between bottom temperature of the winter snow cover (BTS) in March and mean annual surface temperature over five years.	98
Figure 34	Travel time curves of P-wave velocities for active rock glaciers.	99
Figure 35	Travel time curves of P-wave velocities for inactive rock glaciers.	99
Figure 36	Travel time curves of P-wave velocities for relict rock glaciers.	100
Figure 37	Relationship between the length of bouldery rock glacier (L_{RG}) and the average slope length of the source rockwall (L_{RW}).	101
Figure 38	Relationship between the surface angle of rock glacier (α) and the length of bouldery rock glacier (L_{RG}).	102
Figure 39	Relationship between the average slope length of source rockwall (L_{RW}) and the mean annual air temperature at the front of bouldery rock glaciers.	103
Figure 40	Relationship between a parameter combining debris input with slope angle ($L_{RW}\sin\alpha$) and the mean annual air temperature at the front of bouldery rock glaciers.	104
Figure 41	Rock glacier dynamics near the lower limit of mountain permafrost.	105

List of tables

Table 1	Results of hammer seismic soundings.	106
Table 2	Bottom temperatures of the winter snow cover (BTS), mean annual surface temperatures (MAST) and calculated depth of the base of a low P-wave velocity ($<1500 \text{ m s}^{-1}$) layer (D).	107

Chapter 1 Introduction

1.1. Mountain permafrost and rock glaciers

Permafrost, defined as ground kept below 0°C at least for two years, occurs in more than 20 percent of the ground in the world, large part of which lies in polar regions (e.g. Washburn, 1979; French, 1996). In mid-latitude regions, although the total extent is limited, permafrost occurs on many high mountains isolated by the surrounding permafrost-free lowlands. This type of permafrost, called alpine or mountain permafrost (e.g. Fujii and Higuchi, 1978; Haeberli *et al.*, 1993), has a more complicated distribution pattern than polar permafrost, because spatial variations in altitudes, aspects and slope angles within a small area control thermal conditions on the ground (e.g. Haeberli *et al.*, 1993).

Rock glaciers are the best geomorphological indicator of permafrost in steep mountainous regions, because steep slopes and narrow valleys hinder the development of the other indicators such as large polygons, pingos and palsas (Barsch, 1996). Rock glaciers are tongue-shaped or lobate landforms covered with angular debris, which resemble lava streams or small glaciers (Figure 1). In general, rock glaciers have a length of the order of 10 to 1000 m and a thickness between 10 and 100 m. The steep frontal slope and ridge-furrow topography on the upper surface also characterize the morphology of rock glaciers. Most rock glaciers originate from a talus or moraine (e.g. Corte, 1987). Rock glaciers are, therefore, classified in terms of the source landforms and materials into ‘talus rock glaciers’ and ‘morainic (debris) rock glaciers.’

Since rock glaciers have been observed under cold environments, their viscous appearance has mainly been attributed to gravity-driven deformation of the

subsurface ice (e.g. Capps, 1910; Wahrhaftig and Cox, 1959; Outcalt and Benedict, 1965; Whalley and Martin, 1992; Barsch, 1996). Thus, the thickness, slope angle and creep properties of rock glaciers have been considered to be the primary controls on their dynamics. In addition, long-term development of rock glaciers requires continuous debris/ice supply and thermal conditions favorable for the maintenance of the subsurface ice.

Although ice is a vital component of rock glaciers, the ice origin is problematic where a large rock glacier develops from a cirque floor or the head of a U-shaped valley. Some researchers have supported the glacial origin (e.g. Whalley and Martin, 1992; Clark *et al.*, 1998), while the others the periglacial origin (e.g. Haeberli, 1985; Barsch, 1996). In the latter, the ice is attributed to frozen groundwater or buried snow banks. Authors who emphasize the periglacial origin of talus rock glaciers distinguish ‘talus-derived rock glaciers’ from ‘glacier-derived rock glaciers’ (e.g. Humlum, 1988; Ishikawa *et al.*, 2001). Despite such a debate on the ice origin, subsurface ice in rock glaciers is called permafrost in this study, because this study focuses on talus-derived rock glaciers that have no glacier or moraine.

In terms of the activity status and the presence of permafrost, rock glaciers are classified into active, inactive and relict types (e.g. Martin and Whalley, 1987; Barsch, 1996). Active rock glaciers are moving downslope by internal ice deformation. Inactive rock glaciers are stagnant, but still contain permafrost. These two types are designated together as ‘intact rock glaciers’ (Haeberli, 1985). Relict rock glaciers lack both movement and ice, and indicate former presence of permafrost.

1.2. Internal structure and thermal conditions of rock glaciers

The internal structure of rock glaciers has been investigated directly by borehole

observations (Barsch, 1979; Vonder Mühll and Holub, 1992; Clark *et al.*, 1996; Guglielmin *et al.*, 2001; Arenson *et al.*, 2002) and by natural and artificial outcrop observations (e.g. Fisch *et al.*, 1977; Elconin and LaChapelle, 1997). These studies show that the ice content in rock glaciers widely ranges from 40 % (ice-cemented debris) to nearly 100 % (massive ice). The subsurface ice bodies have also been sounded indirectly by electrical DC resistivity (e.g. Fisch *et al.*, 1977; King *et al.*, 1987; Vonder Mühll and Schmid, 1993; Ishikawa *et al.*, 2001), seismic refraction (e.g. Potter, 1972; Haeberli and Patzelt, 1982; Vonder Mühll and Schmid, 1993; Musil *et al.*, 2002), electromagnetic reflection (e.g. King *et al.*, 1987; Berthling *et al.*, 2000; Degenhardt and Giardino, 2003), electromagnetic induction (Hauck *et al.*, 2001) and gravity (Vonder Mühll and Klingelé, 1994). These soundings indicate that permafrost is a few meters to several tens meters thick in intact rock glaciers in mid-latitude mountains. Haeberli *et al.* (1998) proposed a three-layered structure consisting of the top blocky active layer, middle ice-rich permafrost layer and bottom blocky layer: the last one is derived from the block accumulation at the foot of the steep frontal slope.

Permafrost temperatures in rock glaciers have been measured in some boreholes (Johnson and Nickling, 1979; Vonder Mühll and Haeberli, 1990; Arenson *et al.*, 2002; Vonder Mühll *et al.*, 2003). The mean annual temperatures at the permafrost table are from -2°C to 0°C , because all of the investigated sites are located near the lower limit of mountain permafrost. The temperature in rock glacier permafrost is generally controlled by heat conduction (Vonder Mühll and Haeberli, 1990). However, the temperature may also be disturbed by unfrozen water intrusion under warm permafrost conditions (Vonder Mühll *et al.*, 2003).

Thermal conditions in the active layer have been monitored on a number of rock glaciers (e.g. Keller and Gubler, 1993; Humlum, 1997; Bernhard *et al.*, 1998,

Hoelzle *et al.*, 1999; Mittaz *et al.*, 2000). The openwork structure of the active layer, which is common on intact rock glaciers, permits intense cooling of the underlying permafrost and the storage of cold air. As a consequence, downslope movement of rock glaciers near the lower limit of mountain permafrost allows the permafrost distribution at lower altitudes compared with the surrounding matrix-supported ground (Ikeda and Matsuoka, 2002).

1.3. Dynamics of rock glaciers

Permafrost creep (gravity driven continuous deformation of frozen materials) in rock glaciers has directly been measured with slope inclinometers installed into boreholes (Johnson and Nickling, 1979; Wagner, 1992; Hoelzle *et al.*, 1998; Arenson *et al.*, 2002). Surface movement resulting from permafrost creep has also been measured by the geodetic survey (e.g. Wahrhaftig and Cox, 1959; Barsch and Zick, 1991; Potter *et al.*, 1998) and aerial photogrammetry (e.g. Barsch and Hell, 1975; Haeberli and Schmid, 1988; Käab *et al.*, 1997, 1998). The observed surface velocities are typically a few centimeters to several tens of centimeters per year, which are two orders of magnitude lower than the typical velocities of alpine warm glaciers (Haeberli, 1985). The ^{14}C ages (mean, 2250 years BP) of moss remains obtained from a borehole on the active Murtèl I rock glacier and isochrones extrapolated from the present-day surface velocity fields indicate that the rock glacier has continuously developed over about 5000 years (Haeberli *et al.*, 1999). In addition, the pattern of ridges and furrows on rock glaciers coincides well with the vertical compression field calculated from the velocity field (Käab *et al.*, 1998).

The activity of rock glaciers depends on a variety of mechanical and thermal factors. Barsch (1992) suggested two kinds of inactivity: climatic and dynamic. The melting of ice in a rock glacier accounts for climatic inactivity. Dynamic inactivity

results from reducing shear stress within the perennially frozen layer in a rock glacier, which is caused either by a temporal decrease in debris input or by a downslope decrease in slope gradient.

Climatic inactivity is associated with the lower limit of mountain permafrost. The active layer of a climatic inactive rock glacier may reach 10 m or thicker near the front (Barsch, 1996). Ikeda and Matsuoka (2002) demonstrated that inactive rock glaciers have warmer ground thermal conditions than active rock glaciers near the lower limit of mountain permafrost. However, warming of permafrost may not always inactivate but may temporarily accelerate a rock glacier, because ice and frozen soils become more deformable with rising temperature toward the melting point (e.g. Morgenstern *et al.* 1980). In fact, a positive correlation has been found between the permafrost temperature and mean annual or seasonal surface velocity on rock glaciers located near the lower limit of mountain permafrost (Hoelzle *et al.*, 1998; Arenson *et al.*, 2002; Kääb *et al.*, 2003). Similarly, high surface velocities ($>0.2 \text{ m a}^{-1}$) were observed only on the rock glaciers of which the front reached near the lower limit of mountain permafrost (Frauenfelder *et al.*, 2003).

In contrast to climatic inactivity, dynamic inactivity occurs also in the continuous permafrost zone, where the distribution and activity of a rock glacier depend mainly on debris input and slope gradient rather than on climatic parameters (e.g. Calkin *et al.*, 1987; Solid and Sørbel, 1992). A numerical simulation indicates that a sudden decrease in debris input leads to gradual deceleration of an advancing rock glacier (Olyphant 1987). In addition, Kirkbride and Brazier (1995) proposed a conceptual model compiling the schematic fluctuation of temperatures and debris supply to explain the formation of multiple lobes on a rock glacier.

1.4. Purpose of this study

Although mechanical and thermal conditions have been considered to affect the movement of rock glaciers, few field studies have explored both conditions. In particular, the studies on debris supply have rarely focused on a change in rock glacier dynamics but on the amount of mass movements (e.g. Barsch, 1977, Frich and Brandt, 1985; Barsch and Jakob, 1998; Humlum, 2000). In addition, direct observations of permafrost creep in rock glaciers are still rare.

In this paper, contemporary and long-term dynamics of rock glacier near the lower limit of mountain permafrost is evaluated from field studies on both thermal conditions and mass balance. The first half addresses the contemporary dynamics of two small rock glaciers in the eastern Swiss Alps. Since small rock glaciers are vulnerable to environmental changes, monitoring and analysis are more convenient than those of a large rock glacier. The investigations involved excavation with portable drills, triangulation survey, inclinometer measurement, seismic and two-dimensional DC resistivity soundings, ground temperature monitoring and rockfall monitoring. Part of the results is reported in Ikeda *et al.* (2003). The second half focuses on the difference in activity status of rock glaciers on a regional scale, which may reflect long-term variations in climate and debris supply. For this purpose, ground surface temperatures, active layer thickness and terrain parameters (altitude, aspect, slope angle and size of source rockwalls) are compared between a number of active, inactive and relict rock glaciers in the eastern Swiss Alps. The techniques involved mapping including measurements of the terrain parameters, seismic soundings and ground temperature monitoring. The second part extends ideas presented in an early report (Ikeda and Matsuoka, 2002).

Chapter 2 Study areas and sites

2.1. Upper Engadin and Davos

Field investigations were undertaken in two mountain regions in eastern Switzerland (Figure 2). The main study area is the Upper Engadin, where a large extent of high mountain slopes permits the widespread occurrence of contemporary permafrost (Figure 2a). The second area is Davos, where lower elevations of mountain slopes indicate enlargement of permafrost during some past cold periods (Figure 2b).

In the Upper Engadin, apart from the Bernina group with high mountain peaks (the highest, Piz Bernina, 4049 m ASL), glaciers are small but a variety of periglacial landforms develop on mountain areas with peaks around 3000 m ASL (Matsuoka *et al.*, 1997). The timberline is located at about 2000–2200 m ASL, the 0°C isotherm of the mean annual air temperature (MAAT) at about 2200–2300 m ASL, the glacial equilibrium line at about 3000 m ASL and the mean annual precipitation amounts to 1000–1500 mm (Haeberli *et al.*, 1992). Between the timberline and an altitude of about 2600–2700 m ASL, alpine meadows are widespread on the ground covered with fine debris; otherwise, bedrock or coarse debris is exposed.

Glacial processes during the Pleistocene basically determined the morphology of mountain slopes in the study area. Rock types appear to be the primary factor controlling landforms in the Last Glacial and Postglacial periods. The bedrock in this region can be broadly divided into crystalline and sedimentary rock groups. Crystalline rocks sustain higher peaks than sedimentary rocks. Bedrock geology also affects the size of debris: crystalline rocks mainly produce coarse debris, while

sedimentary rocks favor fine debris production (Matsuoka *et al.*, 1997). The difference in clast sizes causes a variety of periglacial landforms. In general, coarse debris constructs talus slopes and rock glaciers below high rockwalls, while fine debris promotes development of solifluction lobes and pattern ground. The crystalline rock group consists mainly of granite (including granodiorite), diorite, gneiss and schist, and the sedimentary group mainly of limestone (including dolomite), conglomerate and shale. Rock glaciers develop in all of these rock types, although those composed of shale debris are small (Matsuoka and Ikeda, 2001).

Most of the rock glaciers in the Upper Engadin are talus-derived regardless of the activity status. Some rock glaciers are superimposed by vegetation-free moraines probably formed in the Little Ice Age (e.g. Kneisel, 1998; Maisch *et al.*, 2003). Elevations below 2200 m lack rock glaciers, because they are mostly located on the steep slopes of large U-shaped valleys, which are unfavorable for the rock glacier development (Ikeda and Matsuoka, 2002). Similarly, mountains above 2900 m ASL consist mainly of rockwalls and glaciers which also prevent rock glacier development.

The major study area in the Upper Engadin is Corviglia, a large ski region north of St. Moritz (Figure 3). Granite and limestone are the major lithologies composing rockwalls in the northern Corviglia area (Figure 3a), while conglomerate is exposed on the southern face of Piz Nair in the southern Corviglia area (Figure 3b). Shale composes the north-facing rockwalls of Piz Nair and is also partly exposed on the flank of Piz Padella and Las Trais Fluors.

The Davos area (Figure 2b) was selected as the second study area to compensate the investigation of relict rock glaciers. This mountain area involves a large number of relict talus-derived rock glaciers, because gentle slopes are widespread over slightly lower elevations (2200–2400 m ASL) than similar slopes in the Upper

Engadin. The timberline is located at about 2000–2100 m ASL. The MAAT at Weissfluhjoch (2667 m ASL) is -2.8°C (Barsch, 1969), which equals the MAAT at the same altitude in the Upper Engadin. No glacier lies around the peaks below 2900 m ASL. The bedrock in the Davos area consists mainly of granite, gneiss, schist, serpentinite and limestone.

2.2. Büz rock glaciers

Since July 1998, intensive observations have been undertaken on two small rock glaciers around Piz dal Büz (2955 m ASL) in the northern Corviglia area (Figure 3a): Büz North (BN) rock glacier (Figures 4 and 5a), located on the northeastern slope of Piz dal Büz; and Büz West (BW) rock glacier (Figures 4 and 5b), located on the western slope of the same peak. The surface clasts on the rock glaciers consist mainly of shale pebbles and cobbles, with a few limestone boulders. Both rock glaciers lack vegetation cover.

BN rock glacier originates from the foot of a talus slope at 2840 m ASL and terminates at 2775 m ASL. BN includes an upper lobe (BNU), 70 m long and 120 m wide, and lower lobe (BNL), 90 m long and 100 m wide. BNU has a steep front 10 m high, dipping 35° , while BNL lacks a distinct front. The upper surface is flat and inclines at 25° on BNU and 17° – 22° on BNL. The talus slope above BN is 40 m high, of which the upper to middle part inclines at 35° and the lower part at 40° – 45° . The rockwall above BN has a height of only 2–20 m and the total surface area of about 2000 m².

BW rock glacier consists of adjoining two lobes: the southern BW1 lobe and the northern BW2 lobe. BW2 was investigated in this study. BW2, 95 m long and 80 m wide, originates from the foot of a talus slope at 2860 m ASL and terminates at 2805 m ASL. The frontal slope is 10 m high and dipping at 35° . The talus slope inclines at

35° and grades into the flat upper surface of BW2 dipping at 25°. The rockwall above BW2 has a height of only 2–5 m. The surface area is smaller than 500 m².

Chapter 3 Classification of rock glaciers

3.1. Classification by surface materials

The clast sizes on rock glaciers vary significantly with rock types. The rock glaciers are, therefore, classified in terms of surface clast size into two types (Matsuoka and Ikeda, 2001). The ‘bouldery rock glacier’ is mainly covered with coarse blocks, of which the mean diameter of the intermediate-axis is larger than 20 cm (Figure 6a). In contrast, the ‘pebbly rock glacier’ is mainly covered with pebbles and cobbles, of which the mean diameter of the intermediate-axis is smaller 20 cm (Figure 6b). The pebbly rock glacier is equivalent to the earthy rock glacier defined by Evin (1987). In the study area, pebbly rock glaciers develop on slopes dominated by shale debris, whereas bouldery rock glaciers develop in the other rock types.

These two types of rock glaciers are probably situated under different conditions of debris supply. Block-producing rockwalls above bouldery rock glaciers are generally considered to resist rock weathering (e.g. Whalley, 1984). In contrast, densely jointed rockwalls, such as shale rockwalls in the study area, are susceptible to rock weathering (e.g. Matsuoka, 1990).

3.2. Classification by activity

The three types, active, inactive and relict rock glaciers, are widely distributed over the study area (Figure 2). In the strict sense, the activity status of rock glaciers is determined by the geodetic survey and/or permafrost investigation. In many studies, however, the activity status has been presumed from visual features (e.g. Wahrhaftig and Cox, 1959; Barsch, 1996; Imhof, 1996; Brazier *et al.*, 1998). Active rock glaciers have a steep ($>35^\circ$) vegetation-free frontal slope and load fresh and

unstable boulders on the upper surface (Figure 7a). Inactive rock glaciers show a gentler frontal slope with partial or full vegetation (Figure 7b). They also have a well-developed boulder apron at the foot of the frontal slope and stable boulders on the upper surface. Relict rock glaciers have rounded and subdued topography by permafrost melting as well as vegetation cover on the upper surface (Figure 7c).

In the Alps, the bottom temperature of the winter snow cover (BTS) has widely been used as an indicator of the presence of permafrost (e.g. Haeberli, 1973; Keller *et al.*, 1998). In early winter, the ground surface is cooled well below 0°C by cold air drainage under thin snow cover. Thickening dry snow cover (>80 cm deep) toward late winter prevents cold air drainage and, as a result, the ground surface temperature becomes dependent mainly on the geothermal heat flow. Consequently, BTS rises above -2°C and eventually approaches 0°C in late winter, where permafrost is absent, whereas it is generally maintained below -3°C, where permafrost is present. BTS between -3°C and -2°C is considered to represent the uncertain range of the method and/or a marginal permafrost condition beneath a thick active layer (Haeberli and Patzelt, 1982; Hoelzle *et al.*, 1999). Vonder Mühll *et al.* (1998) demonstrated that such conditions suitable for the BTS method lasted in the observation period (1988–1997) on a typical active rock glacier, Murtèl I, in the Upper Engadin, although the BTS had large inter-annual variation reflecting the differences in thickness and duration of snow cover. Moreover, Hoelzle *et al.* (1993) found the correlation between the permafrost occurrence and vegetation cover, such that 89% of the permafrost sites (BTS < -3°C) are free of vegetation and that 71% of the permafrost-free sites (BTS > -2°C) are covered with alpine meadows or forest.

The comparison between a number of active, inactive and relict types discussed in chapter 6 combines the above two indicators to evaluate the activity status. The

presence of permafrost, or the boundary between inactive and relict rock glaciers, was determined primarily by BTS. For sites lacking a BTS measurement or showing a marginal BTS value, the boundary was estimated by the empirical rule that vegetation cover on the upper surface indicates the absence of permafrost. The latter criterion may include a larger error than that based on BTS, because of different rates between the melting of permafrost and soil development which permits vegetation. Inactive rock glaciers were distinguished from active rock glaciers by the presence of vegetation cover at the frontal slope.

The activity status of a pebbly rock glacier is more difficult to estimate from the vegetation cover, because vegetation can rapidly grow on the upper surface composed of fine materials regardless of the activity. Thus, the estimated activity status of pebbly rock glaciers may have a larger error than that of bouldery rock glaciers.

Chapter 4 Techniques

4.1. Mapping and measurements of terrain parameters

The distribution of rock glaciers was traced on the 1/25000 topographic maps of Switzerland and the 1/15000 farmland-name map of Celerina on the basis of field and air photograph surveys. Previous information on the distribution of rock glaciers in the Upper Engadin by Hoelzle (1998) and Frauenfelder *et al.* (2001) were also incorporated in the mapping. Then, terrain parameters representative of climatic and mechanical conditions were measured on the maps of 77 bouldery rock glaciers to evaluate relationships between these parameters and rock glacier dynamics.

Debris supply and slope angle are the main mechanical parameters controlling the rock glacier activity (e.g. Barsch, 1992). The amount of debris supply on a rock glacier reflects various conditions of the source rockwall, such as size, strength, temperature and water content. Except for the size of rockwall, however, these parameters are difficult to determine without field measurements. Thus, the size of source rockwall was assumed to represent the amount of debris supply. This evaluation is applied to bouldery rock glaciers, because of the limited distribution of pebbly rock glaciers in the study area. Rock glaciers superimposed by moraines were excluded from the measurement, because the processes of debris supply are different from the other talus-derived rock glaciers. The slope angle of the upper surface is assumed to equal the angle of the base of a creeping layer.

The measured parameters for a rock glacier are the altitudes at the upper edge and foot of the front, aspect of the front, length (L_{RG}), average slope angle of the upper surface (α), width of the rooting zone (W), area of the source rockwall (A_{RW}) and slope angle of the source rockwall (β) (Figure 8). The L_{RG} and α values were

measured parallel to the flow line and W perpendicular to the flow line. Then, debris supply was represented by the average slope length of the source rockwall (L_{RW}):

$$L_{RW} = A_{RW} / (W \sin \beta) \quad (1).$$

The altitude and aspect of a rock glacier relate to thermal conditions: air temperature and incoming radiation, respectively. MAATs at the front were evaluated using the altitude of 0°C isotherm (2200 m ASL) and the lapse rate (5.6°C km⁻¹) in the study area (cf. Hoelzle, 1992).

4.2. Temperature monitoring

4.2.1. Ground surface temperature

BTS can be measured by manual installation of a temperature probe or automated recording with a data logger (e.g. Hoelzle *et al.*, 1999). The former permits understanding of spatial variation in BTS at a particular time in winter, whereas the latter provides temporal variation at a particular site. Both measurements were undertaken in the Corviglia region in the Upper Engadin and the Davos area. The study areas have snow cover commonly 1–2 m deep in a normal winter.

The manual measurements were carried out on March 2–7, 1999, with a thermistor probe 2–3 m long pushed through the snow cover to the ground surface (Hoelzle *et al.*, 1999). Automated monitoring was undertaken with nine miniature data loggers (Thermo Recorders TR-51 and 51A, manufactured by T & D, Japan) placed on nine rock glaciers (O1, O4, PN3, PN5, PS2, PS3, PS4, NS5, BNL) in early August 1998, five loggers on five rock glaciers (O2, NS2, BNU, NN8, NN12) in early August 1999, two loggers on two rock glaciers (BN3, BN4) in early August 2000 and three loggers on three rock glaciers (W1, W2, W3) in late July 2001 (see

Figures 2 and 3 for the locations). On BW2 rock glacier, ground temperatures were recorded with a multi-channel data logger (EXL-007-8A, manufactured by LOG Electronics, Japan) from early August 1998. On PN1 rock glacier, a multi-channel logger (LG-C1, manufactured by LOG Electronics, Japan) was used to monitor ground temperatures from early August 1999. These loggers recorded surface temperatures under the uppermost clast 2–5 cm thick at 1 h intervals with a resolution of 0.1°C except for the EXL-007-8A logger at 2 h intervals. The recorded data were calibrated by fitting the constant temperature below the wet snow cover in spring into 0.0°C; hence, the error near 0°C was $\pm 0.1^\circ\text{C}$. In addition to BTS in late winter, the mean annual surface temperature (MAST), which is averaged for 365 days from early or middle August, was determined from the first (1998–1999) to fourth (2001–2002) years. MAST in the fifth year was averaged from middle July 2002.

4.2.2. Subsurface temperature

The excavation and drilling were performed on BNU rock glacier in early August 2000. A 3-m deep pit was excavated and then an additional 2.4 m deep borehole (6 cm in diameter) was drilled down from the bottom of the pit. Seven thermocouple probes were installed at depths of 0, 0.5, 1, 2, 3, 4 and 5 m. The hole was backfilled immediately after the installation. These data have been recorded in a data logger (KADEC-UN, manufactured by Kona System, Japan) at 3 h intervals with a resolution of 0.1°C from August 9, 2000, to July 15, 2003. The recorded data were calibrated by means of fitting the long-lasting constant temperature near the melting point into 0.0°C, thus, the monitoring error near 0°C is $\pm 0.1^\circ\text{C}$.

4.3. Geophysical soundings

4.3.1. Hammer seismic sounding

The depth of the frost table or bedrock was investigated by 19 seismic refraction soundings performed on the rock glaciers. Seismic refraction sounding using a sledgehammer permits us to detect the frost table, because the P-wave velocity of frozen ground ($1500\text{--}4700\text{ m s}^{-1}$) is much higher than that of the dry active layer ($300\text{--}800\text{ m s}^{-1}$) (e.g. Hunter, 1973; Haeberli and Patzelt, 1982; Barsch, 1996). In this paper, a high velocity layer ($\geq 2000\text{ m s}^{-1}$) is regarded to be frozen where it underlies a low velocity layer ($< 1500\text{ m s}^{-1}$) much thinner than the apparent thickness of the rock glacier.

A 3-channel seismograph, McSEIS-3 (manufactured by Oyo, Japan) was used for the survey. This seismograph can cumulate up to 99 signals to improve the signal-to-noise ratio. A 4-kg sledgehammer produced a seismic pulse. The shot points were mostly placed at 5 or 6 m intervals and at 2 or 2.5 m intervals near the receivers. A survey line was 30–63.5 m long. The P-wave velocities of two or three layers and the depth of the boundaries between these layers were determined after a correction with regard to the dip of the boundary (Heiland, 1940). The soundings were carried out from middle July to middle August in 2000–2003.

4.3.2. DC resistivity imaging

Electrical DC resistivity in ground mostly depends on its liquid water content, which is controlled by various factors. DC resistivity in ground increases when ground temperature falls below 0°C because of a decrease in liquid water content (e.g. Hoekstra and McNeill, 1973). Thus, if water content is homogeneous in the ground, permafrost is detected by means of electrical DC resistivity sounding. In fact, a middle layer having DC resistivities higher than those of the upper and lower

layers in thick sediment has been usually interpreted as permafrost in a cold environment (e.g. Guglielmin *et al.*, 1994; Ishikawa and Hirakawa, 2000), although the water content varies between the active layer and permafrost and/or between layers having different grain size distribution.

In the studies on rock glaciers, electrical DC resistivity sounding has been useful for the detection of subsurface ‘ice-rich’ permafrost which is supersaturated with ice, because ice bodies with no or little debris generally has a lower electric conductivity than most of the unfrozen sediments. Rock glacier permafrost mostly shows high resistivities (10–2000 k Ω m) which are considered to be ice-rich (Haeberli and Vonder Mühll, 1996; Haeberli *et al.*, 1998), while ice-cemented permafrost near the melting point shows resistivities lower than 10 k Ω m (e.g. Hoekstra and McNeill, 1973). If the presence of permafrost is detected by other methods (e.g. drilling, seismic soundings), an absolute value of resistivity is a useful indicator of relative unfrozen water content in permafrost, which reflects ground temperature and grain-size distribution.

The two-dimensional internal structures of BN and BW rock glaciers were estimated by means of the DC resistivity imaging. The electrode configuration of the soundings was Wenner-Schlumberger array, which combines Wenner and Schlumberger configurations in a profile. The sounding profiles were set parallel to the flow line, on which electrodes were placed at 5 m intervals. The profile on BN was 165 m long and the profile on BW 145 m long. The resistivity meter for the sounding was SYSCAL JUNIOR (manufactured by Iris Instruments, France). Two-dimensional modeled DC resistivity distributions were computed with the software RES2DINV ver. 3.4 invented by M. H. Loke.

4.4. Monitoring mass movements

4.4.1. Triangulation survey

The surface velocity of BN and BW was measured annually from August 1998 to July 2003 by the triangulation survey of marker boulders. Three benchmarks were placed on limestone outcrops around the rock glaciers by anchoring a steel bolt. Twenty-four survey points were constructed on the rock glaciers. They consisted of 11 points on BW2, 5 points on BNU and 8 points on BNL. A total station was used for the survey. To provide accuracy of the millimeter scale, the tapered tip of a reflector was inserted in an 8 mm-diameter drill hole on the marker boulders. The total error produced by the survey system is less than 1 cm a^{-1} . The benchmarks and survey points were established on August 11, 1998. These points were resurveyed on July 22, 1999, July 24, 2000, August 2, 2001, July 19, 2002 and August 13, 2003.

4.4.2. Inclinator measurement

Internal movement of BNU was monitored with inclinometers from August 9, 2000, to July 15, 2003. Two inclinometers (BKJ-A-10-D, manufactured by Kyowa Electronic Instruments, Japan), 35 cm long and 2.7 cm in diameter, were installed at 4 m and 5 m depth in the borehole. The inclinometers sensed internal movement along two directions perpendicular to each other. The inclinometer can measure inclination within $\pm 12.2^\circ$ from the vertical, with a resolution of 0.005° . The inclinations were recorded in a data logger (EXL-007A-8, manufactured by LOG Electronics, Japan) at 3 h intervals.

An inclination at a depth was calculated from the sum of the horizontal vectors, which were defined as the tangents of the measured inclinations for the two axes. The inclinations were used to calculate a creep parameter in a simple flow law for glacier ice:

$$\dot{\epsilon} = dV/dz = A\tau^n \quad (2)$$

where $\dot{\epsilon}$ is the strain rate, V is the downslope velocity at a depth, z is the depth perpendicular to the surface, τ is the shear stress, A is the constant for a given temperature and ice type and n is an experimentally derived exponent (Glen 1955, Paterson 1994). The strain rate $\dot{\epsilon}$ is identical with the vertical velocity gradient (dV/dz). The shear stress at a depth of z is:

$$\tau = \rho g |z| \sin \alpha \quad (3)$$

where ρ is the mean density of rock glacier components, g is the acceleration due to gravity (9.8 m s^{-2}), $|z|$ is the absolute value of z and α is the surface gradient. The exponent n was fixed to 3 (cf. Morgenstern et al. 1980). The creep parameter A was calculated for the two depths using $\rho = 1800 \text{ kg m}^{-3}$ and $\alpha = 25^\circ$.

4.5. Rockfall monitoring

The quantity of debris supply on BN rock glacier was evaluated by collecting fragments detached from painted rock faces. Four $50 \times 50 \text{ cm}^2$ quadrangles were painted on the rockwall above BN (Figure 4). All painted fragments below the rock faces were collected annually in late July to early August. The total volume of the detached fragments divided by the painted area represents the annual retreat rate of the rockwall. Then, the annual volume of debris supply above BN was estimated from multiplying the obtained retreat rates by the source rockwall area (2000 m^2).

Chapter 5 Contemporary dynamics of Büz rock glaciers

5.1. Internal structure

The pit and borehole on BNU displayed that angular shale pebbles and cobbles filled with sand and silt are the major components, except for the uppermost 40 cm of an openwork layer (Figure 9). The frost table lay at about 1 m depth on August 3, 2000. Below the frost table, the debris was entirely ice-cemented to the bottom and lacked visible air voids. A number of small ice lenses (<2 cm thick) were observed below 2 m depth. The gravimetric ice content, which was measured from the borehole cores (c. 10 cm long), was 50% at 4 m depth and 28% at 5 m depth. If the cores had no air void, the volumetric ice content was about 60% at 4 m depth and 45% at 5 m depth. The borehole did not reach the bedrock at the bottom (5.4 m deep).

Seismic refraction soundings revealed two-layered structure in BN and BW (Figure 10, Table 1, see also Figure 4 for the locations). The second layer with a high P-wave velocity (2000–3400 m s⁻¹) indicates permafrost and the first layer with a low P-wave velocity (350–470 m s⁻¹) the active layer. The seismic refraction of BNU, the upper part of BNL (BNLa) and the upper part of BW2 show active layers shallower than 3 m, whereas that of lower part of BNL (BNLb) and the lower part of BW2 show active layers deeper than 4 m. The lower ends of both rock glaciers have 5 to 6 m thick active layers, which imply permafrost degradation at the lower parts.

The DC resistivity tomogram shows that the resistivity values in BN are of the order of 1 kΩm (Figure 11), which is the lowest range for permafrost in intact rock glaciers (Haeberli & Vonder Mühl 1996). Such low values probably result from the debris-rich frozen layer at temperatures close to the melting point. Massive ice,

which has a high DC resistivity ($>10 \text{ k}\Omega\text{m}$), is unlikely to exist in the rock glacier.

Two elliptic layers in BN with relatively high DC resistivities ($>4.5 \text{ k}\Omega\text{m}$), which are distinguished from the surroundings by a large resistivity gradient, underlie the frontal part of BNU and the upper part of BNL (Figure 11). The former is about 20 m thick and the latter about 10 m thick. The higher DC resistivities in these layers may reflect slightly colder permafrost than the other part (cf. Hoekstra & McNeil 1973). In contrast, the upper part of BNU and the lower part of BNL show low DC resistivities ($<2 \text{ k}\Omega\text{m}$). These parts probably lie at the melting point or higher temperatures. Thus, the permafrost layer observed in the borehole is thin and situated at the margin of this permafrost body. In the lower part of BNL, the thick active layer indicated by the seismic sounding suggests that resistivity lower than $1 \text{ k}\Omega\text{m}$ lie under a melting condition of permafrost.

The resistivity values in BW are $0.5\text{--}1 \text{ k}\Omega\text{m}$ (Figure 12), which is lower than those in BN. The low values suggest that permafrost is probably thin and at the melting point. Such a warm condition is also verified by the thick active layer indicated by the seismic sounding.

5.2. Thermal conditions

5.2.1. Snow thickness

In the eastern Swiss Alps, snow conditions on ground are usually suitable for the BTS method (e.g. Vonder Mühl *et al.*, 1998). In a normal winter, ground is cooled below thin snow cover in early winter, and then thickening dry snow cover ($>80 \text{ cm}$ deep) in late winter insulates ground from air temperature (Haeberli and Patzelt, 1982; Hoelzle *et al.*, 1999). The observed first and second years (1998–2000) had such normal winter (Ikeda and Matsuoka, 1999, 2002). In the third and fourth years (2000–2002), however, the snow condition did not suit the BTS method: heavy

snowfalls in October and November 2000 prevented ground from cooling; and lack of notable snowfalls until late January 2002 resulted in intensive ground cooling irrespective of the presence or absence of permafrost (Hoelzle *et al.*, 2003).

The snow thickness directly observed on BN and BW in March 1999, 2001 and 2002 supported the abnormal snow conditions in the third and fourth years. On March 3, 1999, the snow depth spatially ranged from 1.5 to 2.8 m (average 2.3 m) among 8 points on BN and from 1.0 to 1.7 m (average 1.3 m) among 6 points on BW2, while the snow depth in the fourth year (March 22, 2001) exceeded 5 m on the upper part of BNL and 4 m on BNU. In addition, the snow depth was about 3.5 m on BW2 and on the lower part of BNL. In the fifth year (March 6, 2002), the snow depth on BNU and the upper part of BNL ranged from 0.8 to 2.4 m among 11 points (average 1.6 m); BW and the lower part of BNL were only covered with snow thinner than 0.8 m.

5.2.2. Bottom temperature of the winter snow cover

Figure 13 displays four to five years of ground surface temperatures (daily mean values) recorded on BN and BW. The records on BNL were interrupted from August 3 to September 11, 2000, and the records on BW for 4 days in early August 2001. The average BTS values for March and MASTs at all logger sites are also listed in Table 2 with the depths of the low P-wave velocity layers.

The ground surface temperature on BN is affected by a long snow-covered duration. Continuous and stable subzero temperatures below 0°C indicate that BN was covered with snow for more than nine months per year. In the first and second years, BTS on BNL gradually decreased in early winter, and remained nearly constant at about -1°C until middle May when BTS rapidly rose to 0°C by damping of snow. In the third year, the lowest BTS on BNL was -0.5°C, which was slightly

higher than the previous two years, because the extremely thick snow cover prevented the ground from cooling; then the snow cover became entirely wet in late May. In the fourth year, the extremely snow-poor condition resulted in the lowest BTS value (-4°C) on BNL in late January, and then BTS gradually increased to -1°C until early June when BTS rapidly rose to 0°C . In the fifth year, BTS was kept above -0.5°C in early winter and gradually decreased to -1°C in late winter; then BTS rapidly increased to 0°C in middle May 2003. BTS in the fifth year suggests that the snow condition was intermediate between the normal winters and the snow-rich third winter.

Temperatures on BNU displayed seasonal and inter-annual variations similar to those on BNL, while BTS on BNU reached slightly lower values than that of BNL. The rapid increase in BTS on BNU coincided with that of BNL. The lowest BTS values on BNU were -2.5°C in the second year, -0.5°C in the third year, -5°C in the fourth year and -1.5°C in the fifth year.

The average BTS values for March on BN were higher than -2°C through the five years (Table 2). Despite the regionally normal conditions of snow cover in the first and second years, such a high BTS was inconsistent with the presence of permafrost revealed by the excavation and seismic refraction soundings. This is because BN was generally covered with thick snow keeping the ground a warm condition in early winter (cf. Hoelzle *et al.*, 2003). The high altitude and northern exposure of BN probably cause the regionally exceptional condition. In addition, the high BTS was also attributed to the matrix-supported active layer, which prevents advective cooling in ground under snow cover (Ikeda and Matsuoka, 1999), while low BTS values were recorded on other pebbly rock glaciers in the same area (cf. Table 2).

In contrast to BN, the winter surface temperature on BW largely fluctuated in

the first, second and fourth years, although daily variations in temperature were small through the winter. Such a condition probably resulting from thin snow cover did not fulfill the requirement for the BTS method. The windward location near a col may be unfavorable for snow accumulation on BW. BTS in the snow-rich third and fifth years reached constant values at -1°C in late winter 2001 and at -2°C in late winter 2003. The average BTS value for March in the fifth year (-2.3°C) indicates the marginal condition of permafrost presence, whereas that in the extraordinary snow-rich third year (-1.1°C) disagrees with the presence of permafrost demonstrated by the result of the seismic sounding (see Figure 10 and Table 1). A rapid rise in temperature by damping of snow occurred in the end of April in 1999, in late April in 2000, in early May in 2001, in late May 2002 and in middle to late April 2003.

5.2.3. Mean annual surface temperature

MASTs on both BNU and BNL ranged from 0.0 to 1.6°C . The increase in MAST on BNL from the first to second year (from 0.4 to 0.9°C) reflected the earlier snowmelt in the second year. MAST on BNU (0.4°C) in the second year was slightly lower than that of BNL (0.7°C) in the third year. Such a rise in MAST resulted mainly from the high BTS despite the longer duration of snow cover. The lowest MAST (0.0°C on both sites) was recorded in the fourth year, which was caused by the extremely thin snow cover in early winter 2002. In contrast, the highest MASTs (1.6°C on BNL and 1.4°C on BNU) were observed in the fifth year, which probably reflected thick snow cover in early winter and extremely hot summer in 2003.

MASTs on BW also showed inter-annual variation, which mainly reflected the snow thickness. MASTs for the years with thick winter snow cover (0.7°C in the third year and 1.6°C in the fifth year) are much higher than those in the first and

second years (-0.4°C , and -0.9°C , respectively) having normal snow conditions. The fourth year with much smaller amount of snow had MAST (-0.8°C) similar to those in normal years.

The high BTS and slightly positive MAST in the normal years imply that permafrost in BN has a temperature close to the melting point. In contrast, the slightly negative MASTs in the normal years suggest that BW is more favorable for the maintenance of permafrost than BN. However, the thick active layer of BW indicates degradation of permafrost, which possibly results from thin snow cover and well-drained steep slope minimizing water supply in the snow melting season.

5.2.4. Subsurface temperature

Figure 14 presents three years of variations in ground temperatures recorded in BNU. The data show that the permafrost temperature is close to the melting point, as indirectly indicated from the high DC resistivity, high BTS and slightly positive MAST. The maximum thickness of the active layer slightly exceeded 2 m in the summer of 2001 and 2002. Permafrost temperatures (at 3–5 m depths) were nearly constant at the melting point through the three years. In particular, those at 4 and 5 m depths were between -0.1 and 0.0°C . The temperatures at 3 m depth reached slightly lower values (-0.2°C in spring 2002 and -0.3°C in winter 2003).

The thermal regime of the active layer in BNU varied inter-annually, reflecting the difference in thickness of the snow cover. The temperatures at 1 to 3 m depth remained at -0.1 to 0.0°C throughout the third winter (2000–2001), because the thick snow cover in the early winter prevented the ground from cooling. In contrast, temperatures in the uppermost 2 m decreased below the thin snow cover in the fourth winter (2001–2002). The minimum temperatures at 0.5, 1 and 2 m depths were -3.0°C , -1.8°C and -0.5°C , respectively. In the fifth winter (2002–2003),

when the snow cover hindered ground cooling in the early winter and allowed ground cooling in the late winter, temperatures at 0.5 and 1 m depths gradually decreased to -0.9°C and -0.6°C until the end of winter, respectively.

Freezing of water in the active layer delayed cooling from the melting point. For example, the temperature at 2 m depth in BNU dropped below -0.1°C in late February 2002, while the surface temperature dropped below -0.1°C three and half months earlier. As a result, the active layer consisting of matrix-supported pebbles and cobbles prevents permafrost from seasonal cooling on BNU under the slightly positive MAST. Such a condition contrasts with that in the openwork blocky active layer, where the cold air can directly move through air voids (e.g. Humlum, 1997; Harris and Pederson, 1998; Sawada *et al.*, 2003).

5.3. Movement

5.3.1. Surface movement of BN rock glacier

Surface movement on BN showed large spatial and temporal variations (Figure 15). All points moved downslope in consistent directions over the five years. The marker boulders on BNU showed much higher velocities than those on BNL. In the first year, the horizontal velocities (V_H) of boulders on BNU were $47\text{--}70\text{ cm a}^{-1}$, while those on BNL were $1.5\text{--}19\text{ cm a}^{-1}$. The downslope velocities (V_N), which were evaluated from V_H and the vertical velocities, were $49\text{--}82\text{ cm a}^{-1}$ on BNU, while those on BNL were only at $2\text{--}19\text{ cm a}^{-1}$. The frontal slope of BNU ($V_N = 49\text{--}58\text{ cm a}^{-1}$) moved slower than the upper surface ($V_N = 74\text{--}82\text{ cm a}^{-1}$). The velocities on BNL also decreased from the upper part ($V_N = 8\text{--}19\text{ cm a}^{-1}$) to the lower part ($V_N < 7\text{ cm a}^{-1}$). Similar spatial variation in velocity was observed in the following four years.

Downslope movement slightly accelerated in the second year. The V_N values

were, on average, 1.2 times as fast as the first year, reaching 66–95 cm a⁻¹ on BNU and 2–23 cm a⁻¹ on BNL. In the third year, the V_N values significantly increased up to twice the first year: 109–146 cm a⁻¹ on BNU and 4–37 cm a⁻¹ on BNL. In the fourth year, BNU decelerated, while BNL maintained the velocities. The V_N values were 78–96 cm a⁻¹ on BNU and 3–33 cm a⁻¹ on BNL, which were 1.3 times and 1.7 times larger than those in the first year, respectively. Movement slightly accelerated from the fourth to fifth year, except for the lower part of BNL. The V_N values in the fifth year were 83–104 cm a⁻¹ on BNU and 3–36 cm a⁻¹ on BNL, which were 1.4 times and 1.8 times larger than those in the first year, respectively. The average V_N values for the five years were 94–103 cm a⁻¹ at the three points on the upper surface of BNU, 77–81 cm a⁻¹ at the two points on the frontal slope of BNU, 14–29 cm a⁻¹ at the five points on the upper part of BNL and 2–7 cm a⁻¹ at the three points on the lower part of BNL.

Most of the marker boulders on BNU moved nearly parallel to the upper surface, indicating the advance of the front (Figure 16). The amount of uplift or subsidence (ΔH) is given by the value expected from the horizontal displacement multiplied by the tangent of the inclination of the upper surface plus the observed vertical displacement (<0 in the downward direction). Positive ΔH values indicate uplift and negative ones subsidence. The boulders on the frontal slope were uplifted ($\Delta H = 20$ to 50 cm in the five years). In contrast, the uppermost point on BNU subsided ($\Delta H = -70$ cm in the five years), which apparently compensated the frontal advance.

The upper part of BNL moved upward, while the lower part of BNL moved roughly parallel to the surface (Figure 16). The ΔH values in the five years ranged from 10 to 30 cm on the upper part of BNL. In particular, boulders moving slowly showed significant uplift, which probably reflected the compressive stress field between the rapidly creeping BNU and the slowly moving lower BNL. In addition,

small ridges (c. 30 cm high) just below the western margin of BNU indicate that the uplift resulted from both of the compression in permafrost and the thickening of the active layer (Figure 17).

Despite the presence of silty matrix in the active layer, the most part of the surface velocity is attributed to the movement within permafrost, because buried flexible probes moved at only 0.4 cm a^{-1} downslope on the upper part of BNL (Figure 18a). In addition, the marker boulders are not susceptible to solifluction in the active layer. These movements are also unlikely to have resulted from active layer slides or debris flow, because the marker boulders did not exhibit any movement due to such a rapid flow during the observation period.

5.3.2. Surface movement of BW rock glacier

All marker boulders on BW moved slowly (Figure 19). The average horizontal velocities (V_H) were $0.5\text{--}2.5 \text{ cm a}^{-1}$ during the five years, except for the northernmost boulder having moved at 4 cm a^{-1} . The V_H values fluctuated inter-annually, although the fluctuation was inconsistent between the boulders in 1998–2002. In this period, the inter-annual variation in velocity was within $\pm 2 \text{ cm a}^{-1}$. The velocities decreased in the fifth year (2002–2003) to values half in the fourth year.

All boulders but the northernmost one on BW subsided (Figure 20). The vectors of the downslope displacements dipped over 30° , indicating the subsidence of the upper surface with the average slope angle of 25° . The vertical displacements were $6.5\text{--}12 \text{ cm}$ for the five years, except for the lowermost boulders with V_H of only 0.5 cm a^{-1} . The amount of uplift or subsidence (ΔH) is given by the value expected from the horizontal displacement multiplied by the tangent of the inclination of the upper surface plus the observed vertical displacement (<0 in the downward direction). A

positive ΔH value indicates uplift and negative one subsidence. The ΔH values for the five years were -0.5 to -9 cm (average 4 cm). The subsidence probably reflects ongoing melting of ice lenses in permafrost.

The small velocity of BW is comparable with the rate of solifluction (cf. Matsuoka, 2001). Actually, four buried flexible probes moved downslope at 0.5 – 1.4 cm a^{-1} on the surface of BW during four years, which is attributed to solifluction (Figure 18b). Thus, permafrost creep in BW is almost inactive.

5.3.3. Internal movement of BN rock glacier

The two inclinometers installed in BNU indicated large downslope tilting in permafrost, which is consistent with the large surface velocity. Both continuously inclined downslope from early August 2000 to middle July 2003 (Figure 21). The directions of inclinations were consistent during the three years. Inclination at 5 m depth was larger than that at 4 m depth, and inclination for one of the two axes at 5 m depth finally exceeded the measurement limit (12.2°) on February 3, 2003. However, the observed total inclination at 5 m depth exceeds this limit, because the inclinometer was originally installed with slightly upslope tilting. After reaching the limit, the inclination at 5 m depth was estimated from the measured inclination to the other axis using the linear relationship between inclinations to the two axes ($r^2 = 0.9995$). The inclination rates at 4 and 5 m depth in the observed period were, on average, $2.7^\circ a^{-1}$ and $6.1^\circ a^{-1}$, respectively.

The strain rates calculated from the inclinations display seasonal and inter-annual variations (Figure 21). The strain rates at 4 m depth ranged from $0.00 a^{-1}$ to $0.11 a^{-1}$ and those at 5 m depth from $0.01 a^{-1}$ and $0.28 a^{-1}$. Annual strain rates for 2000–2001, 2001–2002, 2002–2003 were calculated to be $0.058 a^{-1}$, $0.031 a^{-1}$ and $0.042 a^{-1}$ at 4 m depth and $0.18 a^{-1}$, $0.089 a^{-1}$ and $0.10 a^{-1}$ at 5 m depth,

respectively. These variations paralleled the inter-annual variation in surface velocities (see Figure 15). In addition, the strain rates at both depths gradually decreased from February to April in the later two years, while the rates rapidly increased in May, reaching the annual maximum in the third and fourth years (2000–2002). Note that the ordinal numbers of the years are counted from the summer 1998 when the temperature monitoring was started on BN.

Using equations (2) and (3) defined in chapter 4, creep parameters A in the third, fourth and fifth years were calculated to be $8.1 \times 10^{-14} \text{ kPa}^{-3} \text{ s}^{-1}$, $4.4 \times 10^{-14} \text{ kPa}^{-3} \text{ s}^{-1}$ and $5.9 \times 10^{-14} \text{ kPa}^{-3} \text{ s}^{-1}$ at 4 m depth ($|z| = 3.8 \text{ m}$) and $1.3 \times 10^{-13} \text{ kPa}^{-3} \text{ s}^{-1}$, $6.5 \times 10^{-14} \text{ kPa}^{-3} \text{ s}^{-1}$ and $7.6 \times 10^{-14} \text{ kPa}^{-3} \text{ s}^{-1}$ at 5 m depth ($|z| = 4.7 \text{ m}$), respectively. Assuming that an average of the two measured strain rates represents the strain rate over 4–5 m depth ($|z| = 3.8\text{--}4.7 \text{ m}$), the A values in the third, fourth and fifth years were calculated to be $1.2 \times 10^{-13} \text{ kPa}^{-3} \text{ s}^{-1}$, $5.9 \times 10^{-14} \text{ kPa}^{-3} \text{ s}^{-1}$ and $7.2 \times 10^{-14} \text{ kPa}^{-3} \text{ s}^{-1}$, respectively. $|z|$ is the absolute value of a depth perpendicular to the surface.

The next step is to estimate the thickness of the moving debris H . From equations (2) and (3), we obtain

$$V_S = A(\rho g \sin \alpha)^n \int_0^H |z|^n dz \quad (4)$$

where V_S is the downslope velocity at the surface, ρ is the mean density of rock glacier components, g is the acceleration due to gravity (9.8 m s^{-2}) and α is the surface gradient. Assuming that the average creep parameters over 4–5 m deep is representative of the whole frozen layer, neglecting deformation of the active layer (in the uppermost 2 m) and using the observed average V_S for each year, $\rho = 1800 \text{ kg m}^{-3}$, $\alpha = 25^\circ$ and $n = 3$, extrapolation shows that the movement of BN results from deformation of about 9 m thick ($|z| = 8 \text{ m}$) rock glacier (Figure 22). The calculation

indicates that 90% of the surface velocity originates from deformation below 5 m depth. The depths of the deformation base were consistent in the three years and the estimated thickness approximated the frontal height (c. 10 m) of BNU, although the calculation includes a number of assumptions such as a constant A through the frozen layer, the use of n for ice or ice-rich soil and neglect of the snow weight.

5.4. Rock glacier dynamics in a marginal permafrost condition

5.4.1. The origin of rapid permafrost creep

Both triangulation and inclinometer measurements showed large deformation of permafrost in BNU. An analysis based on the observed inclinations indicated that deformation of BNU occurred entirely within the top 10 m. The large deformation probably reflected the permafrost temperature close to the melting point, which is indicated directly by the ground temperatures and indirectly by the low DC resistivities (see Figures 11 and 14).

The calculated creep parameter A is significantly higher than the previously reported values for ice and ice-rich permafrost. For example, the A values (4.4×10^{-14} – 1.3×10^{-13} kPa⁻³ s⁻¹) at BNU are one to two orders of magnitude higher than a value at -1°C calculated from the borehole deformation of Murtèl I rock glacier (5.0×10^{-15} kPa^{-2.9} s⁻¹; Wagner, 1992), a value of ice at -1°C from several laboratory tests (1.4×10^{-15} kPa⁻³ s⁻¹; Morgenstern *et al.*, 1980) and an average value of glacier ice at 0°C from several references (6.8×10^{-15} kPa⁻³ s⁻¹; Paterson, 1994). Budd and Jacka (1989) proposed a slightly higher A value for ice at 0°C (9.3×10^{-15} kPa⁻³ s⁻¹) from laboratory tests, but the value is still lower than those of BNU. Thus, the deformation of BNU is likely to be too large to originate from simple deformation of ice at the melting point.

The unusually large deformation observed in BNU is probably associated with

the presence of water. First, the unfrozen water content of frozen ground increases with rising temperature and surface area of soil particles (e.g. Anderson and Morgenstern, 1973; Dash et al. 1995). The permafrost layer in BNU probably includes a certain amount of unfrozen water because of the significant content of interstitial sand and silt and the temperature close to 0°C. Whereas interlocked debris tends to strengthen permafrost (e.g. Hooke et al. 1972), such unfrozen water may weaken the shear resistance of permafrost by reducing effective stress near the melting point (e.g. Arenson et al. 2002). Cohen (2000) displayed unusually large A values (1.4×10^{-13} – 1.4×10^{-14} kPa⁻³ s⁻¹) for dirty basal ice below a 210 m thick temperate glacier by means of a 3-dimensional simulation, and explained the large values due to unbound water between ice lamellae and sediment layers in the dirty ice.

Second, the rapid increase in strain rates in BNU during the snowmelt period, as indicated by the constant surface temperatures at 0°C, implies that snow meltwater infiltrated into the permafrost (Figure 23). The maximum strain rate in May and July 2001 appears to have resulted from a large amount of meltwater derived from the unusually thick snow cover. In contrast, the small acceleration of the inclinometers in the next spring (2002) corresponded to the unusually thin snow cover. Meltwater intrusion, which increases unfrozen water content in permafrost, destabilizes a rock glacier by reducing the effective stress (e.g. Arenson *et al.*, 2002). The significant permeability of a rock glacier was demonstrated by the recent studies on the boreholes drilled through an active rock glacier, Murtèl I, where warm and heterogeneous permafrost occasionally allows unfrozen water intrusion (Arenson *et al.*, 2002; Vonder Mühl *et al.*, 2003). In addition, such acceleration in a snowmelt season was also observed on a small rock glacier in the Furggentälti area, western Swiss Alps (Mihajlovic *et al.*, 2003), while a large bouldery rock glacier, Muragl I,

was seasonally accelerated three to four months after the snow damping (Kääb *et al.*, 2003). The increase in strain rates in BNU, however, started two weeks before the snow damping at the monitoring site. The reason for such earlier acceleration is uncertain, but one possibility is that the meltwater penetrating into BNU originated from the thinner snow cover on the talus slope than that on the monitoring site.

Unfrozen water content in permafrost at the melting point may significantly fluctuate, because the strain rates responded to the ground surface temperatures in spite of the constant temperature ($\approx 0^{\circ}\text{C}$) at the monitoring depths (Figure 23). The lack of ground cooling in the third winter (2000–2001) may have prevented unfrozen water that infiltrated in the preceding spring and summer from freezing. As a result, the continuous large inclination was observed in the third year. The significant lowering of the ground surface temperatures in the fourth winter (2001–2002) is likely to have resulted in the deceleration of the inclination, indicating the freezing of unfrozen water that infiltrated in the preceding spring and summer.

Temperature of shallow permafrost responds significantly to seasonal to inter-annual variations in thermal conditions at ground surface (e.g. Harris 2001). Simultaneously, a large fluctuation also occurs in the deformation properties of permafrost near the melting point. Small rock glaciers in a marginal permafrost condition moves rapidly, primary because the permafrost close to the melting point contains a significant amount of unfrozen water. In addition, the movement is sensitive to seasonal and inter-annual change in ground thermal conditions which are mainly controlled by the thickness and duration of snow cover. Such a movement of a small rock glacier, showing extremely large creep parameters and responding rapidly to the change in ground surface temperature, is possibly due to the permeable structure allowing unfrozen water intrusion into the permafrost.

5.4.2. Temporary acceleration followed by deceleration of permafrost creep: numerical simulation based on mass balance model

In contrast to the rapid movement of BNU, the lower part of BNL moves very slowly (see Figures 15) and has a thick active layer (see Figure 10). Inactive BW2 also has a thick active layer but shows subsidence of the upper surface (see Figures 10 and 20). These results demonstrate ongoing degradation of the permafrost, which inactivates these rock glaciers. Both MAST and BTS on the upper part of BNL were higher than those of BNU (see Figure 13 and Table 2). Although no temperature data are available, these values are considered to rise toward the lower part of BNL, because seasonal snow cover disappears much earlier in the lower part. This condition favors the degradation of permafrost close to the melting point. The inactive BW2, however, have lower MASTs than BN in the years with a normal or poor snow condition. The limited water supply from the thin snow cover and long snow-free duration may be unsuitable for the maintenance of permafrost (see Figure 13 and Table 2).

The spatial variations in the velocity, active layer thickness and surface temperature appear to demonstrate temporally climatic inactivation of rock glaciers from the fast BNU to slow BNL. Further advance of BNU toward the warmer part of the slope may eventually degrade permafrost and inactivate BNU.

In the light of the mass balance, the amount of debris supply also influences the movement of BN. The rapid movement of BNU is unlikely to balance with the debris supply, because the rockwall above BNU is too small to feed a large amount of debris. The mass balance was evaluated in terms of downslope debris discharge by permafrost creep. The discharge per unit width of a rock glacier (Q) is given by

$$Q = H\bar{V} \quad (5)$$

$$\bar{V} = \frac{1}{H} \int_0^H V dz \quad (6)$$

where H is the thickness of moving debris, V is the downslope velocity at a depth and z is the depth perpendicular to the surface. The substitution of equations (2) and (3), defined in chapter 4, into equation (6) yields

$$\bar{V} = \frac{1}{5} A (\rho g \sin \alpha)^3 H^4 \quad (7)$$

where A is the creep parameter, ρ is the mean density of the rock glacier components, g is the acceleration due to gravity (9.8 m s^{-2}) and α is the surface gradient. Using the average A values ($7.4 \times 10^{-14} \text{ kPa}^{-3} \text{ s}^{-1}$), ρ and α defined in chapter 4 ($\rho = 1800 \text{ kg m}^{-3}$, $\alpha = 25^\circ$) and the estimated H (8.0 m; see Figure 22), the equations (5) and (7) yield the discharge of BNU to be $6.4 \text{ m}^3 \text{ a}^{-1}$ per unit width. In contrast, directly observed retreat rates of the rockwall were only 0.031 mm a^{-1} in 2000–2001 and 0.027 mm a^{-1} in 2001–2002. The volume of debris input from a source rockwall per unit width per unit time (I) is given by

$$I = RL_{RW} / (1 - \gamma) \quad (8)$$

where R is the retreat rate of the rockwall, L_{RW} is the average slope length of the source rockwall given by equation (1) and γ is the porosity of the talus. The L_{RW} value of BNU was calculated to be 15 m using the area of the source rockwall (2000 m^3), the width of the rock glacier at the talus foot (130 m) and the average slope angle of the rockwall (57°). With the parameters of $L_{RW} = 15 \text{ m}$, $\gamma = 0.5$ and $R = 2.9 \times 10^{-5} \text{ m a}^{-1}$ (observed average value), equation (8) then yields $I = 8.7 \times 10^{-4} \text{ m}^3 \text{ a}^{-1}$ per unit width, which is four orders of magnitude smaller than the discharge of BNU. Thus, the present movement of BNU does not balance with the debris supply from the rockwall.

In such an unbalanced condition, the continuous permafrost creep will probably thin BNU, which may in turn result in deceleration of movement (cf. Olyphant 1987). In fact, the subsidence of the surface was observed on the uppermost marker boulder (see Figure 16). The steep lower part of the talus slope (40°–45°) behind BNU also indicates recent debris lost from there, which may result from the subsidence of the upper part of BNU (see Figure 16). In addition, long-lasting large discharge by the observed permafrost creep ($6.4 \text{ m}^3 \text{ a}^{-1}$ per unit width) has to result in a large rock glacier far exceeding the observed slope geometry of BNU (the upper surface 45 m in length and the front 10 m in height). Thus, the present high velocities may reflect recent short-term acceleration.

Such acceleration indicates warming of permafrost in recent years. The warming may partly result from the downslope advance of the rock glacier, which has lowered its front to the warmer elevation. Regional climatic changes in recent years may also lead the acceleration. In fact, a slowly moving large rock glacier in the study area, Murtèl I, slightly accelerated between 1991 and 1995, which corresponded to an increase in temperature (c. 0.5°C) in the deformed layer (Arenson *et al.*, 2002). A similar relationship between air temperature and acceleration of a rock glacier was also observed on a rapidly moving small rock glacier in the Furggentälti area, western Swiss Alps (Mihajlovic *et al.*, 2003).

In order to predict the future movement of BNU, change in the longitudinal profile was simulated on the basis of a numerical model developed by Olyphant (1983, 1987). The model follows the conservation of mass:

$$\partial Q / \partial x + \partial H / \partial t = 0 \quad (9)$$

where x is the distance along the flow line and t is time. Incorporation of equations (5), (7), (8) and (9) gives rock glacier development as a function of time.

The original model by Olyphant lacked a talus slope between a rock glacier and a rockwall, although rock glaciers generally have a talus slope with a well-defined nick point at the talus foot. BNU also has such a nick point. The difference in the slope angle between the talus slope and the upper surface of a rock glacier probably reflects different processes: permafrost creep in a rock glacier and rockfall and debris flow on a talus slope. Thus, the change of a talus profile, which is controlled by the angle of repose and angle of maximum slope (cf. Carson and Kirkby, 1972), is also incorporated in the numerical model in this study. The simulation is programmed to shift the angle of talus slope within a short distance (Δx) to the angle of repose without any volume loss in the section when the slope angle exceeds the maximum angle of slope (Figure 24). In the simulation, the angle of repose is fixed at the minimum angle of the talus slope above BNU (35°) and the angle of maximum slope at the maximum angle of the talus slope (45°).

For calculation using a computer, equation (9) is arranged as

$$\Delta Q/\Delta x + \Delta H/\Delta t = 0 \quad (10).$$

In this study, Δx is fixed at 2 m. Δt is determined to insure a stable solution: 12 h in the initial stage of the simulation (<20 years) and increases to 24 h in the second stage (20–30 years) and to 120 h in the final stage (30–50 years). The values of the parameters introduced to the simulation, such as A , ρ , α , R , L_{RW} and γ , are the same as used in the evaluation of the mass balance. The Q value at the upper end of the simulated profile is replaced with I given by equation (8). The longitudinal profile of BNU (see Figure 16) is simplified for the simulation. The rock glacier is assumed to move by laminar flow down a semi-infinite plane inclined at angle α to the horizontal (Figure 25). The initial thickness H of the rock glacier is set at 8 m, which corresponds to the estimated deforming thickness of BNU (see Figure 22). The

horizontal length of talus slope is set at 56 m, which corresponds to the length of the talus slope above BNU, and the initial angle of the talus slope at the angle of repose (35°). The initial horizontal length of the rock glacier is set at 40 m, which is slight shorter than that of the upper surface of BNU (45 m), to create the steep (40° – 45°) lower part of the talus slope above BNU (15 m in horizontal length) when the simulated upper surface of the rock glacier becomes about 45 m long.

The simulated profile similar to the present profile of BNU is formed in the first decade, keeping a nearly constant velocity at the front (Figure 26). Then, the frontal advance significantly decelerates in the next two decades, because the thinning of the rock glacier starts near the front. As a result, the downslope velocity at the front in the 30th year becomes one third of that in the first year. The frontal velocity finally decreases to one fourth of that of the first year in the 50th year. This result indicates that the observed rapid movement will not last over the next 10 years, because the rock glacier will thin itself and the debris supply by the erosion of the talus slope will not be enough to sustain the rapid movement. Although the simulation includes a number of assumptions, such as the sharp discontinuity of the controlling parameters between the rock glacier and talus slope, the laminar movement and the consistent creep parameter in the whole rock glacier and neglect of the movement of BNL, the small amount of the debris supply from the rockwall and talus slope probably prevent the rapid advance of BNU within two decades, unless a catastrophic landslide originates from the talus slope.

Consequently, small rock glaciers located near the lower limit of mountain permafrost experience large seasonal, inter-annual and decadal variations in movement responding to change in thermal conditions. The decadal variation involves temporary acceleration reflecting the maximum creep parameter of permafrost at the melting point and subsequent deceleration because of the

unbalanced condition between the debris supply from the rockwall and talus slope and the rapid movement of the rock glacier. Large rock glaciers may respond to thermal change much slowly and need longer duration for such temporary acceleration and subsequent deceleration.

Chapter 6 Long-term variations in rock glacier dynamics

6.1. Parameters relating to climatic conditions

6.1.1. Altitude and aspect

Rock glaciers are distributed in all aspects over elevations between 2100 m and 2900 m ASL (Figures 2 and 27). The lower limit of the mountain permafrost zone, which is indicated by the terminus of the lowest intact rock glacier, lies at 2250 m ASL in the northern exposures, rising to 2550 m ASL in the southern exposures. The former elevation corresponds to the 0°C isotherm of MAAT, while the latter is nearly equivalent to the -2°C isotherm. In addition, most of the south-facing rock glaciers are inactive or relict. The difference in the elevation and activity status basically reflects the amount of incoming radiation.

6.1.2. Ground surface temperature

Near the lower limit of the discontinuous permafrost zone, the permafrost distribution at a local scale depends on the ground surface conditions. Figure 3 displays the distribution of rock glaciers and BTS values in March 1999 in the Corviglia area. BTS values derived from the manual measurements roughly corresponded to the surface features. Low BTS values ($<-3^{\circ}\text{C}$) mostly occurred on ‘apparently’ intact rock glaciers, which have no vegetation cover on the upper surface; in this paper, the word ‘apparently’ designates the activity status presumed only by the visual features. In contrast, apparently relict rock glaciers and slopes lacking blocks showed BTS values near 0°C. In the following, BTS and MAST are used to distinguish thermal conditions between active, inactive and relict rock glaciers.

Figures 28–32 show ground surface temperatures (daily mean values) recorded at all logger sites in the observation period (1998–2003) (see Figures 2 and 3 for the locations). The average BTS values for March and MASTs are also listed in Table 2 with the depths of the low P-wave velocity layers. The large inter-annual variation in snow conditions, which has been mentioned in Chapter 5, resulted in an inter-annual variation in ground surface temperature in the study area. The observed first and second years (1998–2000) had a normal winter suitable for the BTS method (Ikeda and Matsuoka, 1999, 2002). In the third and fourth years (2000–2002), however, the BTS method was inapplicable because of the extraordinary snow conditions: heavy snowfalls in October and November 2000 and the lack of notable snowfalls until late January 2003 (Hoelzle *et al.*, 2003).

First and second years: In the first and second years having a normal winter, BTS values on the apparently intact bouldery rock glaciers (O1, O2, O4, PN1, PN5, PS2, PS3, NS2) and the pebbly rock glaciers (NN8, NN12) decreased in the early winter, then remained nearly constant below -2°C or slowly increased toward the end of the winter (Figures 28–31). The average BTS values for March were lower than -3°C on these intact rock glaciers (Table 2), indicating the presence of permafrost (Hoelzle *et al.*, 1999). In contrast, BTS values above -2°C in the late winter on apparently relict rock glaciers (PN3, NS5) indicates the absence of permafrost (Figure 32). BTS on PS4 rock glacier shows an intermediate condition (average -2°C) between inactive and relict. However, both vegetation-free surface and low manual BTS values ($<-3^{\circ}\text{C}$) at 6 points (see Figure 3a) imply that PS4 is possibly inactive rather than relict. BN and BW are located at exceptional sites for the BTS method, because the former is usually covered with thick snow already in early winter and the latter with thin snow throughout winter (*cf.* Chapter 5). Whereas the BTS condition was similar between the first and second years, the earlier

snowmelt in the second year caused slightly higher MAST than that in the first year except for BW (Table 2, see also Figures 28–32).

Third year: The heavy snowfalls in early winter 2000 resulted in a warm ground condition throughout the third winter. All BTS values were higher than -3°C . High BTS values indicative of the absence of permafrost ($>-2^{\circ}\text{C}$) were recorded on all active and inactive pebbly rock glaciers (BN, BN3, BW, NN8, NN12) and two inactive bouldery rock glaciers (PS3, PS4), while the other active and inactive bouldery rock glaciers (O1, O4, PN1, PN5, NS2) had marginal BTS values (-2°C to -3°C). Such warm winter temperature caused higher MAST than that in the previous two years on many rock glaciers (O1, O4, PN5, NS2, BNU, BW, NN8, NN12), while the prolonged snow cover which prevented the ground from warming during mid-summer offset the high winter ground temperature, resulting in MAST not dissimilar to that in the second year on the other rock glaciers (PN1, PS3, PS4, PN3, NS5).

Fourth year: The snow-poor condition in the fourth winter (2001–2002) permitted intensive cooling of the ground until January. However, BTS increased gradually until the wet-snow front reached at the ground (Figures 28–32). In late winter (February to April), two relict rock glaciers showed a significant increase from -4°C to -1.5°C on PN3 and from -5°C to -0.5°C on W1 (Figure 32). Such a large temporal variation was unfavorable for the BTS method (Hoelzle *et al.*, 2003), although the average BTS value for March in the fourth year was similar to that in a normal winter on most rock glaciers (Table 2). Reflecting the cold winter condition, MASTs in the fourth year were the lowest during the observation period except on O4, NS5 and BW (Table 2).

Fifth year: In the fifth year (2002–2003), weak cooling and the subsequent warming in the early winter probably reflected heavy snowfalls (Figures 28–32).

Then, BTS on the intact rock glaciers decreased gradually and reached below -2°C except on PS4 and BN (Figures 28–31, see also Table 2). In contrast, BTS on the relict rock glaciers was maintained above -1°C throughout the winter (Figures 31 and 32). BTS on PS4 and BN showed an intermediate condition between intact and relict rock glaciers (Figures 29 and 30, see also Table 2). Although the thick snow cover prevented the ground from intensive cooling in the early winter, the snow cover was probably thinner than that in the third year, which resulted in gradual cooling of the ground beneath the snow cover. In spite of such a snow-rich condition, the fifth year experienced early snowmelt because of the extremely hot summer in 2003 (Figures 28–32). As a result, MASTs were highest during the five years except on PN5 and NN8 (Table 2).

Figure 33 relates BTS to MAST at the monitoring sites, except for BN and BW, where the snow condition is unfavorable for the BTS method. The BTS values in this figure represent averages for March evaluated from the logger data. The relationship between the two parameters is grouped into three regions according to the rock glacier activity, although BTS and MAST varied year by year. The intact rock glaciers have higher BTS than the relict rock glaciers, and the active rock glaciers have lower MASTs than the inactive rock glaciers. When the snow condition was normal (1998–2000), MAST was lower than 0°C and BTS was also low ($<-3^{\circ}\text{C}$) on the active rock glaciers (O1, O2, PN1, PN5, NN12). In contrast, the inactive rock glaciers (O4, PS2, PS3, PS4, NS2, NN8) showed low BTS ($<-2^{\circ}\text{C}$) despite MAST above 0°C . This suggests that under a positive MAST close to 1°C , permafrost may still be maintained but its progressive melting inactivates rock glaciers. MAST near 0°C on O1 and PN1 may indicate the boundary condition between the active and inactive states. In fact, vegetation is growing on the frontal slope of the two rock glaciers. Positive MAST and high BTS ($>-2^{\circ}\text{C}$) occurred on

the relict rock glaciers (PN3, NS5). The average values of BTS and MAST for the five years also show a pattern similar to the normal years in the diagram, because the values in the cold year (2001–2002) offset those in the warm years (2000–2001, 2002–2003).

6.1.3. Active layer thickness

Seismic refraction soundings revealed a difference in thickness of the uppermost low P-wave velocity layer between the active, inactive and relict rock glaciers, which reflects the preservation or degradation of permafrost (Table 1, see Figures 2, 3 and 4 for the locations). Figures 34–36 display travel time curves for the three types of rock glaciers. The active (PN1, PN5, BNU, BNLa, NN12) and half of the inactive (O4, PS3, NS2, BN3) rock glaciers show a high velocity layer (2100–4400 m s⁻¹) underlying a low velocity layer (330–690 m s⁻¹) thinner than 4 m (Table 1), whereas the rest of the inactive (PS4, W2, BW2, NN8) and the relict (PN3, PS1, NS5, W1, W3) rock glaciers have a low velocity layer (340–950 m s⁻¹) thicker than 4 m (Table 1). An exceptional case is the slowly creeping (i.e. active) lower part of BNL having an active layer 4 to 6 m thick (BNLb) (cf. Chapter 5). The relict rock glaciers generally have a low velocity layer thicker than that of the inactive rock glaciers. As a result, the sounding confirmed the presence or absence of permafrost evaluated from the BTS method (Table 2).

The P-wave velocity of the bedrock, which was measured on granite and limestone outcrops, ranged from 3200 m s⁻¹ to 3500 m s⁻¹ (Table 1). These values fall within the velocity range for the second layer of the active rock glaciers. However, the upper surface of the second layer is too shallow (1–3 m deep) to be the bedrock surface, because this depth is much smaller than the visual thickness of the rock glacier (≥10 m). Thus, the second layer in the active rock glaciers is regarded as

permafrost.

The second or third layer with a high P-wave velocity occurred also in relict rock glaciers. For instance, NS5 relict rock glacier had the third layer with a velocity of 3100 m s^{-1} , which probably indicates bedrock, because the overlying low velocity layers are too thick (c. 20 m) to be the active layer. The thickness of the low velocity layer in PN3, W1 and W3 (c. 10 m) roughly corresponds to the height of the adjacent frontal or side slope of the rock glaciers. Thus, the high velocity (c. 3000 m s^{-1}) layer in W1 and W3 also implies bedrock rather than permafrost. The velocity of 1600 m s^{-1} in PN3 is likely to indicate unfrozen water-saturated sediment or densely weathered limestone bedrock.

The seismic soundings on W2, BW2 and NN8 inactive rock glaciers demonstrated the progress of permafrost melting, because the low velocity layer had an intermediate thickness between those of active and relict rock glaciers. The high velocity second layer in W2, BW2 and NN8 probably corresponded to permafrost, because the low velocity layer ($\leq 5 \text{ m}$ thick) was shallower than the visual thickness of the rock glaciers ($\geq 10 \text{ m}$ thick). PS4 inactive rock glacier had a thick low velocity layer (c. 9 m), which may indicate considerable progress of permafrost melting. A high velocity (2100 m s^{-1}) observed below 9 m deep is considered to represent permafrost rather than weathered limestone bedrock, because low manual BTS values ($< -3^\circ\text{C}$) were recorded on the rock glacier. In contrast, the low velocity layer corresponding to the active layer is about 2–3 m thick in the other inactive rock glaciers (O4, PS3, NS2, BN3). The thickness similar to that of active rock glaciers suggests that permafrost has not yet degraded in these inactive rock glaciers.

6.2. Parameters relating to dynamic conditions

Figure 37 displays the relationship between the length of bouldery rock glacier

(L_{RG}) and the average slope length of source rockwall (L_{RW}) (see Figure 8 for definition). The active rock glaciers show a positive correlation between L_{RW} and L_{RG} , which indicates that the size of source rockwall is one of the major controls on the rock glacier development. Similar positive correlation between the source rockwall area and surface area of rock glaciers was also reported by several authors (e.g. Wahrhaftig and Cox, 1959; Frauenfelder *et al.*, 2003). The correlation suggests that a large rockwall tends to produce a long rock glacier through the abundant input of debris.

The inactive and relict rock glaciers showed an insignificant correlation between L_{RW} and L_{RG} (Figure 37). In the study area, most of the inactive and relict rock glaciers have L_{RW} shorter than 100 m, whereas most of the active rock glaciers have L_{RW} longer than 100 m. Such a contrast implies that the present debris supply on the inactive and relict rock glaciers is generally less than that of the active rock glaciers. In other words, the active rock glaciers are located at a more favorable place for the continuous development than the inactive and relict rock glaciers.

The angle of the upper surface of bouldery rock glaciers (α) ranged from 6° to 28° (average 16°) (Figure 38). The average angles slightly decreased from active rock glaciers (18°) to relict rock glaciers (14°). No correlation is found between α and L_{RG} , although $\sin\alpha$ is a parameter representing the shear stress in a rock glacier. Thus, debris supply may be more responsible for the development of a rock glacier than slope angle.

6.3. Response of rock glaciers to long-term environmental change

The activity status of rock glaciers was distinguished by parameters relating to thermal conditions, such as altitude, aspect, BTS and MAST in the study areas (Figures 27 and 33). Such spatial variation in thermal conditions indicates the

response of rock glacier dynamics to temporal change in temperature. The difference in altitudes between active and relict rock glaciers in a regional scale has been discussed with regard to palaeoclimate reconstruction (Haeberli, 1983; Kerschner, 1985). In these studies, the difference in MAATs between the fronts of active and relict rock glaciers, which approximately indicates the long-term increase in MAATs causing the disappearance of permafrost from the presently relict rock glaciers, is given by

$$\Delta T_{MAAT} = (E_a - E_r) dT/dE \quad (11)$$

where E is the average altitude of the fronts of active (a) and relict (r) rock glaciers and dT/dE is the lapse rate of air temperature. Likewise, ΔT_{MAST} , which is given by MAST on a relict or climatically inactive rock glacier minus the highest MAST of active rock glaciers (c. 0° in a normal year), is considered to represent the long-term increase in MASTs on the inactive/relict rock glaciers from the beginning of the climatic inactivation.

The ΔT_{MAST} values of the inactive rock glaciers range from 0°C to 1°C (Figure 33), except for those in the extremely snow-rich or snow-poor years (2000–2002). The maximum ΔT_{MAST} of the inactive rock glaciers (1°C) roughly corresponds to the bandwidth of the Holocene climate variation (cf. Frauenfelder et al., 2001). In the study area, active rock glaciers are considered to have continuously moved through the Holocene (e.g. Haeberli *et al.*, 1999; Frauenfelder and Käab, 2000). In contrast, the inactive rock glaciers lying at a slightly warmer situation are likely to have moved only in cold periods during the Holocene, such as the Little Ice Age. Thus, the total duration for the advance of the presently inactive rock glaciers is shorter than that of the presently active rock glaciers during the Holocene. The shorter duration for the advance may result in the length (L_{RG}) of the inactive rock glaciers

generally shorter than 300 m, while half of the active rock glaciers are longer than 300 m (Figure 37).

The relict rock glaciers show ΔT_{MAST} larger than about 1°C (Figure 33), indicating that they have never been active throughout the Holocene, because ΔT_{MAST} exceeds the bandwidth of the Holocene climate variation. Although data on the MASTs on the relict rock glaciers are limited in this study, a previous statistical work by Frauenfelder and Kääb (2000) estimated that MAATs when the relict rock glaciers lay at the lower limit of mountain permafrost was about 2°C lower than the present MAATs on the relict rock glaciers in the study area. Thus, most of the relict rock glaciers are considered to have developed during the Late Glacial period, when the MAAT was 1–4°C colder than that of today (Frauenfelder et al., 2001).

Some inactive rock glaciers having a thin active layer, however, indicate that permafrost melting does not progress in all inactive rock glaciers. Factors other than the thermal conditions may inactivate these rock glaciers. Warm permafrost below such a thin active layer has a large creep parameter, which enables a rock glacier to move rapidly, whereas the continuous movement requires debris supply compensating the volume lost by the movement (cf. Chapter 5). Thus, in the marginal condition of permafrost, rock glaciers may have been inactivated by the shortage of debris supply. In fact, rockwalls above the inactive rock glaciers are generally lower than those above the active ones, which implies that the debris supply on inactive rock glaciers is significantly less than that of active rock glaciers (Figure 37).

MAATs are related to the average slope length of source rockwall (L_{RW}) for active, inactive and relict bouldery rock glaciers to evaluate the contribution of both thermal conditions and debris supply to the activity (Figure 39). The relationship was analyzed separately for four aspects, because the activity status of rock glaciers

is influenced by the difference in incoming radiation (see Figure 27). The slope angle (α), which controls the shear stress in a rock glacier, is incorporated in Figure 40 the analysis using $L_{RW}\sin\alpha$ to improve Figure 39. Both diagrams show a similar relationship that MAATs largely overlap between the active rock glaciers and the other two types. Debris supply may be more responsible for the activity of rock glacier than slope angle. For the same altitude and aspect, the active rock glaciers have a large source rockwall than the inactive and relict rock glaciers. Thus, a large source rockwall is necessary for the continuous development of rock glaciers through the Holocene near the lower limit of mountain permafrost.

The spatial variation in thermal parameters such as MAAT and MAST indicates that long-term change in temperature primarily controls the activity status of rock glaciers near the lower limit of mountain permafrost (Figure 41). In addition, a small amount of debris supply from a small source rockwall would have resulted in the earlier inactivation of rock glaciers in the Holocene. In a transient condition from an active to inactive rock glacier, warm permafrost having a high creep parameter may temporarily accelerate the rock glacier (cf. Chapter 5). Such an unstable condition may be eventually followed by inactivation of the rock glacier because of the insignificant debris input and progressive permafrost melting.

Chapter 7 Conclusions

The first part of this study demonstrates processes controlling contemporary dynamics of a rock glacier. The differences in movement and structure between the upper BN, lower BN and BW, all lying close to the boundary between the permafrost and non-permafrost terrains, indicate a sequence of short-term inactivation of small rock glaciers. Warming of a thin permafrost layer to the melting point makes a rock glacier much unstable and sensitive to seasonal and inter-annual variations in ground temperature. Such an unstable condition is temporary and eventually followed by inactivation of the rock glacier because of insignificant debris supply and progressive permafrost melting.

The present rapid movement of the upper BN ($50\text{--}150\text{ cm a}^{-1}$) is attributed primarily to creep of the frozen debris close to 0°C , which contains a significant amount of unfrozen water. In addition, the movement is sensitive to seasonal and inter-annual changes in ground thermal conditions, which are mainly controlled by the thickness and duration of snow cover. The quick response of movement to change in ground surface temperature may indicate the permeable structure of the permafrost, which allows unfrozen water to percolate into the frozen debris.

The rapid movement of the upper BN is unlikely to balance with the debris supply, because the observed retreat rate of the rockwall ($3 \times 10^{-5}\text{ m a}^{-1}$) above BN is too small to compensate the large volume lost by the rapid downslope deformation. A model of the deformation based on the geometry and creep properties of the upper BN predicts that the observed rapid movement will decline within the next two decades.

The inactive BW and the slowly moving frontal part of BN have a thick active

layer (>5 m) indicating permafrost degradation, although the active layer thickness decreases to about 2 m towards the upper part. In addition, the subsiding surface of BW implies ongoing degradation of ice lenses in permafrost. Such degradation of permafrost may follow the temporary acceleration and subsequent deceleration.

The second part of this study demonstrates long-term change in rock glacier dynamics by means of a comparison between active, inactive and relict rock glaciers in terms of thermal conditions and debris supply. Temperature monitoring and geophysical soundings demonstrate that MAST rises from active rock glaciers to relict rock glaciers. The BTS-MAST diagram distinguishes these three types of rock glaciers clearly. Such a spatial variation in thermal conditions indicates the response of rock glacier dynamics to temporal change in temperature. The difference in the highest MAST between active and inactive rock glaciers roughly corresponds to the bandwidth of the Holocene climate variations (c. -1°C), implying the present inactive rock glaciers were active in the cold periods during the Holocene, such as the Little Ice Age.

The active and inactive rock glaciers are also distinguished by additional parameters: size of the source rockwall and slope angle of the rock glacier, which controls debris supply and slope instability, respectively. Debris supply may be more responsible for the activity of rock glacier than slope angle. A diagram of MAAT and a parameter indicating dynamic conditions ($L_{RW}\sin\alpha$) shows that active rock glaciers have larger $L_{RW}\sin\alpha$ than inactive and relict ones for the same MAAT. Thus, a large amount of debris supply is necessary for the continuous development of rock glaciers through the Holocene near the lower limit of mountain permafrost.

Acknowledgements

This study was conducted as a part of the Japan-Swiss joint research project on periglacial geomorphology. First of all, I should like to express sincere thanks to the Swiss researchers: Dr. Felix Keller (Academia Engadina) for enormous amount of useful information on rock glaciers and permafrost, logistic helps and accommodation during the fieldwork; Prof. Wilfried Haeberli (University of Zurich) for helpful comments on rock glacier development; Dr. Andreas Käab (University of Zurich) for collaboration in the geodetic survey and discussion on rock glacier movement; Dr. Martin Hoelzle (University of Zurich) for useful information on the rock glacier distribution and preparation of BTS probes; Dr. Daniel Vonder Mühl (University of Basel) for technical advice and discussion on electrical sounding; Dr. Regula Frauenfelder (University of Zurich) and Dr. Lukas Arenson (University of Alberta) for helpful discussion on rock glacier distribution and rheology. I also acknowledge Celeriner Bergbahnen for transportation of field equipment.

I would like to thank the following Japanese researchers: Prof. Norikazu Matsuoka (University of Tsukuba) for the guidance to the study, logistic support and advices on both field and laboratory work; and Prof. Kazuomi Hirakawa, Dr. Teiji Watanabe, Dr. Takayuki Shiraiwa, Dr. Shogo Iwasaki (Hokkaido University), Dr. Mamoru Ishikawa (Frontier Observation Research System for Global Change), Dr. Masafumi Aoyama (Tokyo Metropolitan University), Dr. Kotaro Fukui (National Institute for Polar Research) and Mr. Yuki Sawada (Graduate student, Hokkaido University) for numerous advices, discussion and cooperation in the field. I also thank Mr. Toshihiro Terunuma, Ms. Miwa Abe (Yamashita), Mr. Takeshi Date (formerly: Graduate or undergraduate students, University of Tsukuba), Mr.

Masahiro, Abe (Graduate student, University of Tsukuba), Mr. Yoshihiko Eda (Undergraduate student, University of Tsukuba) for assistance in the field. My special thanks go to Prof. Kiichi Moriwaki, Dr. Hideki Miura (National Institute for Polar Research) and Dr. Takanobu Sawagaki (Hokkaido University) for permission to use electrical resistivity meters and drilling machines. Finally, I acknowledge Prof. Yukinori Matsukura, Prof. Masamu Aniya, Prof. Eiji Matsumoto, Dr. Hiroshi Ikeda, Dr. Yuichi Onda and the other staffs and students in the geomorphology section of the Institute of Geoscience, University of Tsukuba, for their helpful comments and discussion.

This study was financially supported by funding from the Japan Science Society; Tokyo Geographical Society; Sumitomo Foundation; Grant-in-Aid for JSPS Fellows.

References

- Anderson, D. M. and Morgenstern, N. R. (1973). Physics, chemistry, and mechanics of frozen ground: a review. In *Proceedings of the Second International Conference on Permafrost*. National Academy of Sciences, Washington, pp. 257-288.
- Arenson, L., Hoelzle, M. and Springman, S. (2002). Borehole deformation measurements and internal structures of some rock glaciers in Switzerland. *Permafrost and Periglacial Processes*, **13**, 117-135.
- Barsch, D. (1969). Permafrost in der oberen subnivalen Stufe der Alpen. *Geographica Helvetica*, **24**, 10-12.
- Barsch, D. (1977). Nature and importance of mass-wasting by rock glaciers in alpine permafrost environments. *Earth Surface Processes*, **2**, 231-245.
- Barsch, D. (1992). Permafrost creep and rockglaciers. *Permafrost and Periglacial Processes*, **3**, 175-188.
- Barsch, D. (1996). *Rock Glaciers. Indicators for the Present and Former Geocology in High Mountain Environments*. Springer, Berlin, 331 pp.
- Barsch, D. and Hell, G. (1975). Photogrammetrische Bewegungsmessungen am Blockgletscher Murtèl I, Oberengadin, Schweizer Alpen. *Zeitschrift für Gletscherkunde und Glazialgeologie*, **11**, 111-142.
- Barsch, D. and Jakob, M. (1998). Mass transport by active rock glaciers in the Khumbu Himalaya. *Geomorphology*, **26**, 215-222.
- Barsch, D. and Zick, W. (1991). Die Bewegungen des Blockgletschers Macun 1 von 1965–1988 (Unterengadin, Graubünden, Schweiz). *Zeitschrift für Geomorphologie N. F.*, **35**, 1-14.

- Barsch, D., Fierz, H. and Haeberli, W. (1979). Shallow core drilling and bore-hole measurements in the permafrost of an active rock glacier near the Grubengletscher, Wallis, Swiss Alps. *Arctic and Alpine Research*, **11**, 215-228.
- Bernhard, L., Sutter, F., Haeberli, W. and Keller, F. (1998). Processes of snow/permafrost-interactions at a high-mountain site, Murtèl/Corvatsch, eastern Swiss Alps. In *Proceedings of the Seventh International Conference on Permafrost*. Centre d'études Nordiques, Sainte-Foy, pp. 35-40.
- Berthling, I., Etzelmüller, B., Isaksen, K. and Solid, J. L. (2000). Rock glaciers on Prins Karls Forland. II: GPR soundings and the development of internal structures. *Permafrost and Periglacial Processes*, **11**, 357-369.
- Brazier, V., Kirkbride, M. P. and Owens, I. F. (1998). The relationship between climate and rock glaciers distribution in the Ben Ohau Range, New Zealand. *Geografiska Annaler*, **80A**, 193-207.
- Budd, W. F. and Jacka, T. H. (1989). A review of ice rheology for ice sheet modeling. *Cold Regions Science and Technology*, **16**, 107-144.
- Calkin, P. E., Haworth, L. A. and Ellis, J. M. (1987). Rock glaciers of central Brooks Range, Alaska, U.S.A. In Giardino, J. R., Shroder, J. F. Jr. and Vitek, J. D. (eds.), *Rock Glaciers*. Allen and Unwin, London, pp. 65-82.
- Capps, S. R. (1910). Rock glaciers in Alaska. *Journal of Geology*, **18**, 359-375.
- Carson, M. A. and Kirkby, M. J. (1972). *Hillslope Form and Process*. Cambridge University Press, London, 475 pp.
- Clark, D. H., Steig, E. J., Potter, N. Jr. and Gillespie, A. R. (1998). Genetic variability of rock glaciers. *Geografiska Annaler*, **80A**, 175-182.
- Clark, D. H., Steig, E. J., Potter, N. Jr., Fitzpatrick, J., Updike, A. B. and Clark, G. M. (1996). Old ice in rock glaciers may provide long-term climate records. *EOS, Transactions, American Geophysical Union*, **77**, 217, 221-222.

- Cohen, D. (2000). Rheology of ice at the bed of Engabreen, Norway. *Journal of Glaciology*, **46**, 611-621.
- Corte, A. E. (1987). Rock glacier taxonomy. In Giardino, J. R., Shroder, J. F. Jr. and Vitek, J. D. (eds.), *Rock Glaciers*. Allen and Unwin, London, pp. 27-39.
- Dash, J. G., Fu, H. and Wettlaufer, J. S. (1995). The premelting of ice and its environmental consequences. *Reports on Progress in Physics*, **58**, 115-167.
- Degenhardt, J. J. and Giardino, J. R. (2003). Subsurface investigation of a rock glacier using ground-penetrating radar: Implications for locating stored water on Mars. *Journal of Geophysical Research*, **108 (E4)**, Art. No. 8036.
- Elconin, R. F. and LaChapelle, E. R. (1997). Flow and internal structure of a rock glacier. *Journal of Glaciology*, **43**, 238-244.
- Evin, M. (1987). Lithology and fracturing control of rock glaciers in southwestern Alps of France and Italy. In Giardino, J. R., Shroder, J. F. Jr. and Vitek, J. D. (eds.), *Rock Glaciers*. Allen and Unwin, London, pp. 83-106.
- Fisch, W. Sr., Fisch, W. Jr. and Haerberli, W. (1977). Electrical D.C. resistivity soundings with long profiles on rock glaciers and moraines in the Alps of Switzerland. *Zeitschrift für Gletscherkunde und Glazialgeologie*, **13**, 239-260.
- Frauenfelder, R. and Kääh, A. (2000). Towards a paleoclimatic model of rock glacier formation in the Swiss Alps. *Annals of Glaciology*, **31**, 281-286.
- Frauenfelder, R., Haerberli, W., Hoelzle, M. and Maisch, M. (2001). Using relict rockglaciers in GIS-based modelling to reconstruct Younger Dryas permafrost distribution patterns in the Err-Julier area, Swiss Alps. *Norsk Geografisk Tidsskrift*, **55**, 195-202.
- Frauenfelder, R., Haerberli, W. and Hoelzle, M. (2003). Rockglacier occurrence and related terrain parameters in a study area of the Eastern Swiss Alps. In *Proceedings of the Eighth International Conference on Permafrost*. Balkema,

- Lisse, pp. 253-258.
- French, H. M. (1996). *Periglacial Environments, Second Edition*. Longman, Harlow, 341 pp.
- Frich, P. and Brandt, E. (1985). Holocene talus accumulation rates, and their influence on rock glacier growth. A case study from Igpiq, Disko, West Greenland. *Geografisk Tidsskrift*, **85**, 32-44.
- Fujii, Y. and Higuchi, K. (1978). Distribution of alpine permafrost in the northern hemisphere and its relation to air temperature. In *Proceedings of the Third International Conference on Permafrost*. National Research Council of Canada, Ottawa, pp. 366-371.
- Glen, J. W. (1955). The creep of polycrystalline ice. *Proceedings of the Royal Society of London, Series A*, **228**, 519-538.
- Guglielmin, M., Lozej, A. and Tellini, C. (1994). Permafrost distribution and rock glaciers in the Livigno Area (Northern Italy). *Permafrost and Periglacial Processes*, **5**, 25-36.
- Guglielmin, M., Cannone, N. and Dramis, F. (2001). Permafrost–glacial evolution during the Holocene in the Italian Central Alps. *Permafrost and Periglacial Processes*, **12**, 111-124.
- Haeberli, W. (1973). Die Basis-Temperatur der winterlichen Schneedecke als möglicher Indikator für die Verbreitung von Permafrost in den Alpen. *Zeitschrift für Gletscherkunde und Glazialgeologie*, **9**, 221-227.
- Haeberli, W. (1983). Permafrost-glacier relationships in the Swiss Alps – today and in the past. In *Proceedings of the Fourth International Conference on Permafrost*. National Academy Press, Washington, pp. 415-420.
- Haeberli, W. (1985). Creep of mountain permafrost: internal structure and flow of alpine rock glaciers. *Versuchsanstalt für Wasserbau, Hydrologie und Glaziologie*

der ETH Zurich, Mitteilungen, **77**, 142 pp.

- Haeberli, W. and Patzelt, G. (1982). Permafrostkartierung im Gebiet der Hochebenkar-Blockgletscher, Obergurgl, Ötztaler Alpen. *Zeitschrift für Gletscherkunde und Glazialgeologie*, **18**, 127-150.
- Haeberli, W. and Schmid, W. (1988). Aerophotogrammetrical monitoring of rock glaciers. In *Proceedings of the Fifth International Conference on Permafrost, Vol. 1*. Tapir, Trondheim, pp. 764-769.
- Haeberli, W. and Vonder Mühl, D. (1996). On the characteristics and possible origins of ice in rock glacier permafrost. *Zeitschrift für Geomorphologie N. F. Suppl.-Bd.*, **104**, 43-57.
- Haeberli, W., King, L. and Flotron, A. (1979). Surface movement and lichen-cover studies at the active rock glacier near the Grubengletscher, Wallis, Swiss Alps. *Arctic and Alpine Research*, **11**, 421-441.
- Haeberli, W., Guodong, C., Gorbunov, A. P. and Harris, S. A. (1993). Mountain permafrost and climatic change. *Permafrost and Periglacial Processes*, **4**, 165-174.
- Haeberli, W., Hoelzle, M., Keller, F., Vonder Mühl, D. and Wagner, S. (1998). Ten years after the drilling through the permafrost of the active rock glacier Murtèl, eastern Swiss Alps: answered questions and new perspectives. In *Proceedings of the Seventh International Conference on Permafrost*. Centre d'études Nordiques, Sainte-Foy, pp. 403-410.
- Haeberli, W., Käab, A., Wagner, S., Vonder Mühl, D., Geissler, P., Haas, J. N., Glatzel-Mattheier, H. and Wagenbach, D. (1999). Pollen analysis and ¹⁴C age of moss remains in a permafrost core recovered from the active rock glacier Murtèl-Corvatsch, Swiss Alps: geomorphological and glaciological implications. *Journal of Glaciology*, **45**, 1-8.

- Haeberli, W., Evin, M., Tenthorey, G., Kensen, H. R., Hoelzle, M., Keller, F., Vonder Mühll, D., Wagner, S., Pelfini, M. and Smiraglia, C. (1992). Permafrost research sites in the Alps: excursions of the international workshop on permafrost and periglacial environments in mountain areas. *Permafrost and Periglacial Processes*, **3**, 189-202.
- Harris, S. A. (2001). Twenty years of data on climate-permafrost-active layer variations at the lower limit of alpine permafrost, Marmot Basin, Jasper National Park, Canada. *Geografiska Annaler*, **83A**, 1-13.
- Harris, S. A. and Pedersen, E. (1998). Thermal regimes beneath coarse blocky materials. *Permafrost and Periglacial Processes*, **9**, 107-120.
- Hauck, C., Guglielmin, M., Isaksen, K. and Vonder Mühll, D. (2001). Applicability of frequency-domain and time-domain electromagnetic methods for mountain permafrost studies. *Permafrost and Periglacial Processes*, **12**, 39-52.
- Heiland, C. A. (1940). *Geophysical Exploration*. Prentice-Hall, New York, 1013 pp.
- Hoekstra, P. and McNeill, D. (1973). Electromagnetic probing of permafrost. In *Proceedings of the Second International Conference on Permafrost*. National Academy of Sciences, Washington, pp. 517-526.
- Hoelzle, M. (1992). Permafrost occurrence from BTS measurements and climatic parameters in the eastern Swiss Alps. *Permafrost and Periglacial Processes*, **3**, 143-147.
- Hoelzle M. (1998). Rock glaciers, Upper Engadin, Switzerland. In IPA Data and Information Working Group, Comp. Circumpolar Active-layer Permafrost System (CAPS), version 1.0. National Snow and Ice Data Center (NSIDC), Boulder, CO, CD-ROM.
- Hoelzle, M., Haeberli, W. and Keller, F. (1993). Application of BTS-measurements for modelling mountain permafrost distribution. In *Proceedings of the Sixth*

- International Conference on Permafrost, Vol. 1.* South China University Technology Press, Wushan, pp. 273-277.
- Hoelzle, M., Haeberli, W. and Stocker-Mittaz, C. (2003). Miniature ground temperature data logger measurements 2000–2002 in the Murtèl-Corvatsch area, Eastern Swiss Alps. In *Proceedings of the Eighth International Conference on Permafrost*. Balkema, Lisse, pp. 419-424.
- Hoelzle, M., Wegmann, M. and Krummenacher, B. (1999). Miniature temperature dataloggers for mapping and monitoring of permafrost in high mountain areas: first experience from the Swiss Alps. *Permafrost and Periglacial Processes*, **10**, 113-124.
- Hoelzle, M., Wagner, S., Kääh, A. and Vonder Mühl, D. (1998). Surface movement and internal deformation of ice-rock mixtures within rock glaciers at Pontresina-Schafberg, Upper Engadin, Switzerland. In *Proceedings of the Seventh International Conference on Permafrost*. Centre d'études Nordiques, Sainte-Foy, pp. 465-471.
- Hooke, R. L., Dahlin, B. B. and Kauper, M. T. (1972). Creep of ice containing dispersed fine sand. *Journal of Glaciology*, **11**, 327-346.
- Humlum, O. (1988). Rock glacier appearance level and rock glacier initiation line altitude: a methodological approach to the study of rock glaciers. *Arctic and Alpine Research*, **20**, 160-178.
- Humlum, O. (1997). Active layer thermal regime at three rock glaciers in Greenland. *Permafrost and Periglacial Processes*, **8**, 383-408.
- Humlum, O. (2000). The geomorphic significance of rock glaciers: estimates of rock glacier debris volumes and headwall recession rates in West Greenland. *Geomorphology*, **35**, 41-67.
- Hunter, J. A. M. (1973). The application of shallow seismic methods to mapping of

- frozen surficial materials. In *Proceedings of the Second International Conference on Permafrost*. National Academy of Sciences, Washington, pp. 527-535.
- Ikeda, A. and Matsuoka, N. (1999). Measurements of bottom temperature of the winter snow cover (BTS) in relation to rock glacier activity, Corviglia, Swiss Alps: a preliminary report. *Annual Report of the Institute of Geoscience, the University of Tsukuba*, **25**, 13-17.
- Ikeda, A. and Matsuoka, N. (2002). Degradation of talus-derived rock glaciers in the Upper Engadin, Swiss Alps. *Permafrost and Periglacial Processes*, **13**, 145-161.
- Ikeda, A., Matsuoka, N. and Kääh, A. (2003). A rapidly moving small rock glacier at the lower limit of the mountain permafrost belt in the Swiss Alps. In *Proceedings of the Eighth International Conference on Permafrost*. Balkema, Lisse, pp. 455-460.
- Imhof, M. (1996). Modelling and verification of the permafrost distribution in the Bernese Alps (Western Switzerland). *Permafrost and Periglacial Processes*, **7**, 267-280.
- Ishikawa, M. and Hirakawa, K. (2000). Mountain permafrost distribution based on BTS measurements and DC resistivity soundings in the Daisetsu Mountains, Hokkaido, Japan. *Permafrost and Periglacial Processes*, **11**, 109-123.
- Ishikawa, M., Watanabe, T. and Nakamura, N. (2001). Genetic differences of rock glaciers and the discontinuous mountain permafrost zone in Kanchanjunga Himal, eastern Nepal. *Permafrost and Periglacial Processes*, **12**, 243-253.
- Johnson, J. P. and Nickling, W. G. (1979). Englacial temperature and deformation of a rock glacier in the Kluane Range, Yukon Territory, Canada. *Canadian Journal of Earth Sciences*, **16**, 2275-2283.
- Kääh, A., Gudmundsson, G. H. and Hoelzle, M. (1998). Surface deformation of creeping mountain permafrost. Photogrammetric investigations on Murtèl rock

- glacier, Swiss Alps. In *Proceedings of the Seventh International Conference on Permafrost*. Centre d'études Nordiques, Sainte-Foy, pp. 531-537.
- Kääb, A., Haeberli, W. and Gudmundsson, G. H. (1997). Analysing the creep of mountain permafrost using high precision aerial photogrammetry: 25 years of monitoring Gruben rock glacier, Swiss Alps. *Permafrost and Periglacial Processes*, **8**, 409-426.
- Kääb, A., Kaufmann, V., Ladstädter, R. and Eiken, T. (2003). Rock glaciers dynamics: implications from high-resolution measurements of surface velocity fields. In *Proceedings of the Eighth International Conference on Permafrost*. Balkema, Lisse, pp. 501-506.
- Keller, F. and Gubler, H. (1993). Interaction between snow cover and high mountain permafrost Murtèl/Corvatsch, Swiss Alps. In *Proceedings of the Sixth International Conference on Permafrost, Vol. 1*. South China University Technology Press, Wushan, pp. 332-337.
- Keller, F., Frauenfelder, R., Gardaz, J., Hoelzle, M., Kneisel, C., Lugon, R., Phillips, M., Reynard, E. and Wenker, L. (1998). Permafrost map of Switzerland. In *Proceedings of the Seventh International Conference on Permafrost*. Centre d'études Nordiques, Sainte-Foy, pp. 557-562.
- Kerschner, H. (1985). Quantitative palaeoclimatic inferences from lateglacial snowline, timberline and rock glacier data, Tyrolean Alps, Austria. *Zeitschrift für Gletscherkunde und Glazialgeologie*, **21**, 363-369.
- King, L., Fisch, W., Haebrli, W. and Wächter, H. P. (1987). Comparison of resistivity and radio-echo soundings on rock glacier permafrost. *Zeitschrift für Gletscherkunde und Glazialgeologie*, **23**, 77-97.
- Kirkbride, M. and Brazier, V. (1995). On the sensitivity of Holocene talus-derived rock glaciers to climate change in the Ben Ohau Range, New Zealand. *Journal of*

Quaternary Science, **10**, 353-365.

- Kneisel, C. (1998). Occurrence of surface ice and ground ice/permafrost in recently deglaciated glacier forefields, St. Moritz area, eastern Swiss Alps. In *Proceedings of the Seventh International Conference on Permafrost*. Centre d'études Nordiques, Sainte-Foy, pp. 575-581.
- Maisch, M., Haeberli, W., Frauenfelder, R., Kääh, A. and Rothenbühler, C. (2003). Lateglacial and Holocene evolution of glaciers and permafrost in the Val Muragl, Upper Engadine, Swiss Alps. In *Proceedings of the Eighth International Conference on Permafrost*. Balkema, Lisse, pp. 717-722.
- Martin, H. E. and Whalley, W. B. (1987). Rock glaciers, part 1: rock glacier morphology, classification and distribution. *Progress in Physical Geography*, **11**, 260-282.
- Matsuoka, N. (1990). The rate of bedrock weathering by frost action: field measurements and a predictive model. *Earth Surface Processes and Landforms*, **15**, 73-90.
- Matsuoka, N. (2001). Solifluction rates, processes and landforms: a global review. *Earth-Science Reviews*, **55**, 107-134.
- Matsuoka, N. and Ikeda, A. (2001). Geological control on the distribution and characteristics of talus-derived rock glaciers. *Annual Report of the Institute of Geoscience, the University of Tsukuba*, **27**, 11-16.
- Matsuoka, N., Hirakawa, K., Watanabe, T. and Moriwaki, K. (1997). Monitoring of periglacial slope processes in the Swiss Alps: the first two years of frost shattering, heave and creep. *Permafrost and Periglacial Processes*, **8**, 155-177.
- Mihajlovic, D., Kölbing, D., Kunz, I., Schwab, S., Kienholz, H., Budmiger, K., Imhof, M. and Krummenacher, B. Developing new methods for monitoring periglacial phenomena. In *Proceedings of the Eighth International Conference on*

- Permafrost*. Balkema, Lisse, pp. 765-770.
- Mittaz, C., Hoelzle, M. and Haeberli, W. (2000). First results and interpretation of energy-flux measurements over Alpine permafrost. *Annals of Glaciology*, **31**, 275-280.
- Morgenstern, N. R., Roggensack, W. D. and Weaver, J. S. (1980). The behavior of friction piles in ice and ice rich soils. *Canadian Geotechnical Journal*, **17**, 405-415.
- Musil, M., Maurer, H., Green, A. G., Horstmeyer, H., Nitsche, F. O., Vonder Mühl, D. and Springman, S. (2002). Shallow seismic surveying of an Alpine rock glacier. *Geophysics*, **67**, 1701-1710.
- Olyphant, G. A. (1983). Computer simulation of rock-glacier development under viscous and pseudoplastic flow. *Geological Society of America Bulletin*, **94**, 499-505.
- Olyphant, G. A. (1987). Rock glacier response to abrupt changes in talus production. In Giardino, J. R., Shroder, J. F. Jr. and Vitek, J. D. (eds.), *Rock Glaciers*. Allen and Unwin, London, pp. 55-64.
- Outcalt, S. I. and Benedict, J. B. (1965). Photo-interpretation of two types of rock glaciers in the Colorado Front Range, U.S.A. *Journal of Glaciology*, **5**, 849-856.
- Paterson, W. S. B. (1981). *The Physics of Glaciers, 3rd Edition*. Elsevier, Oxford, 480 pp.
- Potter, N. Jr. (1972). Ice-cored rock glacier, Galena Creek, northern Absaroka Mountains, Wyoming. *Geological Society of America Bulletin*, **83**, 3025-3057.
- Potter, N. Jr., Steig, E. J., Clark, D. H., Speece, M. A., Clark, G. M. and Updike, A. B. (1998). Galena Creek Rock Glacier revisited – new observations on an old controversy. *Geografiska Annaler*, **80A**, 251-265.
- Sawada, Y., Ishikawa, M. and Ono, Y. (2003). Thermal regime of sporadic

- permafrost in a block slope on Mt. Nishi-Nupukaushinupuri, Hokkaido Island, Northern Japan. *Geomorphology*, **52**, 121-130.
- Solid, J. L. and Sørbel, L. (1992). Rock glaciers in Svalbard and Norway. *Permafrost and Periglacial Processes*, **3**, 215-220.
- Vonder Mühl, D. and Haeberli, W. (1990). Thermal characteristics of the permafrost within an active rock glacier (Murtèl/Corvatsch, Grisons, Swiss Alps). *Journal of Glaciology*, **36**, 151-158.
- Vonder Mühl, D. S. and Holub, P. (1992). Borehole logging in alpine permafrost, Upper Engadin, Swiss Alps. *Permafrost and Periglacial Processes*, **3**, 169-173.
- Vonder Mühl, D. S. and Schmid, W. (1993). Geophysical and photogrammetrical investigation of rock glacier Muragl I, upper Engadin, Swiss Alps. In *Proceedings of the Sixth International Conference on Permafrost, Vol. 1*. South China University Technology Press, Wushan, pp. 654-659.
- Vonder Mühl, D. S. and Klingelé, E. E. (1994). Gravimetric investigation of ice-rich permafrost within the rock glacier Murtèl-Corvatsch (Upper Engadin, Swiss Alps). *Permafrost and Periglacial Processes*, **5**, 13-24.
- Vonder Mühl, D. S., Arenson, L. U. and Springman, S. M. (2003). Temperature conditions in two Alpine rock glaciers. In *Proceedings of the Eighth International Conference on Permafrost*. Balkema, Lisse, pp. 1195-1200.
- Vonder Mühl, D., Stucki, T. and Haeberli, W. (1998). Borehole temperatures in Alpine permafrost: a ten years series. In *Proceedings of the Seventh International Conference on Permafrost*. Centre d'études Nordiques, Sainte-Foy, pp. 1089-1095.
- Wagner, S. (1992). Creep of Alpine permafrost, investigated on the Murtel rock glacier. *Permafrost and Periglacial Processes*, **3**, 157-162.
- Wahrhaftig, C. and Cox, A. (1959). Rock glaciers in the Alaska Range. *Bulletin of*

the Geological Society of America, **70**, 383-436.

Washburn, A. L. (1979). *Geocryology: a survey of periglacial processes and environments*. Edward Arnold, London, 406 pp.

Whalley, W. B. (1984). Rockfalls. In Brunsten, D. and Prior, D. B. (eds.), *Slope Instability*. Wiley, Chichester, pp. 217-256.

Whalley, W. B. and Martin, H. E. (1992). Rock glaciers: II models and mechanisms. *Progress in Physical Geography*, **16**, 127-186.



Figure 1 Typical rock glaciers in the Upper Engadin, Swiss Alps. (a) Murtèl I rock glacier having well-developed ridges and furrows. The steep frontal slope is about 20 m high. (b) Muragl I rock glacier developing from a small cirque. The rock glacier is 800 m long along the flow line.

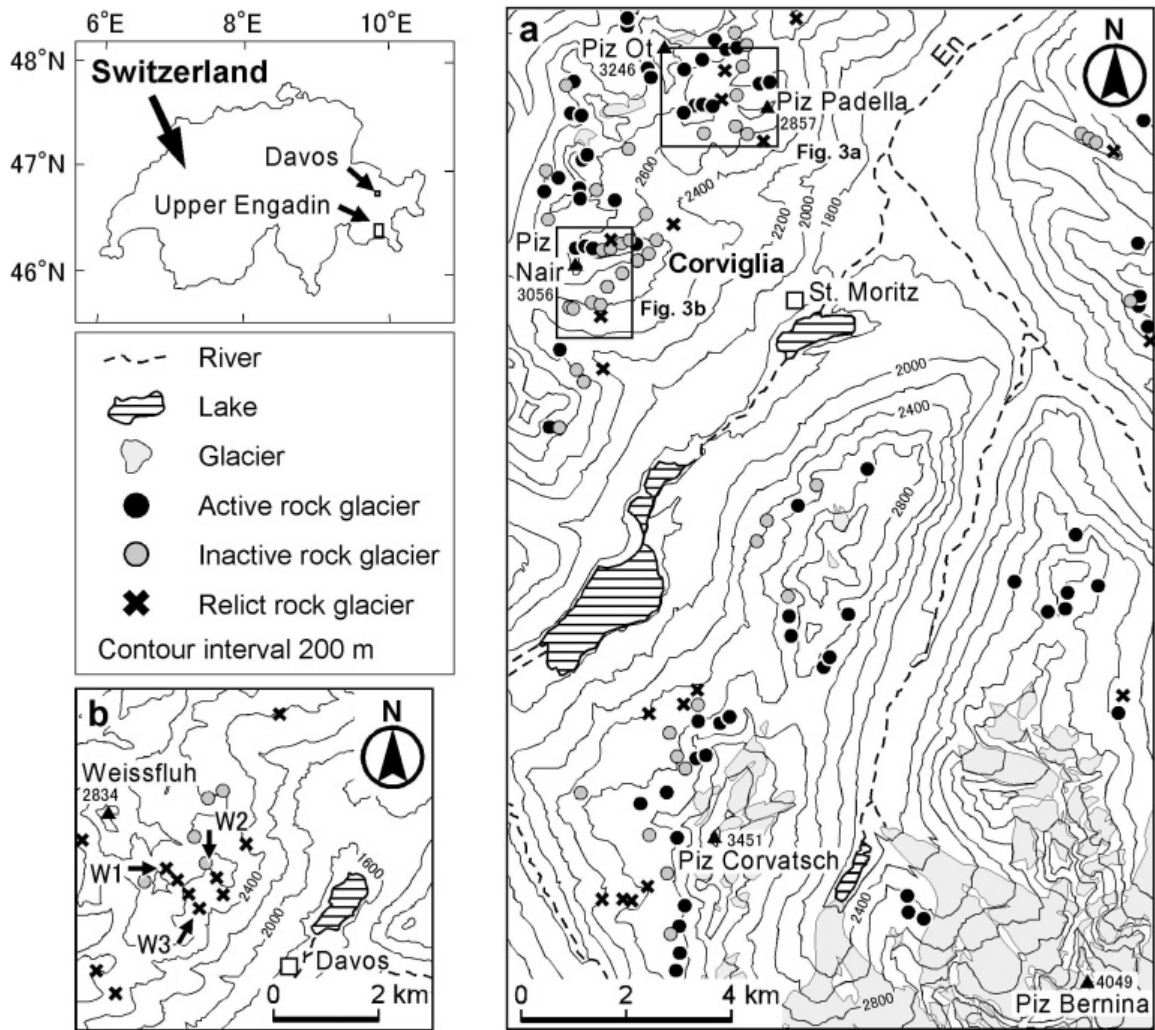


Figure 2 Location of the study areas, shown with distribution of rock glaciers. (a) Upper Engadin. (b) Davos.

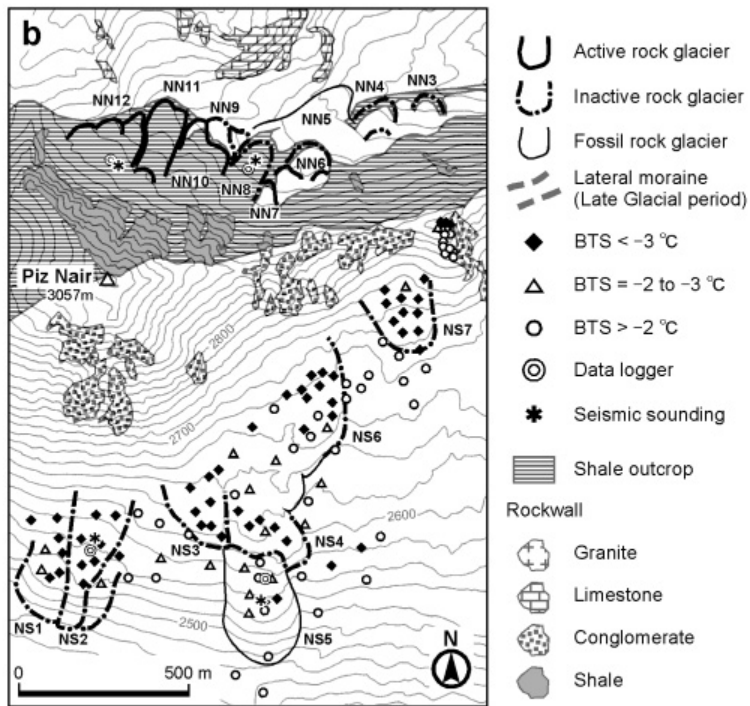
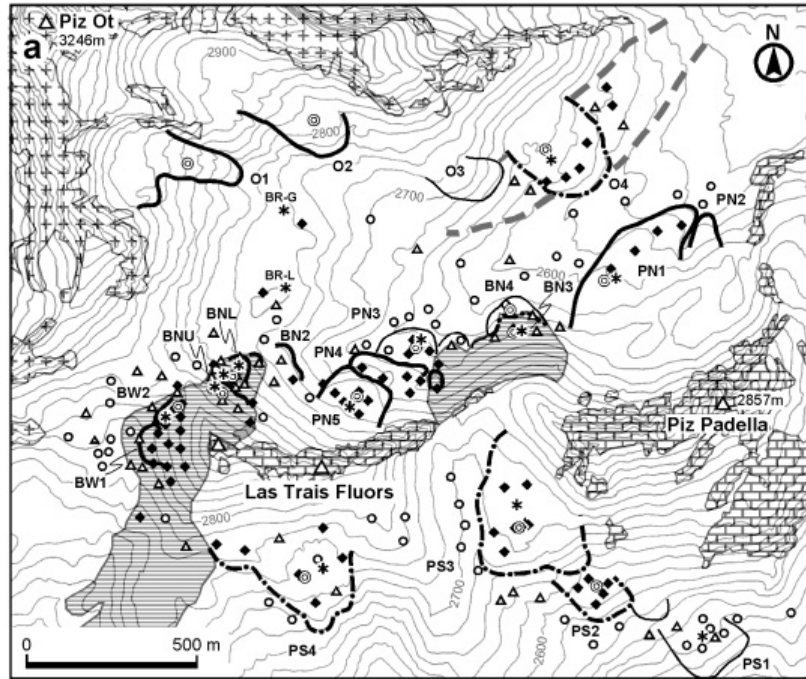


Figure 3 Distribution of rock glaciers in the Corviglia region. (a) Northern area. (b) Southern area. Contour interval 20 m.

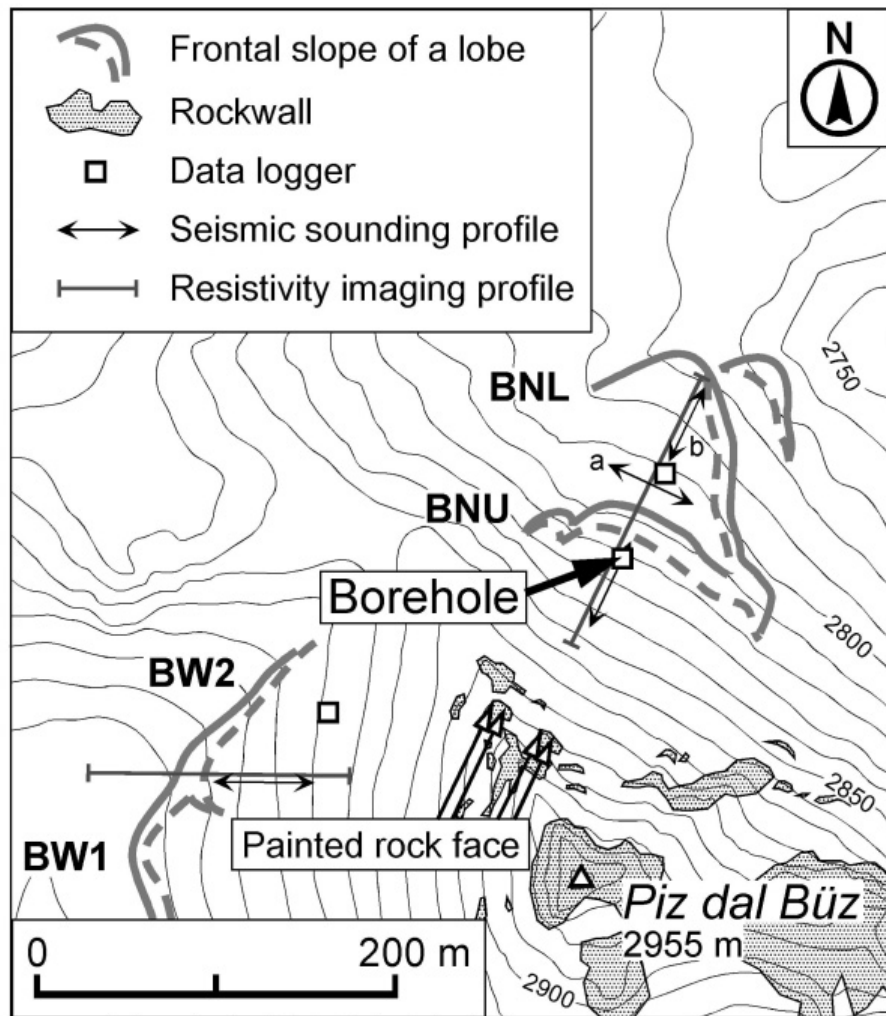


Figure 4 Contour map of Büz rock glaciers. Contour interval 10 m.

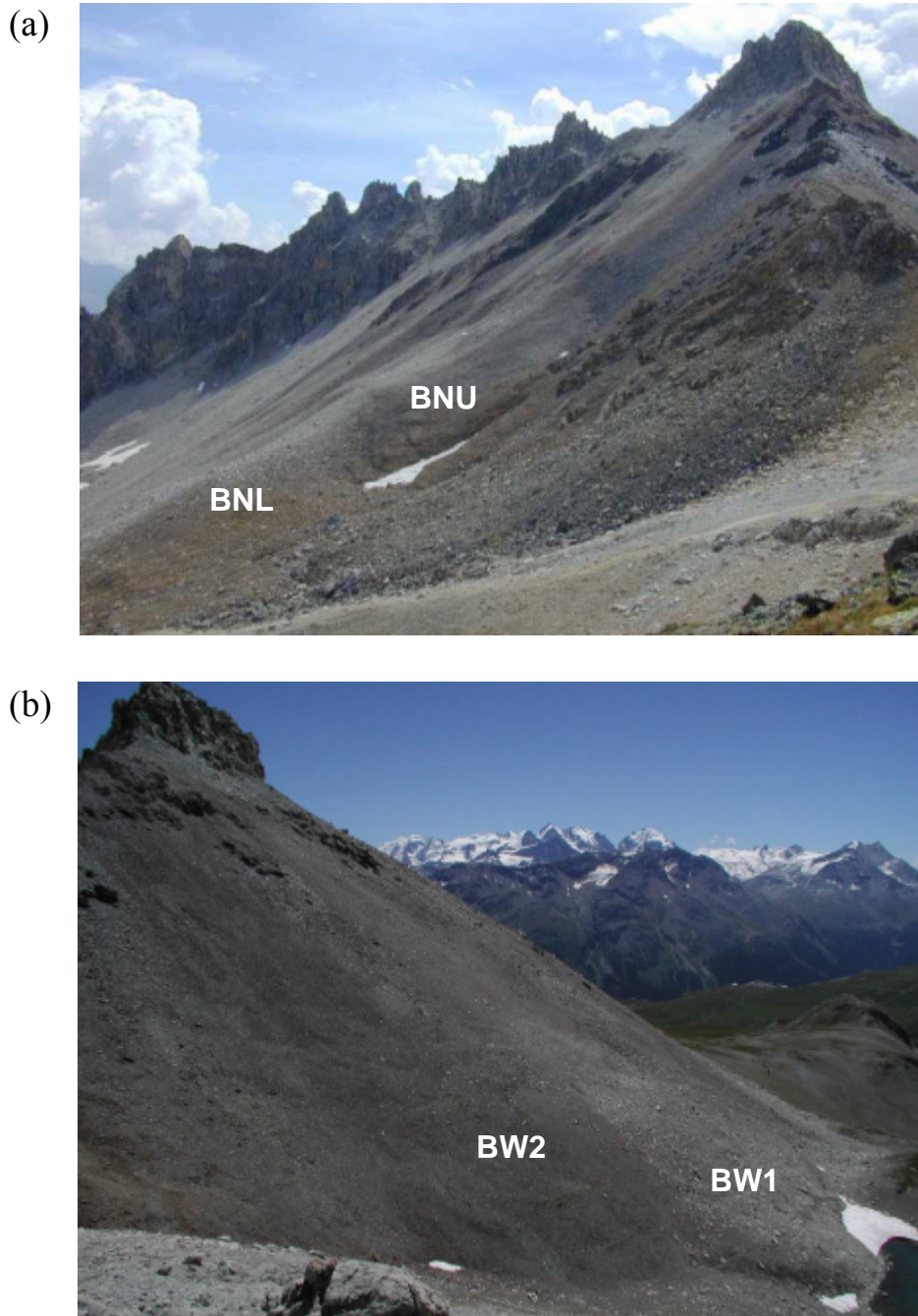


Figure 5 Büz rock glaciers. (a) BN rock glacier consists of an upper lobe (BNU) and lower lobe (BNL), developing on the northern slope of Piz dal Büz. The surface clasts are mainly shale pebbles and cobbles. (b) BW rock glacier consists of adjacent two lobes: BW1 (shale and massive limestone) and BW2 (shale), developing on the western slope of Piz dal Büz.



Figure 6 Bouldery and pebbly rock glaciers. (a) Upper surface of Murtèl I bouldery rock glacier, covered with large gneiss and schist boulders. (b) Pebbly rock glaciers NN10, NN11 and NN12, consisting of shale pebbles and cobbles, developed on the northern slope of Piz Nair.

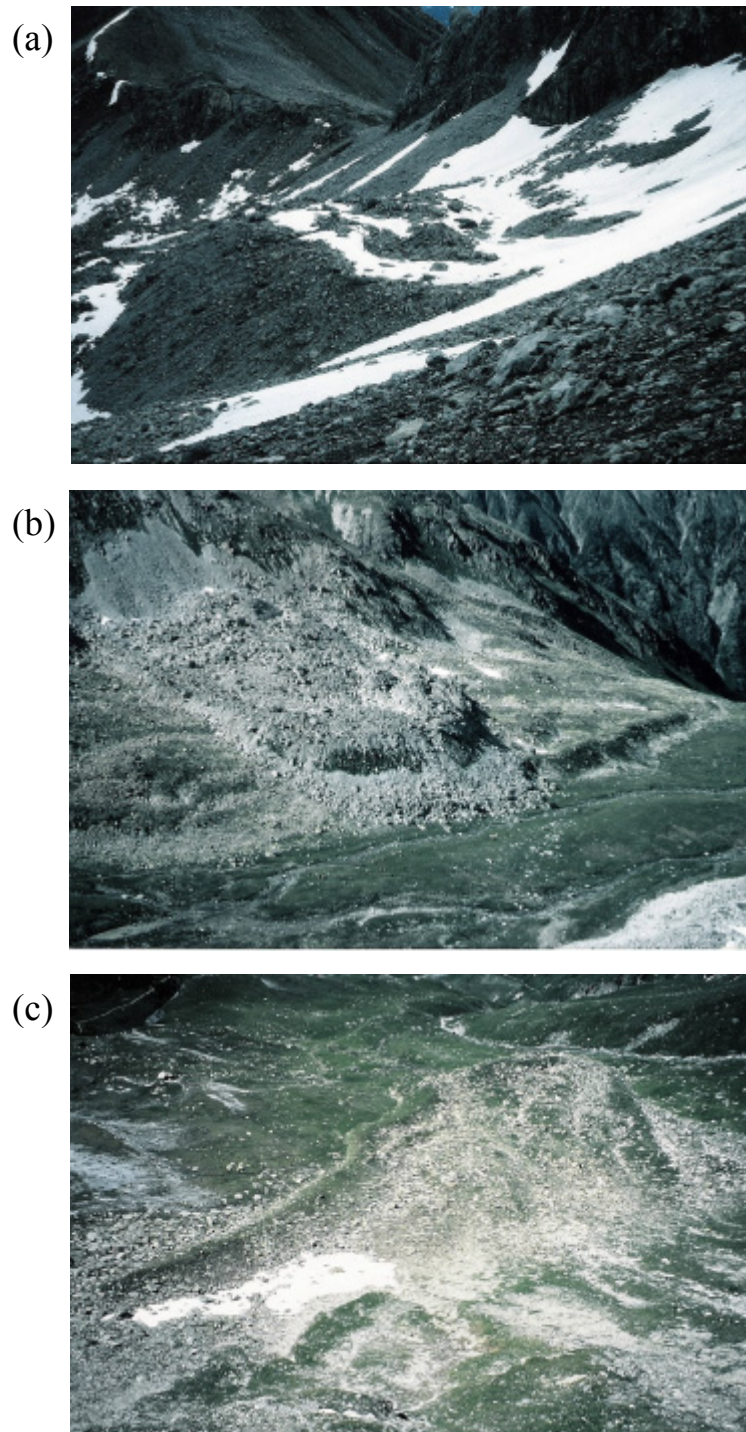


Figure 7 Active, inactive and relict rock glaciers. (a) Active rock glacier PN5, showing a convex-up transverse profile. (b) Inactive rock glacier O4. Vegetation and boulder apron at the frontal slope imply the stationary front. (c) Relict rock glacier C1, showing a large depression fringed by the highest outer ridge.

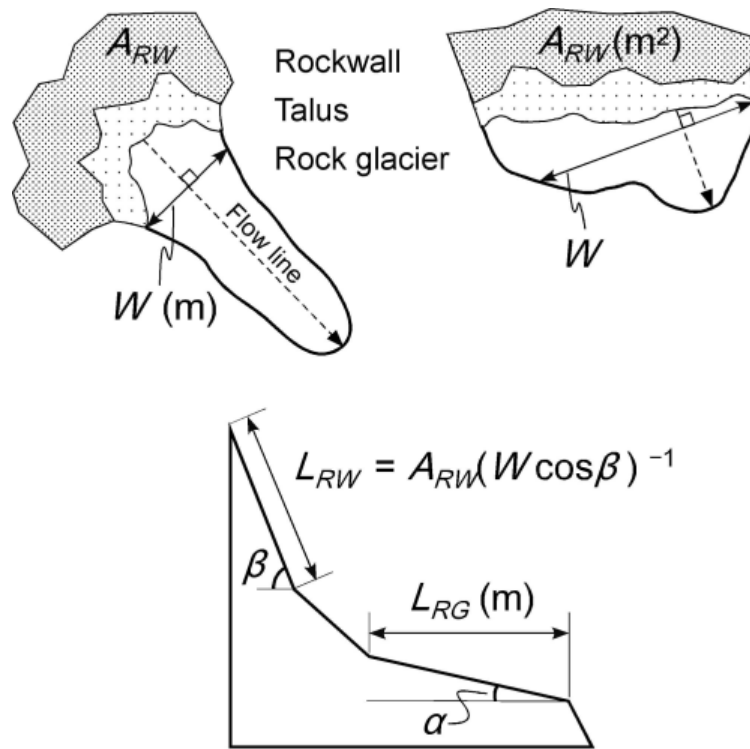


Figure 8 Definition of morphological parameters discussed in the text.

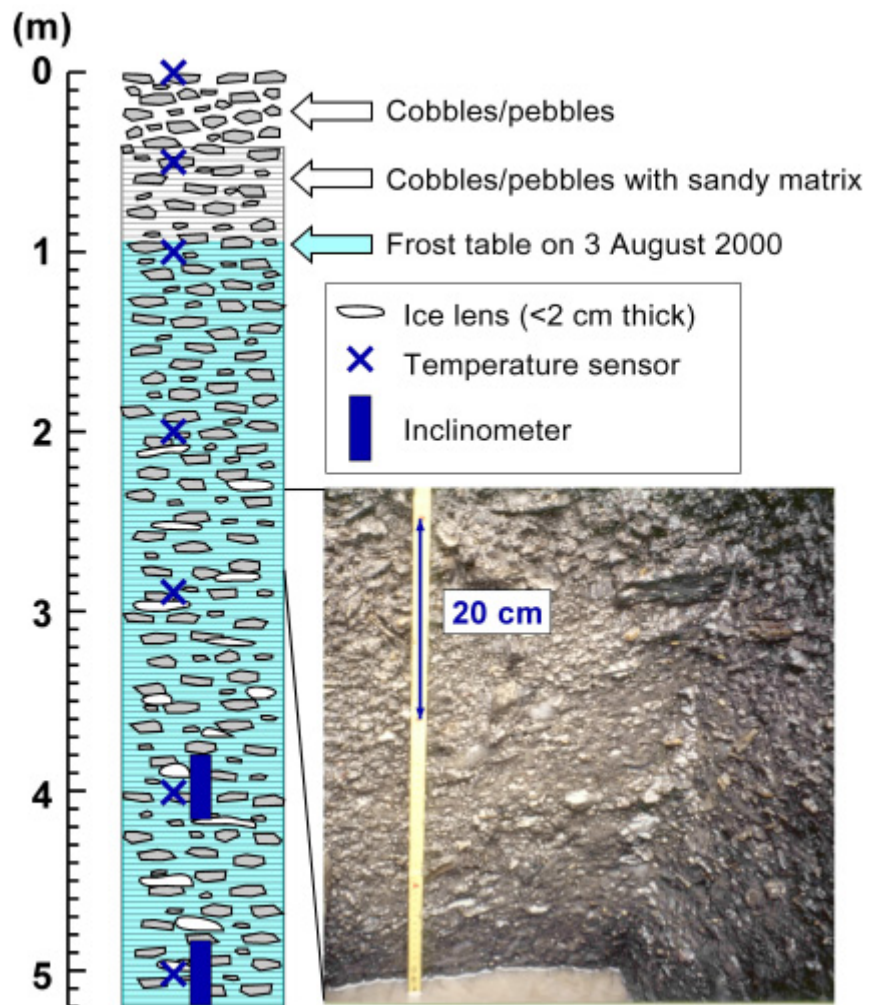


Figure 9 Borehole stratigraphy of the upper lobe of BN rock glacier (BNU).

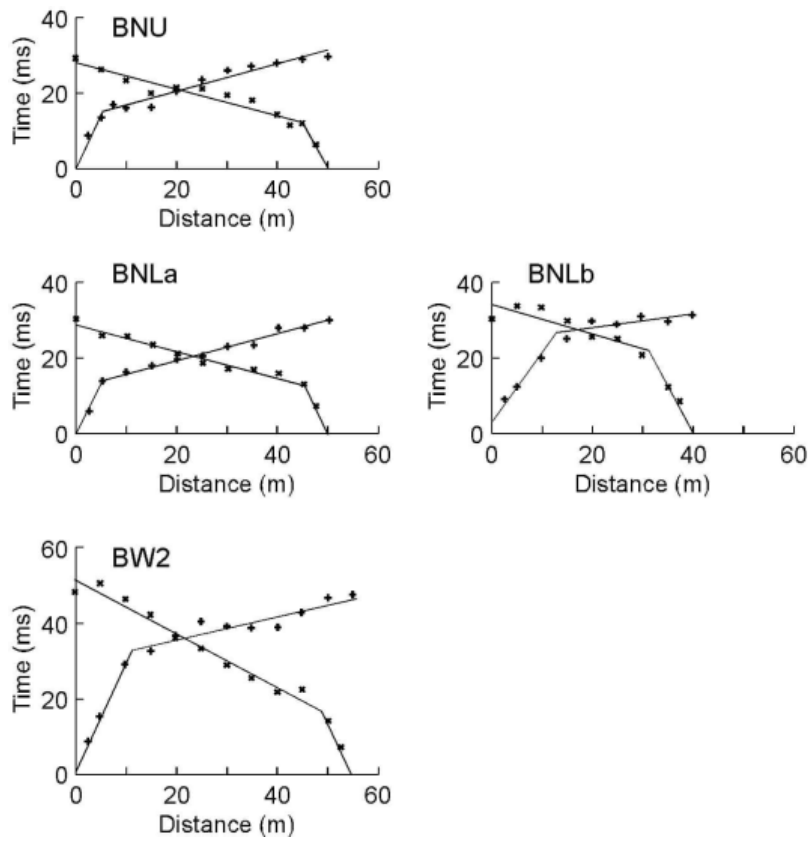


Figure 10 Travel time curves of P-wave velocities for Büz rock glaciers.

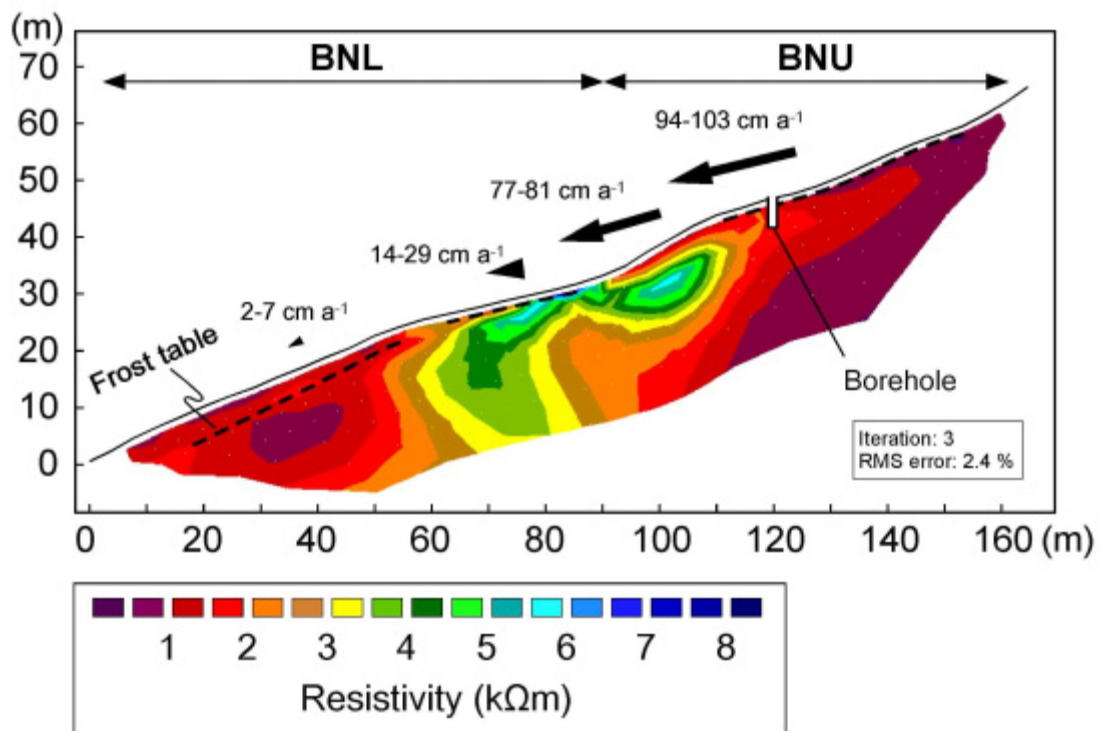


Figure 11 Electrical DC resistivity tomogram of BN rock glacier. The position of the frost table was estimated by means of seismic soundings. The average surface velocities for 1998–2003 are also displayed.

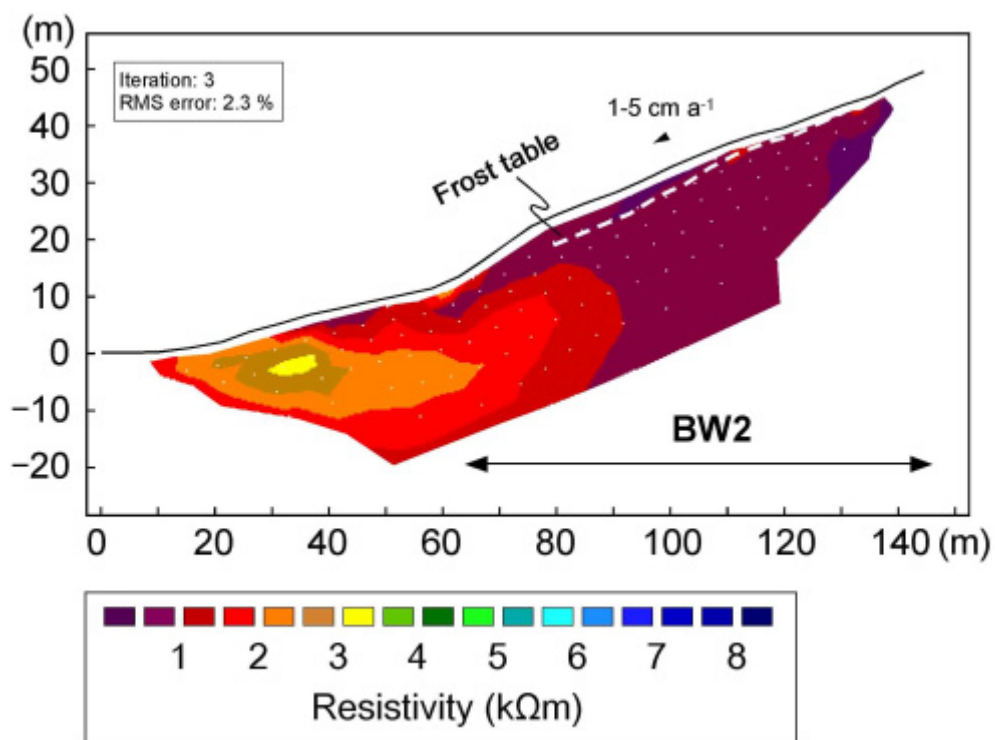


Figure. 12 Electrical DC resistivity tomogram of BW2 rock glacier. The position of the frost table was estimated by means of seismic soundings. The average surface velocities for 1998–2003 are also displayed.

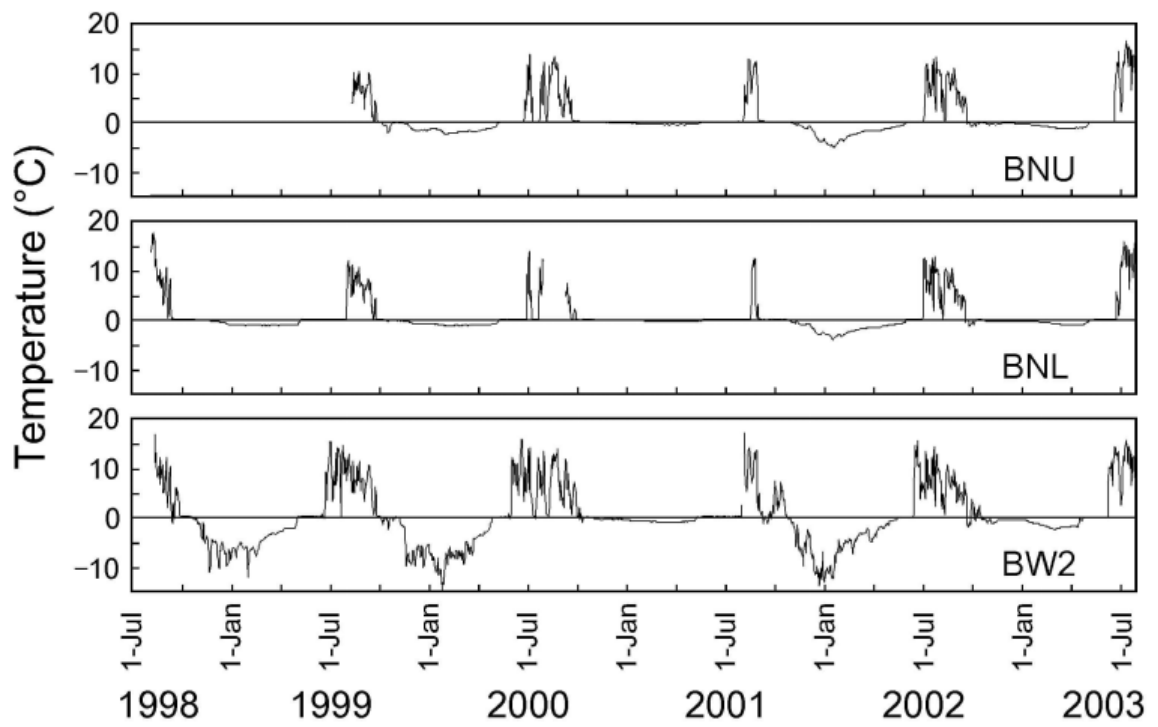


Figure 13 Five years of ground surface temperatures on BNU, BNL and BW2 rock glaciers.

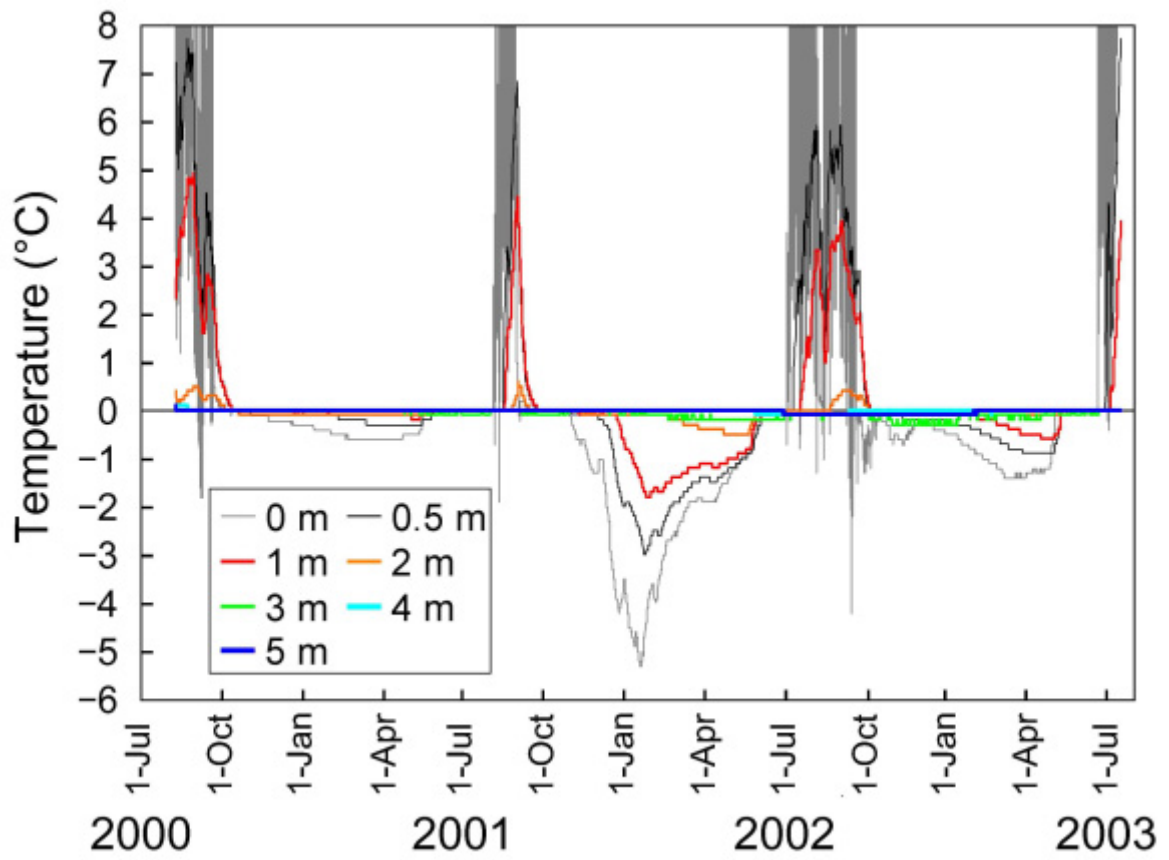


Figure 14 Three years of ground temperatures on BNU.

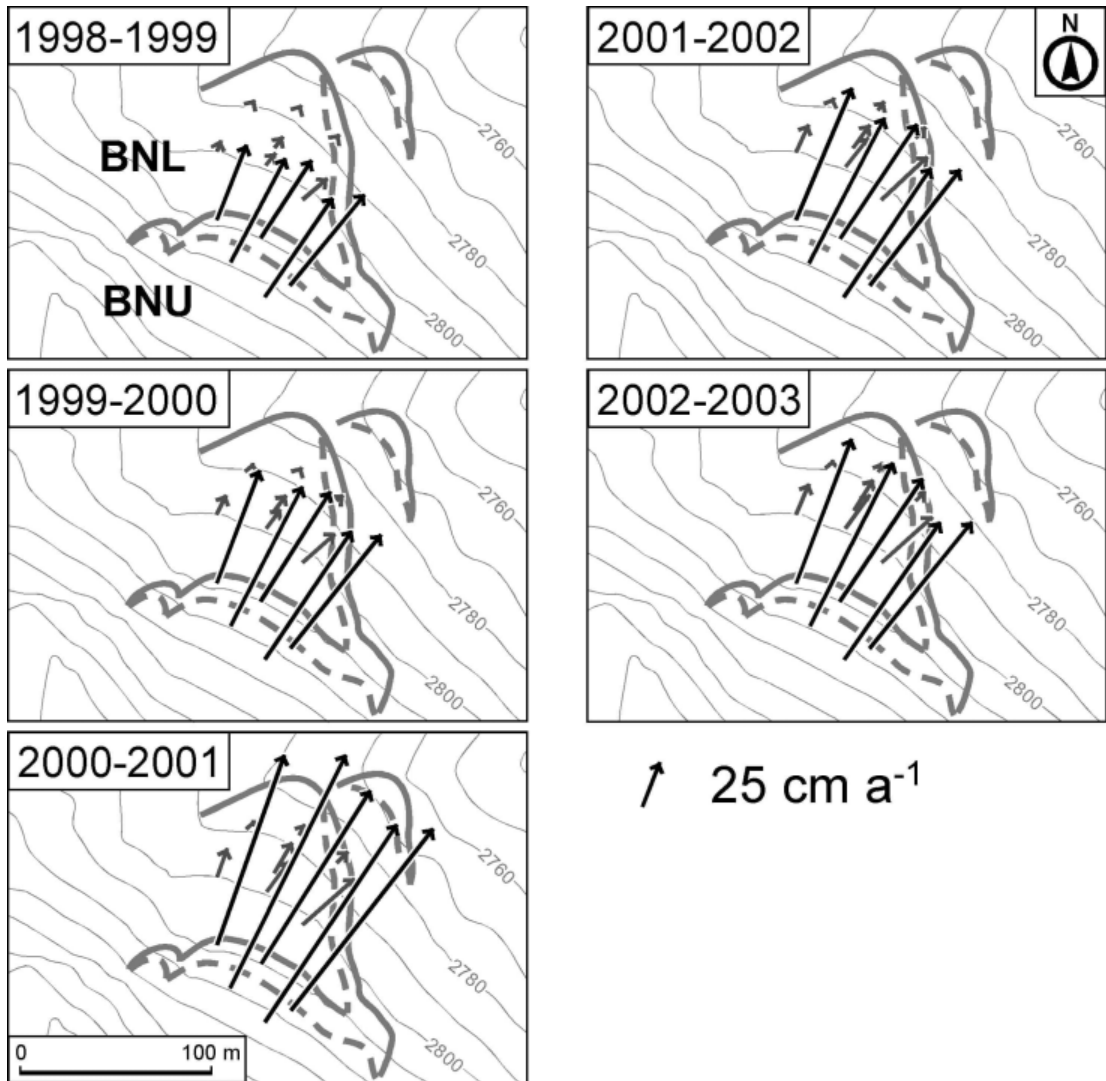


Figure 15 Annual horizontal displacements of boulders on BN rock glacier in 1998–2003.

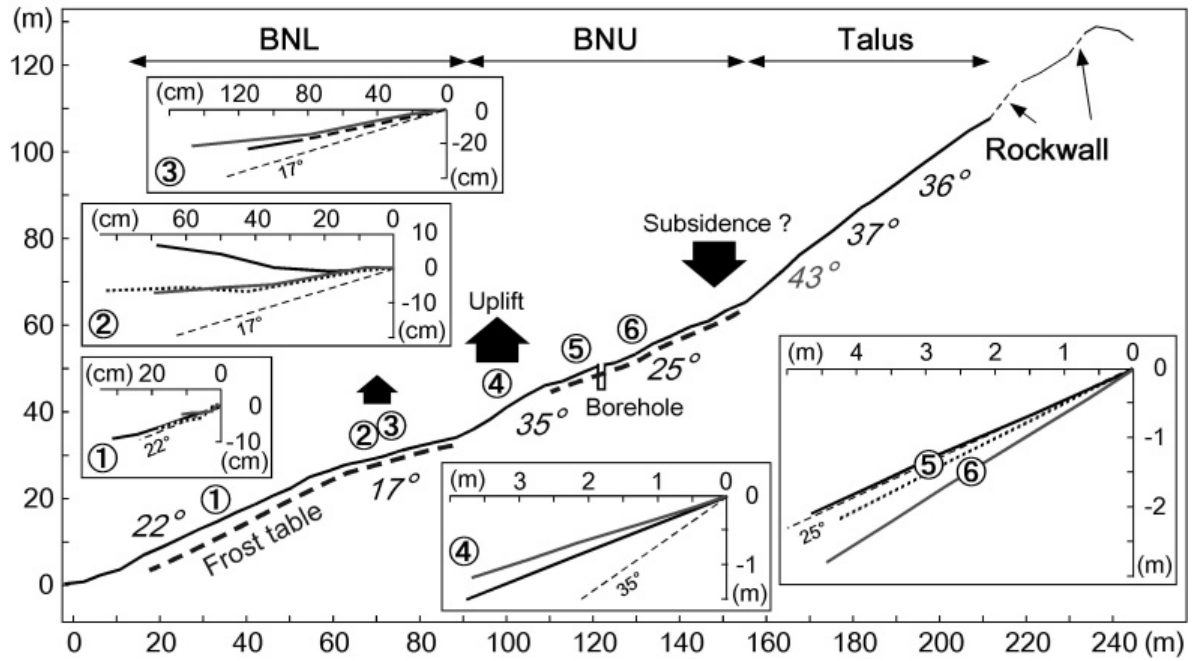


Figure 16 Longitudinal profile of BN rock glacier and talus slope with slope angles in italics. Insets display vertical and horizontal displacements of the marker boulders for five years.



Figure 17 Small ridges (c. 30 cm high) just below the western margin of BNU, indicated by dotted lines.

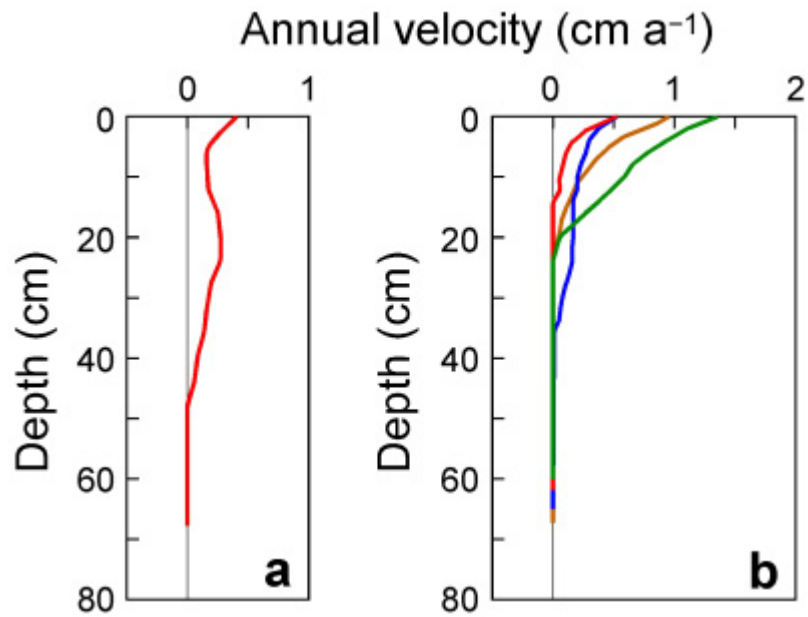


Figure 18 Annual vertical velocity profiles of solifluction movement in BNL and BW2 rock glaciers, measured with flexible probes. (a) A profile in BNL based on the movement for 5 years (1998–2003). (b) Four profiles in BW2 based on the movement for 4 years (1998–2002). The depth is measured perpendicular to the upper surface.

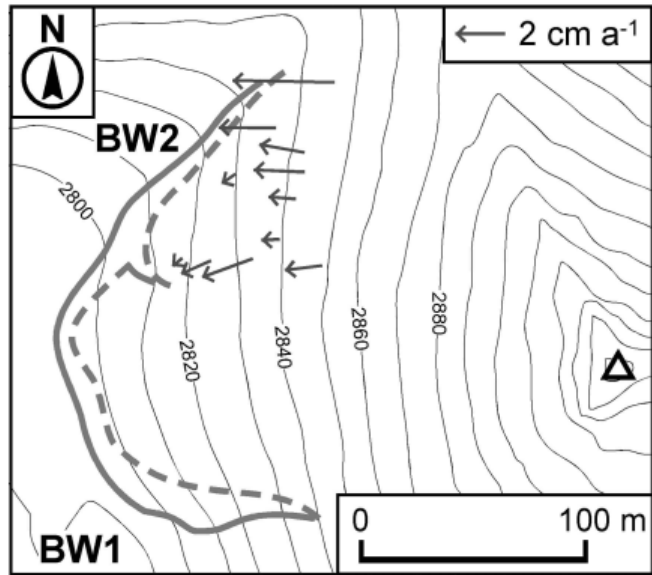


Figure 19 Average annual horizontal displacement of boulders on BW2 rock glacier for five years (1998–2003).

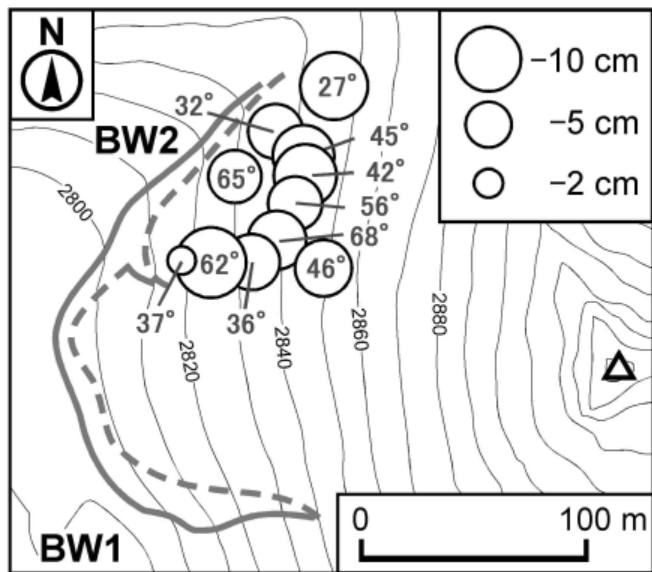


Figure 20 Vertical displacement and downslope dip of displacement vectors on BW2 rock glacier for five years (1998–2003).

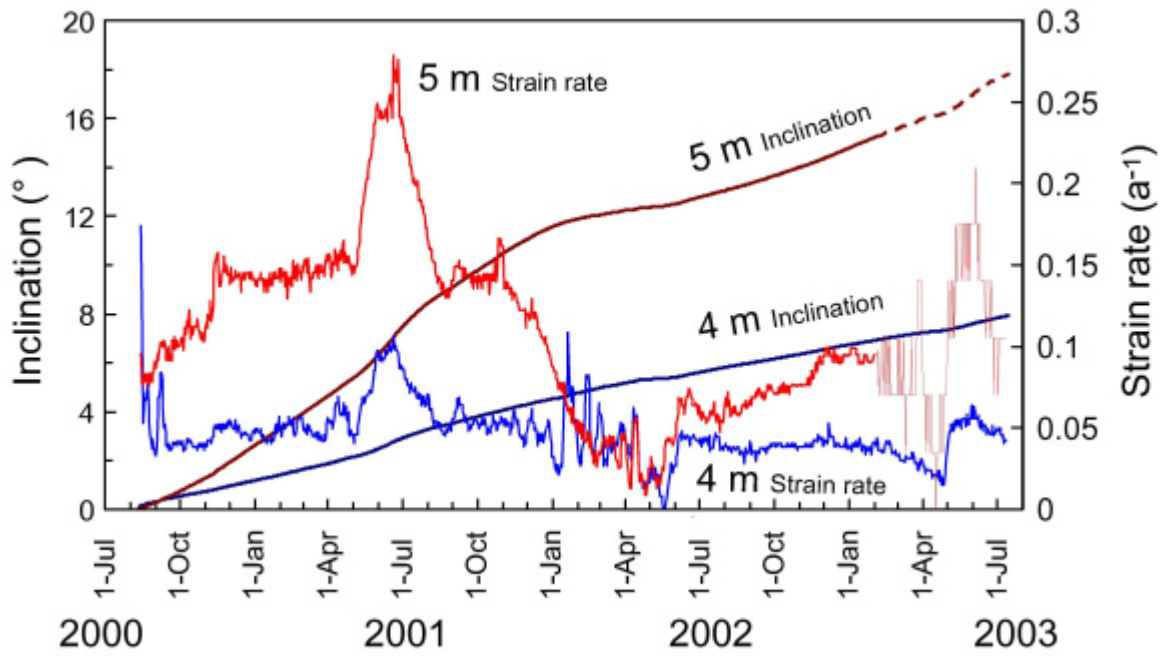


Figure 21 Three years of internal deformation in BNU rock glacier, shown by changes in inclination and calculated strain rates.

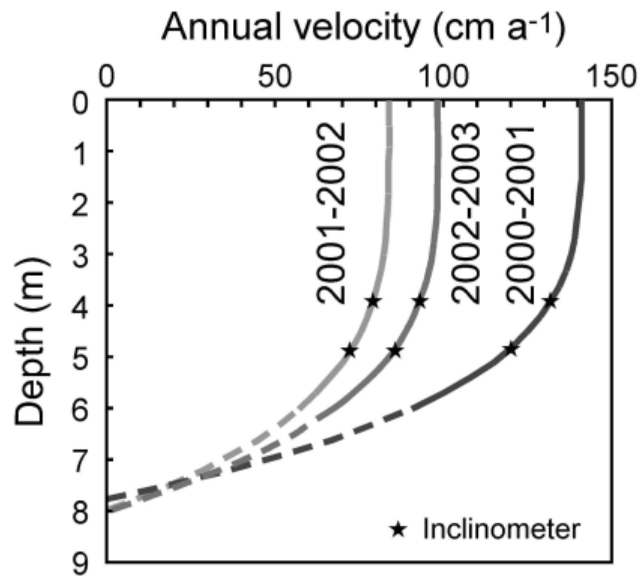


Figure 22 Annual vertical velocity profiles estimated from the observed inclinations at 4 and 5 m depths in BNU rock glacier over three years. The depth is measured perpendicular to the upper surface (25°).

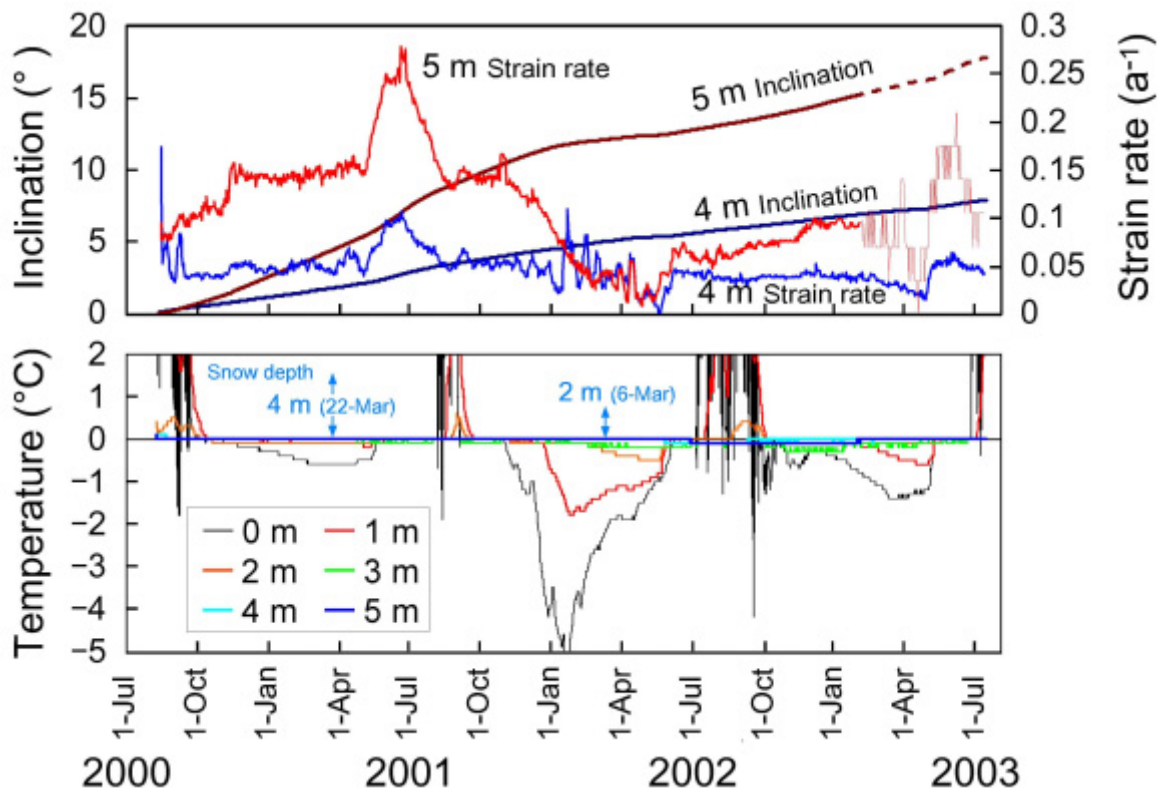


Figure 23 Three years of internal deformation (upper) and ground temperatures (lower) of BNU rock glacier. The blue numbers indicate the snow depth at the manual measurements of BTS.

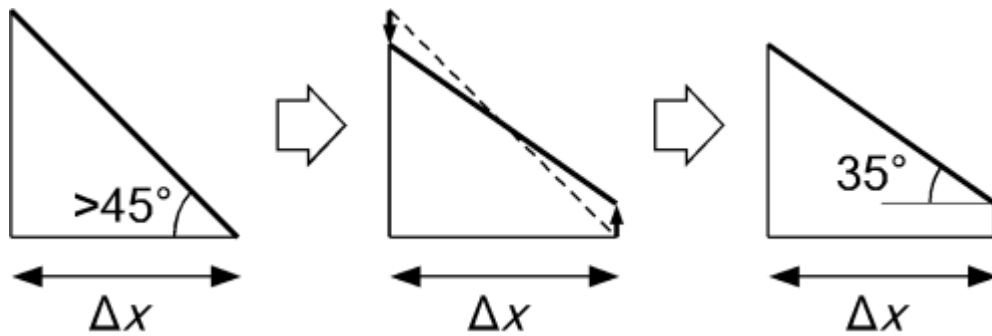


Figure 24 Simulated change in the longitudinal profile of a talus slope. The slope is assumed to change from the maximum angle of the slope to the angle of repose within a short distance (Δx) without any volume loss in the section.

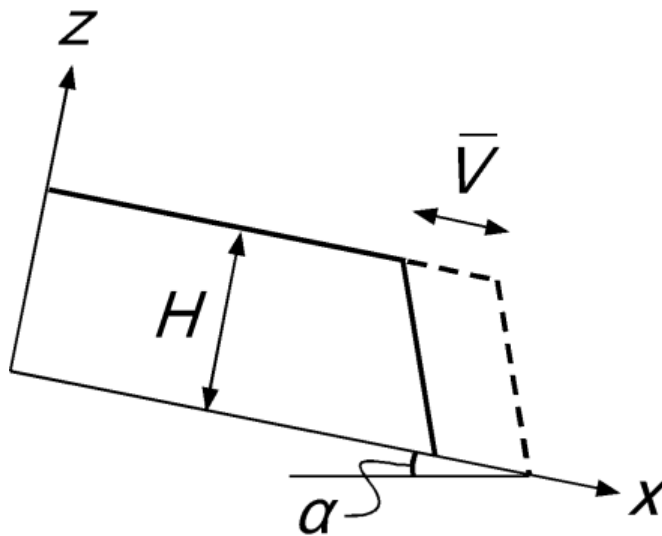


Figure 25 Rock glacier geometry for a numerical simulation discussed in the text. The rock glacier is assumed to move by laminar flow down a semi-infinite plane inclined at angle α to the horizontal (after Olyphant, 1983).

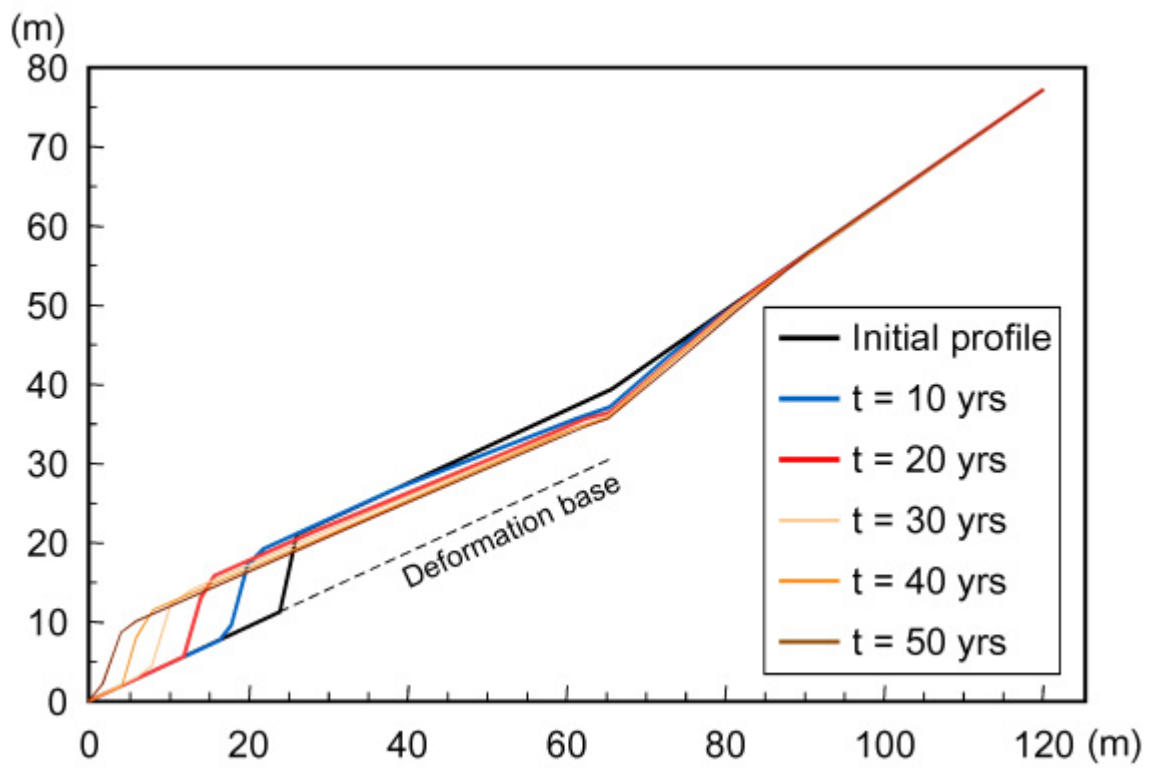


Figure 26 Simulated deformation of BNU rock glacier.

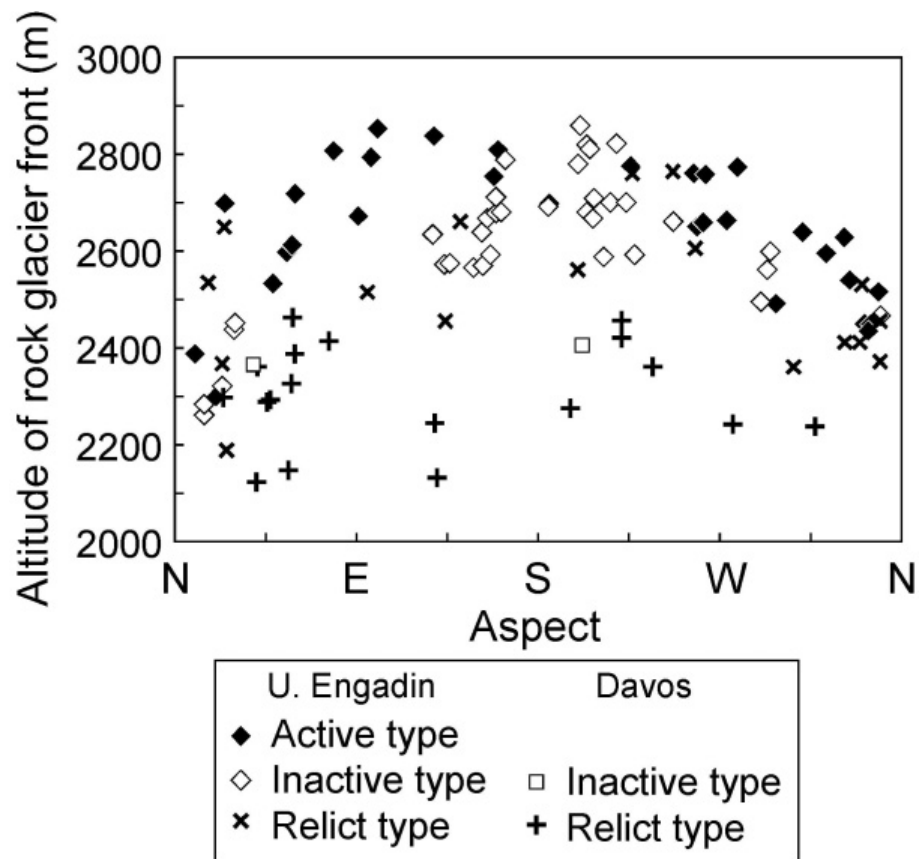


Figure 27 The effect of slope aspect on the altitudinal distribution of the terminus of rock glaciers in the Upper Engadin and Davos.

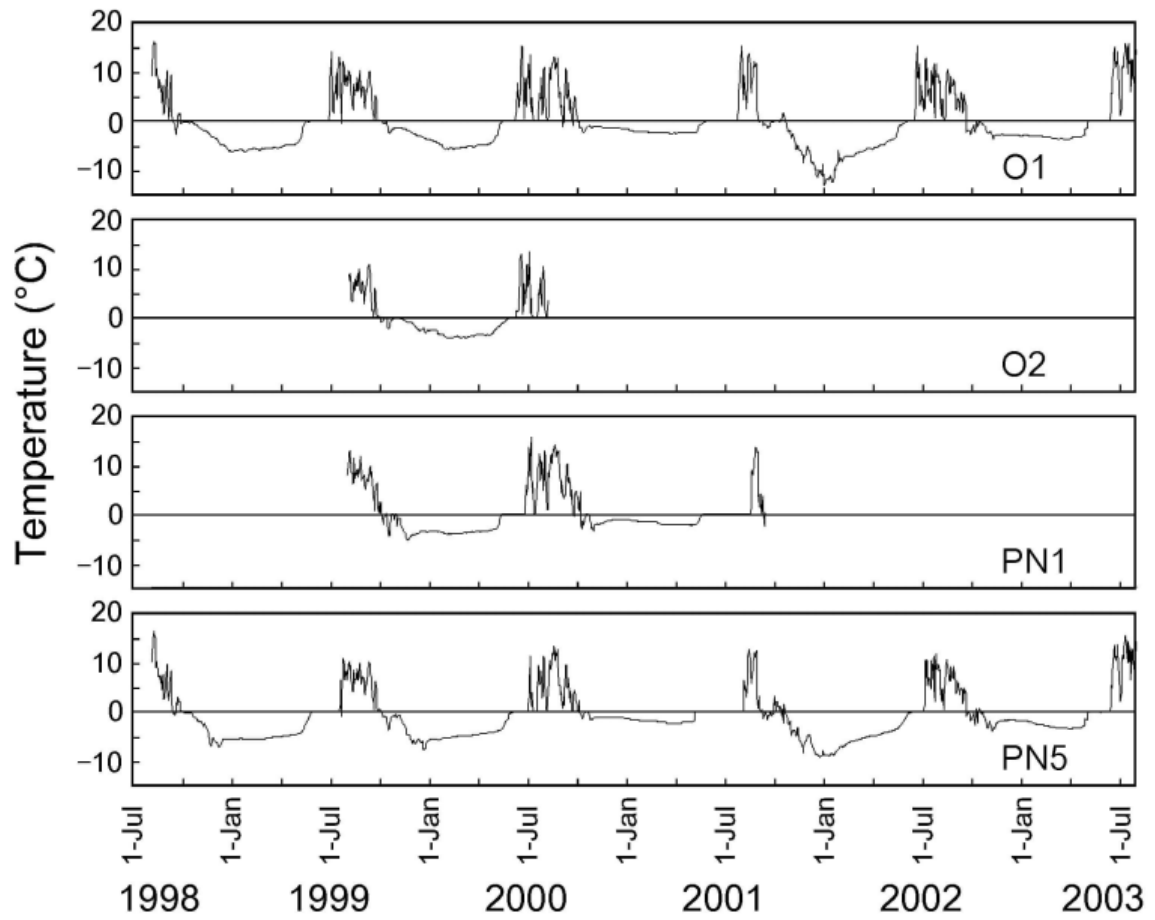


Figure 28 Five years of ground surface temperatures on active bouldery rock glaciers.

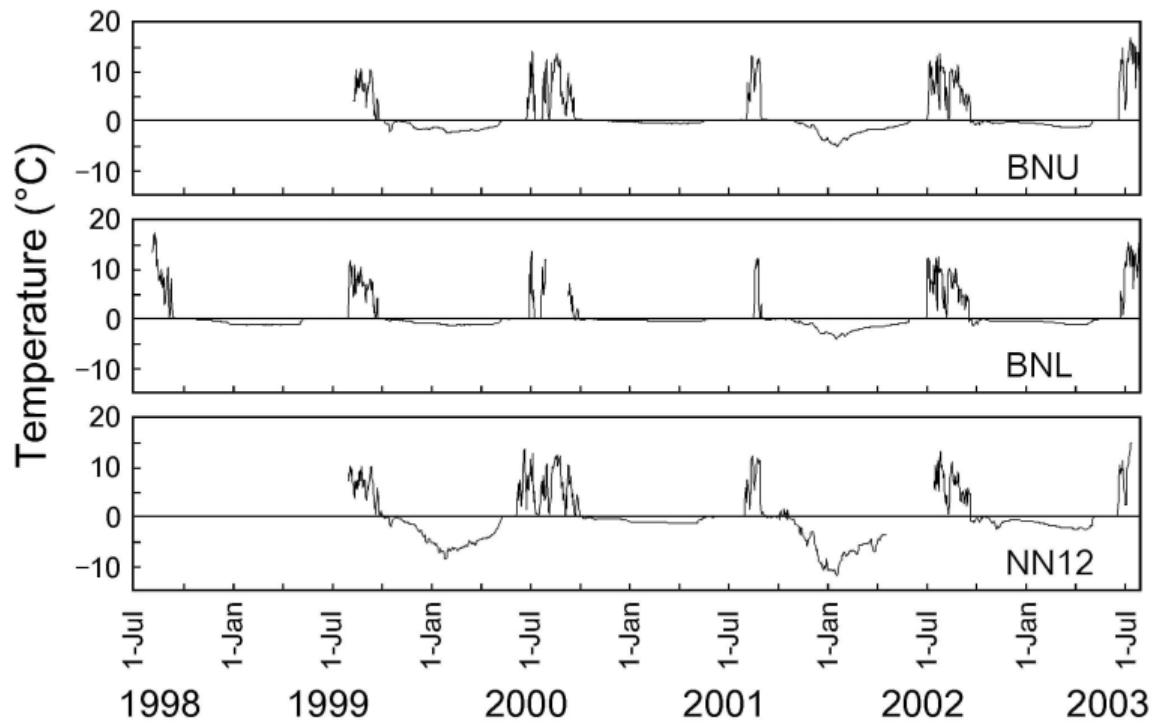


Figure 29 Five years of ground surface temperatures on active pebbly rock glaciers.

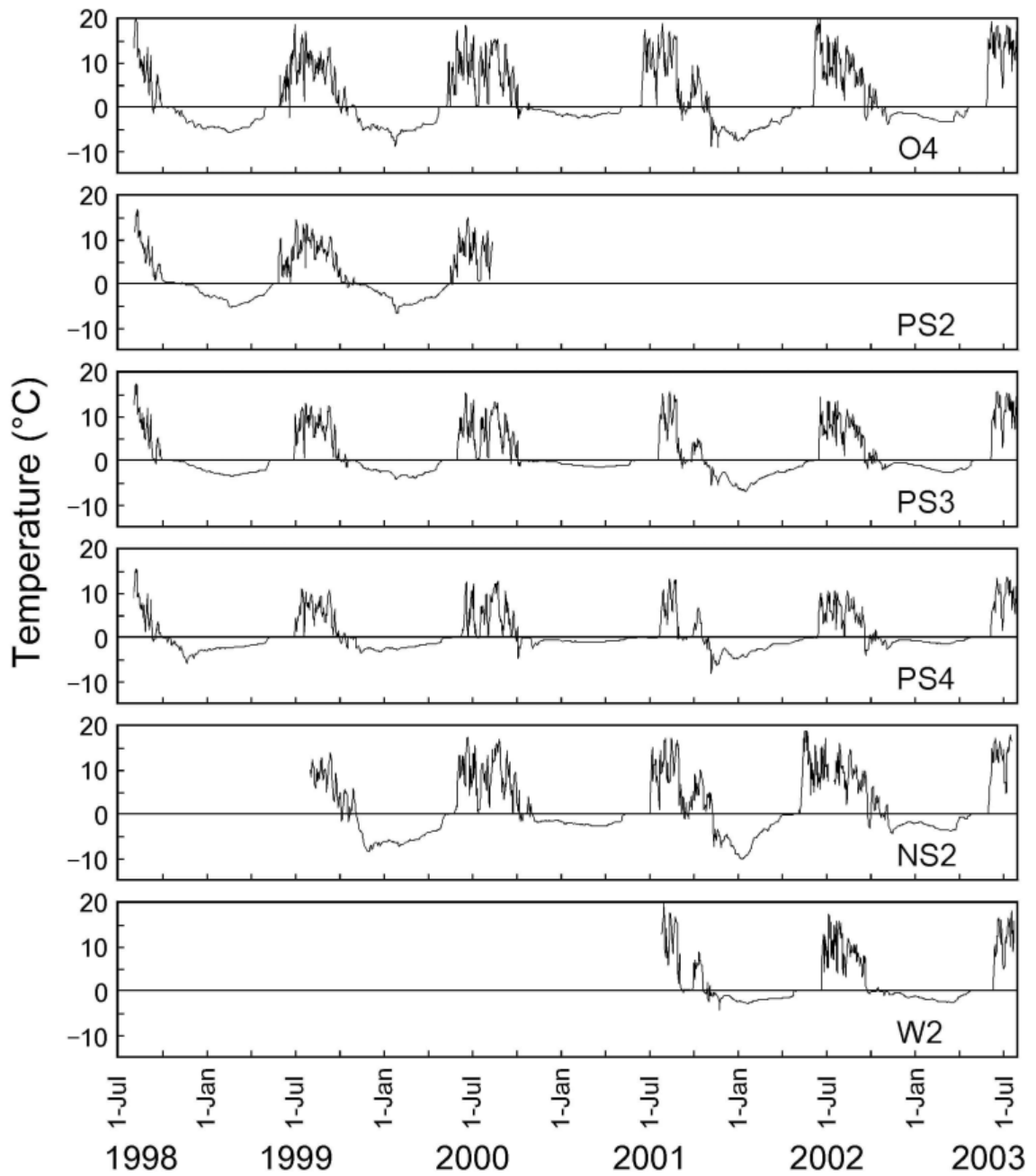


Figure 30 Five years of ground surface temperatures on inactive bouldery rock glaciers.

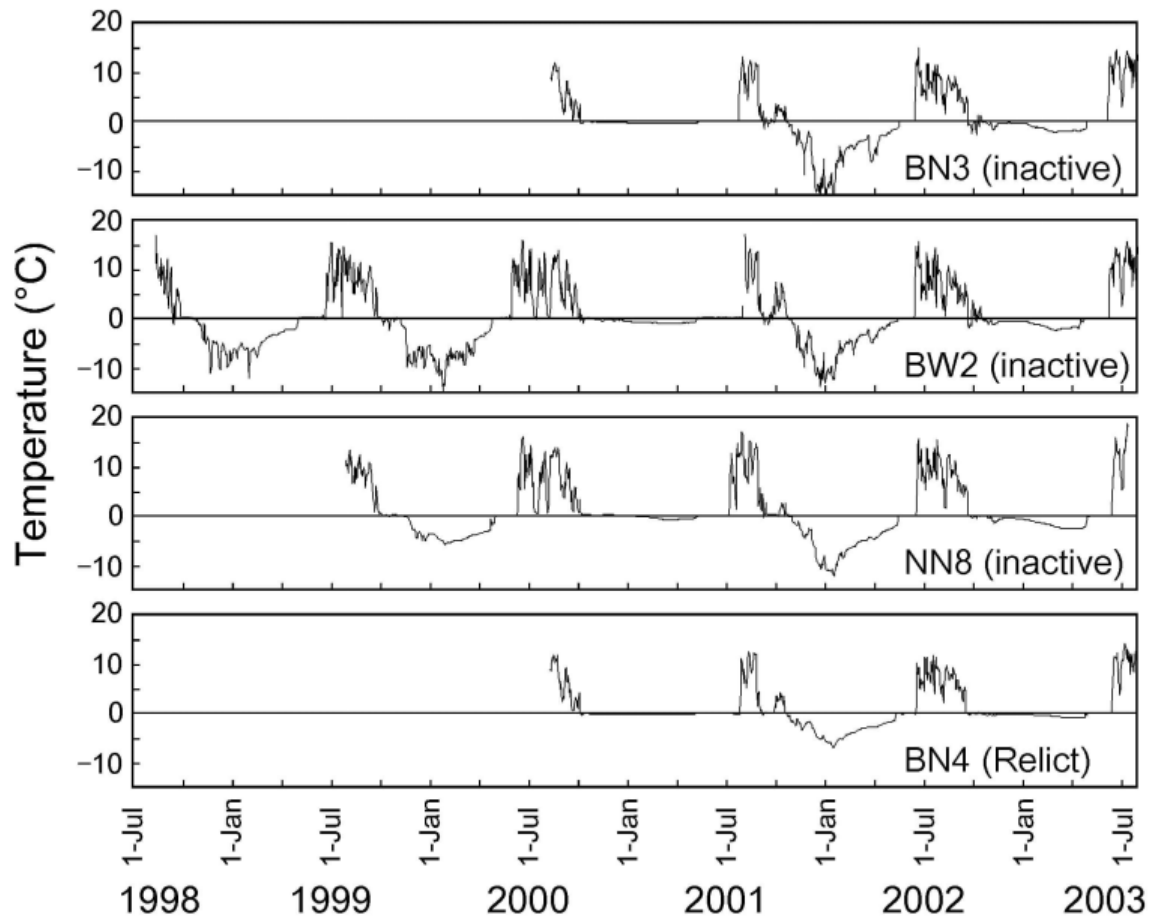


Figure 31 Five years of ground surface temperatures on inactive and possibly relict pebbly rock glaciers.

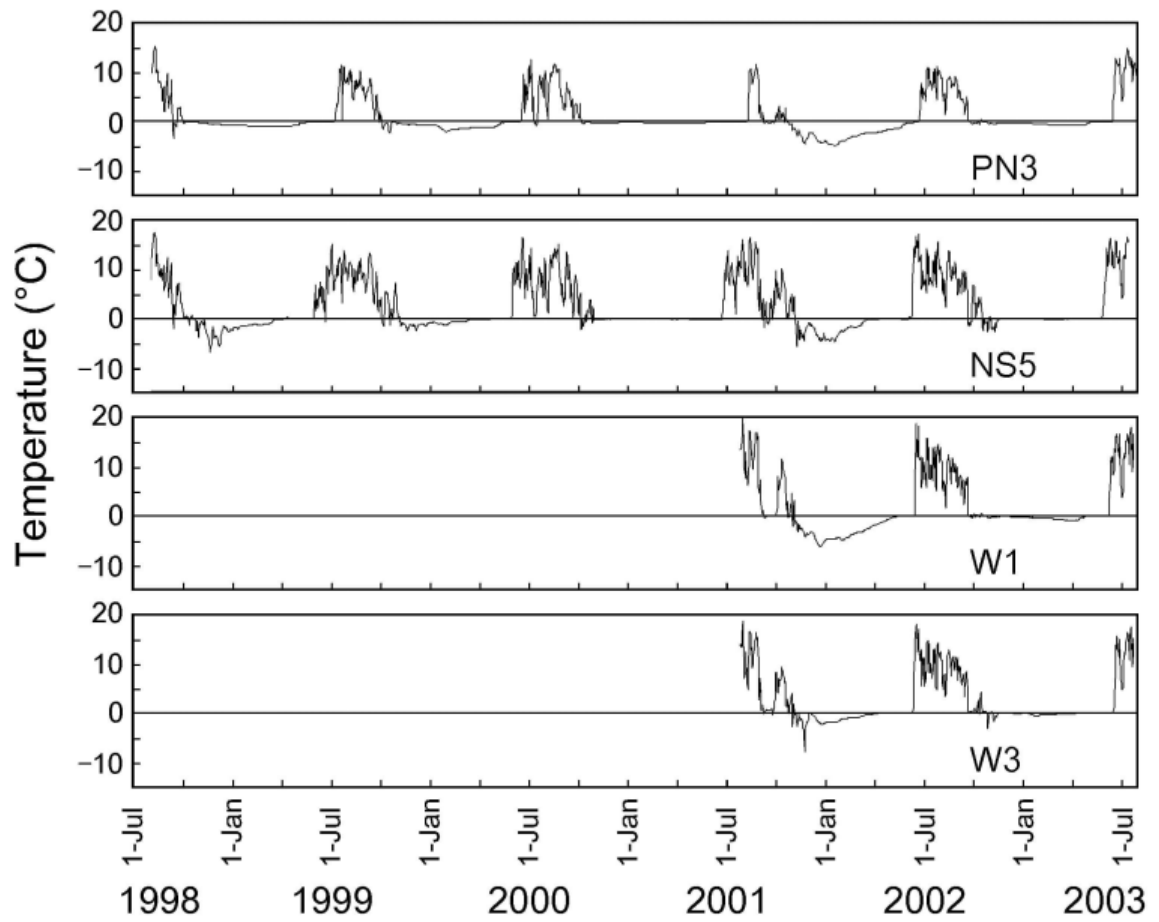


Figure 32 Five years of ground surface temperatures on relict bouldery rock glaciers.

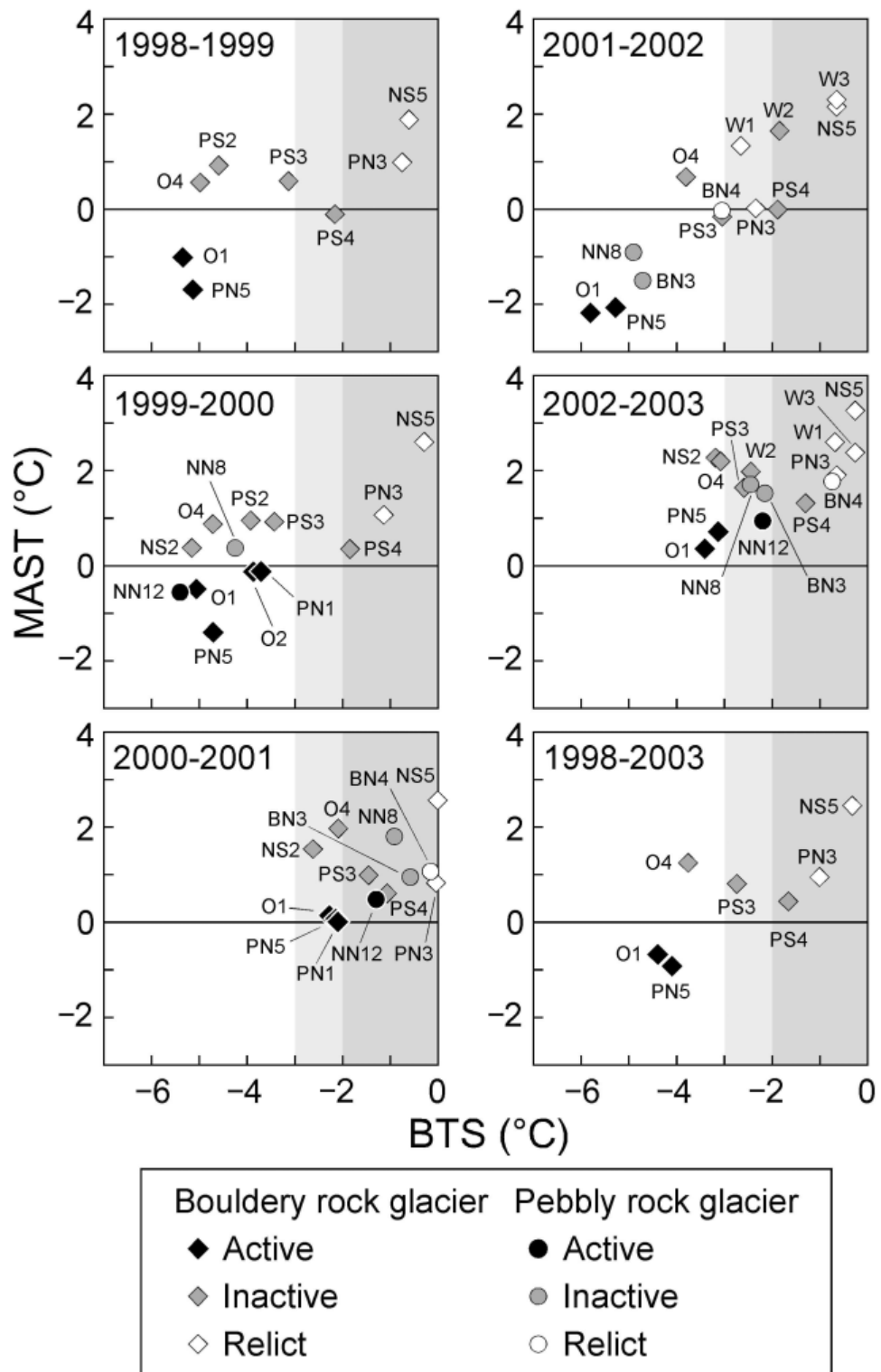


Figure 33 Relationship between bottom temperature of the winter snow cover (BTS) in March and mean annual surface temperature (MAST) over five years.

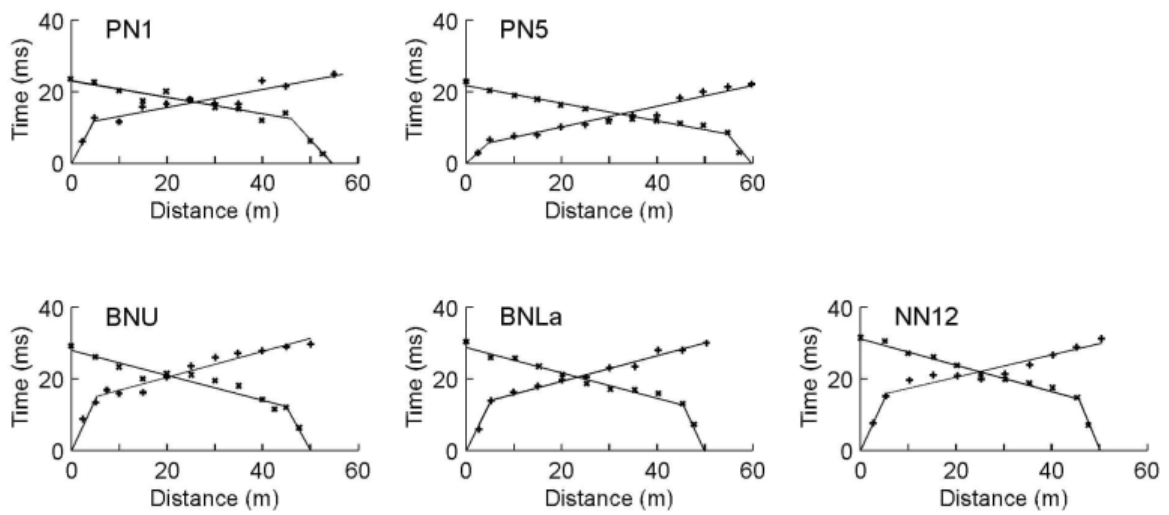


Figure 34 Travel time curves of P-wave velocities for active rock glaciers.

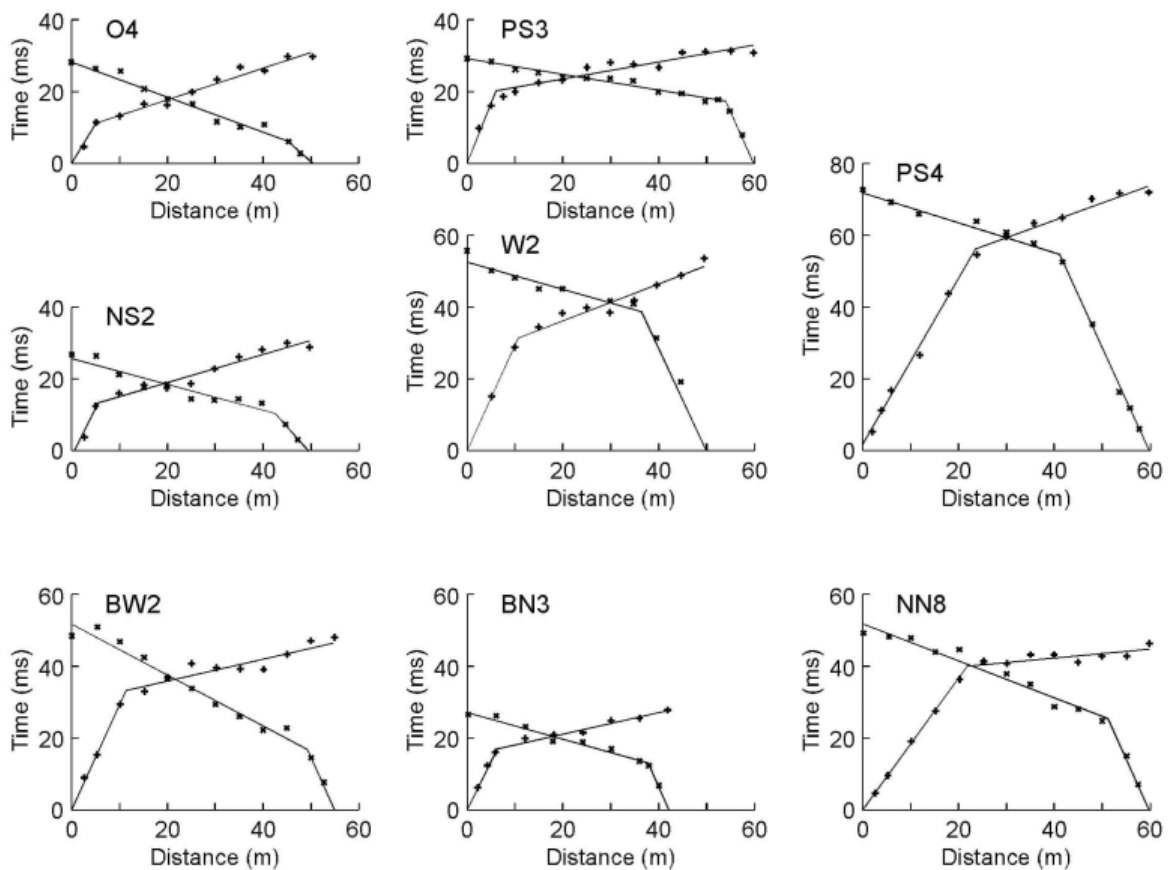


Figure 35 Travel time curves of P-wave velocities for inactive rock glaciers.

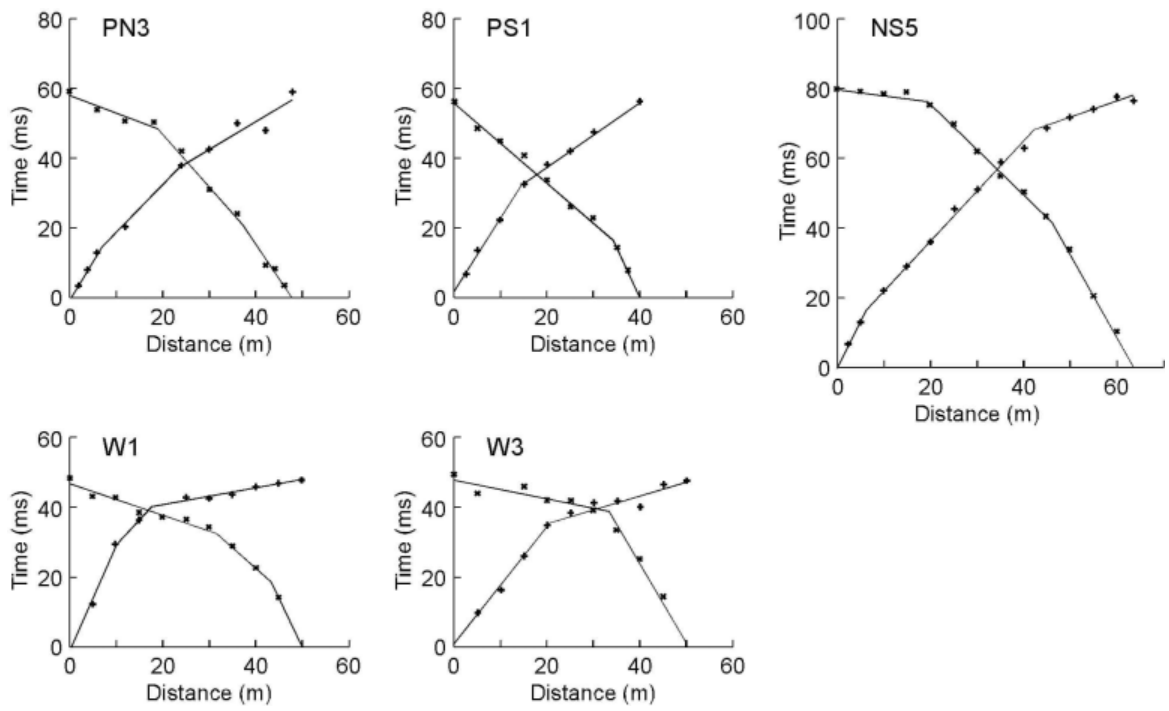


Figure 36 Travel time curves of P-wave velocities for relict rock glaciers.

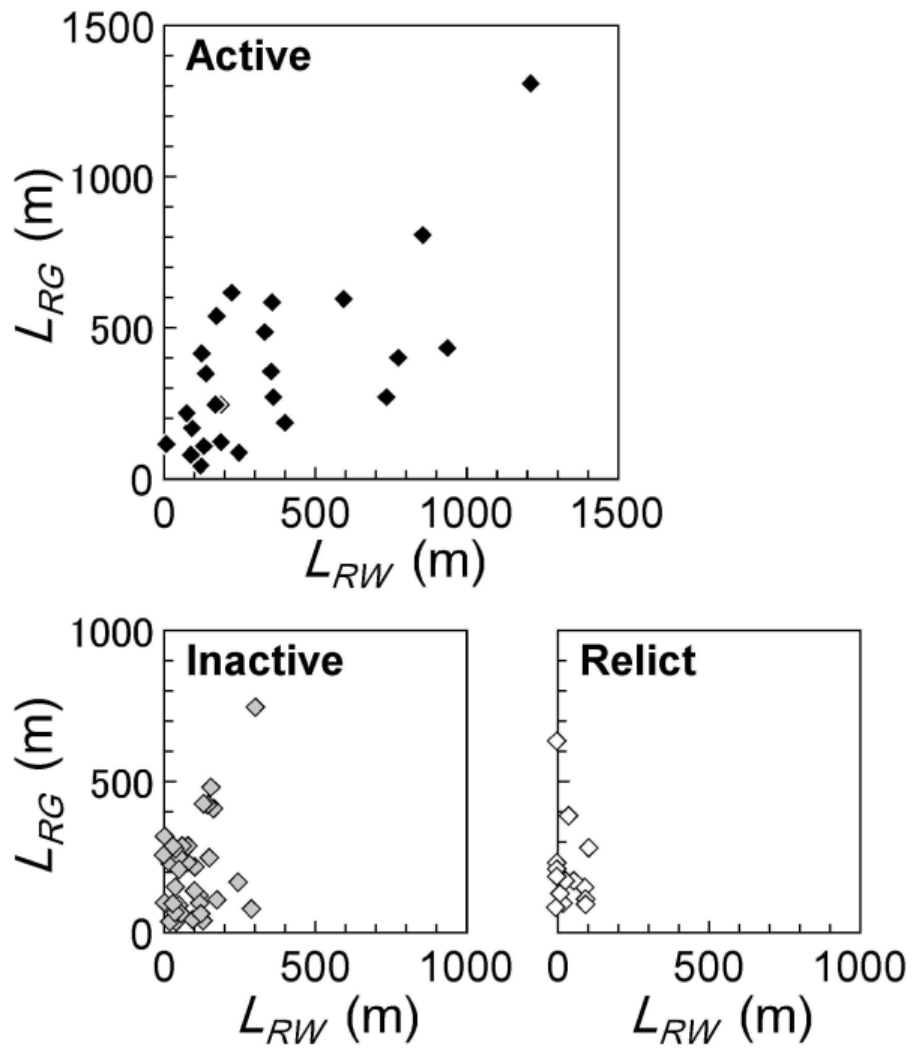


Figure 37 Relationship between the length of bouldery rock glacier (L_{RG}) and the average slope length of the source rockwall (L_{RW}). See Figure 8 for definition.

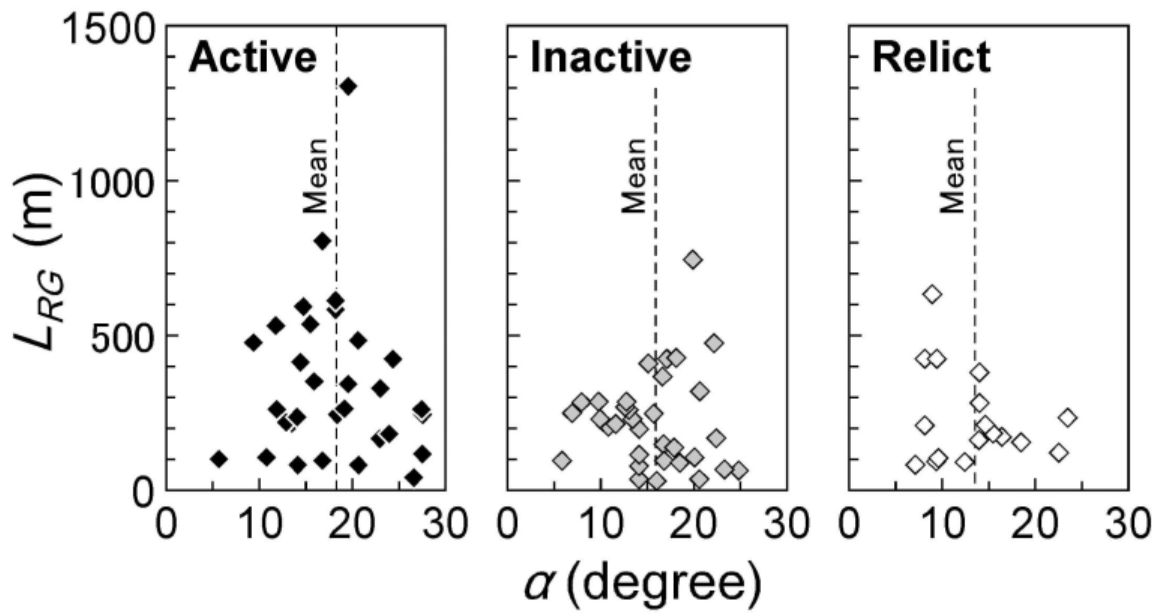


Figure 38 Relationship between the surface angle of rock glacier (α) and the length of bouldery rock glacier (L_{RG}). See Figure 8 for definition.

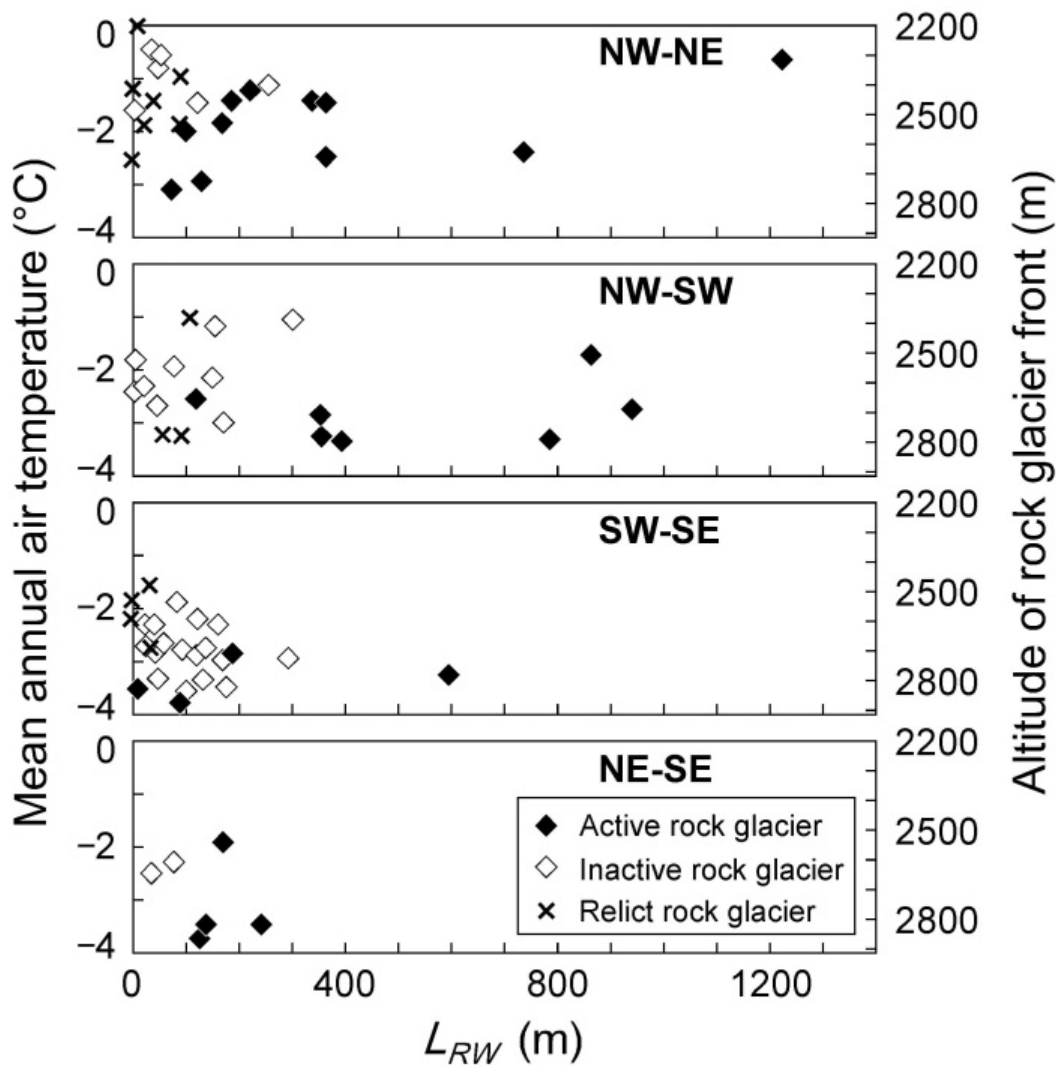


Figure 39 Relationship between the average slope length of source rockwall (L_{RW}) and the mean annual air temperature at the front of bouldery rock glaciers.

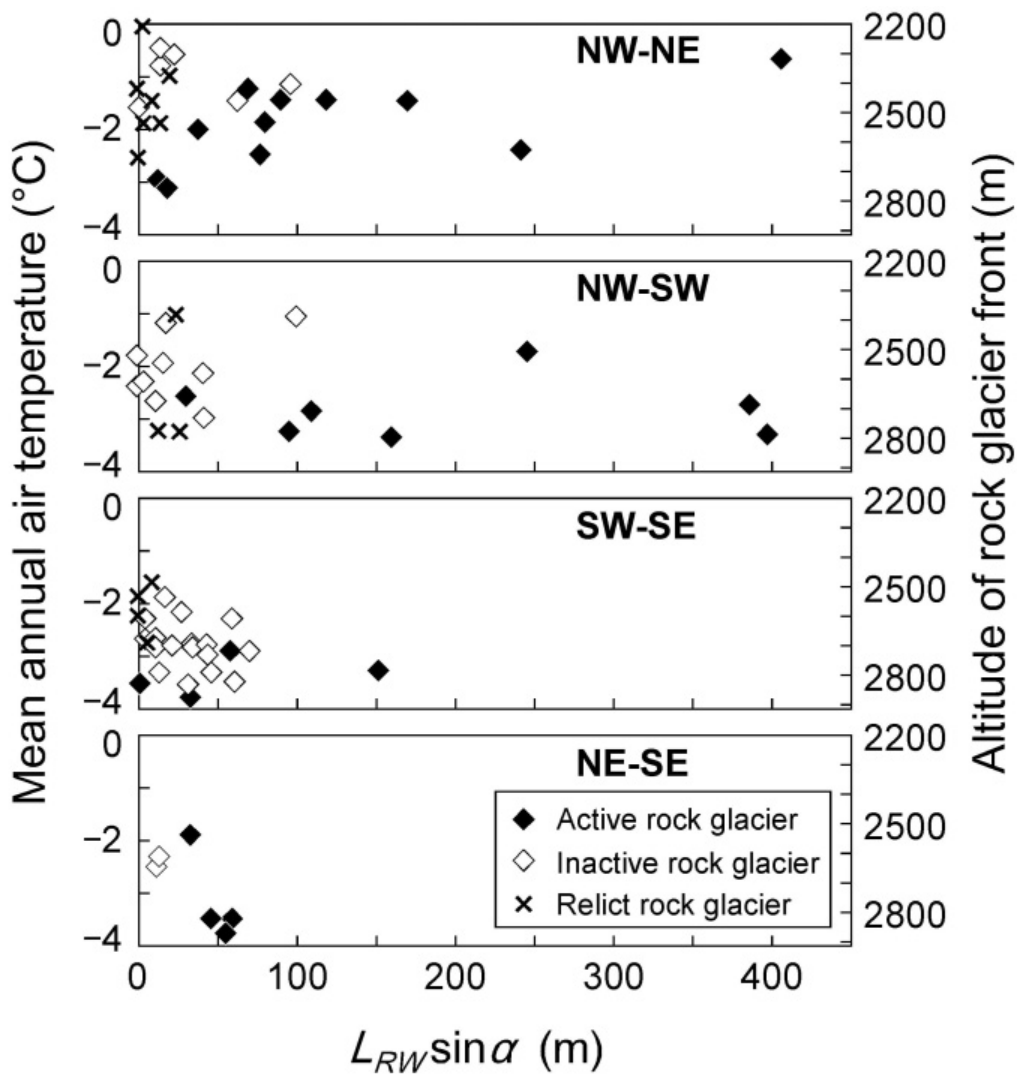


Figure 40 Relationship between a parameter combining debris input with slope angle ($L_{RW} \sin \alpha$) and the mean annual air temperature at the front of bouldery rock glaciers.

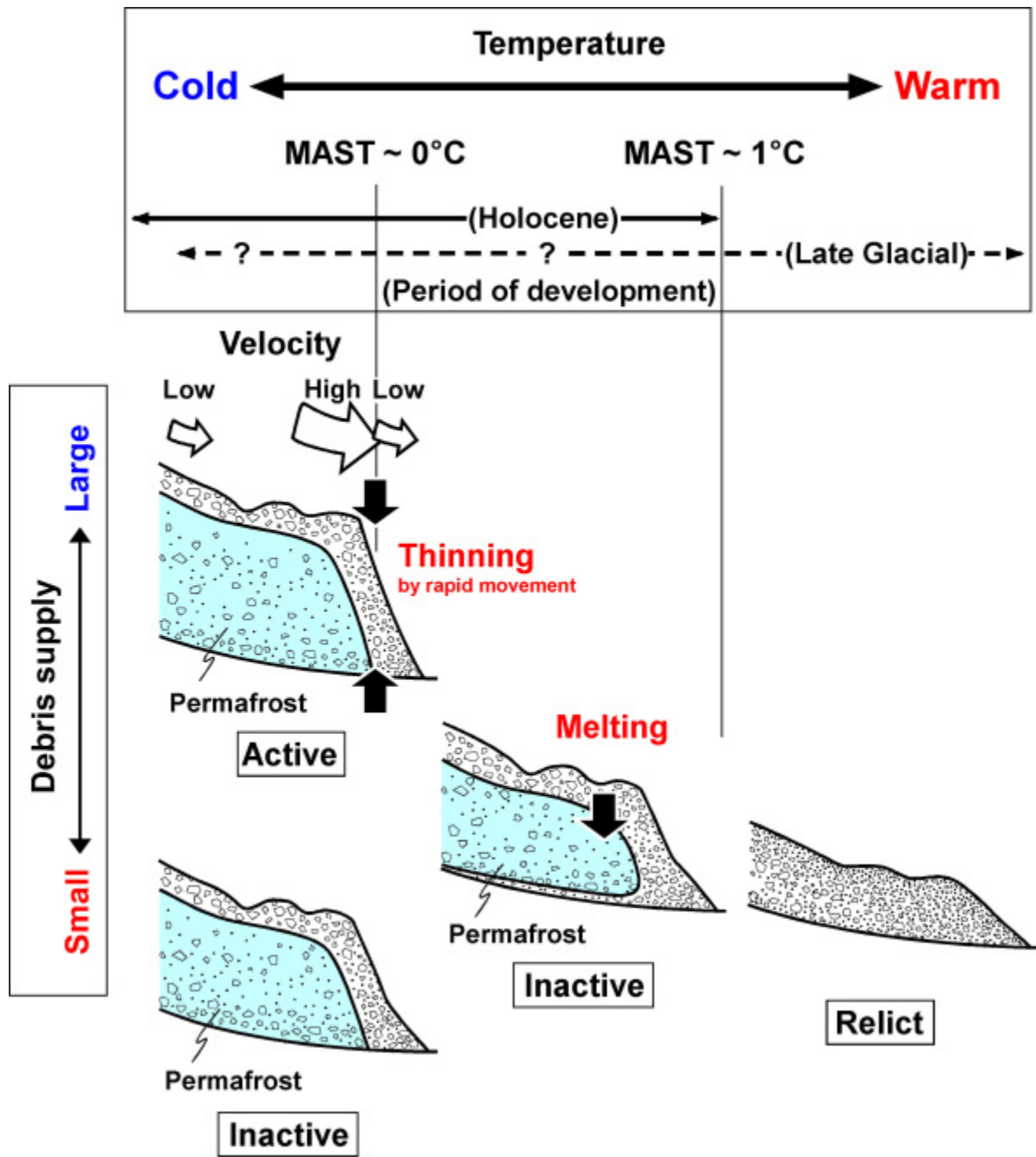


Figure 41 Rock glacier dynamics near the lower limit of mountain permafrost.

Table 1 Results of hammer seismic soundings.

Site	First layer		Second layer		Third layer	AB (m)
	V (m s ⁻¹)	D (m)	V (m s ⁻¹)	D (m)	V (m s ⁻¹)	
Active bouldery rock glaciers						
PN1	550	2.8–2.9	4100			55
PN5	650	1.3–2.4	3700			60
Active pebbly rock glaciers						
BNU	390	2.2–2.6	2800			50
BNLa	370	2.1–2.3	2900			50
BNLb	470	4.4–5.8	3400			40
NN12	340	2.2–2.4	2900			50
Inactive bouldery rock glaciers						
O4	650	1.1–3.1	2100			50
PS3	330	2.6–3.4	4400			60
PS4	380	8.8–9.2	2200			60
NS2	560	2.2–3.2	2700			50
W2	360	4.8–6.2	2300			50
Inactive pebbly rock glaciers						
BW	350	2.3–5.3	2000			55
BN3	350	2.1–2.7	3000			42
NN8	450	4.8–8.6	3200			60
Relict bouldery rock glaciers						
PN3	480	1.5–1.8	700	6.7–12	1600	48
PS1	410	2.2–4.2	950	>12		40
NS5	400	1.8–4.7	730	17–21	3100	64
W1	340	2.2–3.0	800	7.2–11	3000	50
W3	520	7.4–9.2	3100			50
Others						
BR-G	3200					30
BR-L	3500					30

BR-G = granite bedrock; BR-L = limestone bedrock; V = P-wave velocity; D = depth of layer base; AB = length of profile.

Table 2 Bottom temperatures of the winter snow cover (BTS), mean annual ground surface temperatures (MAST) and calculated depth of the base of a low P-wave velocity ($<1500 \text{ m s}^{-1}$) layer (D).

Site	BTS/MAST ($^{\circ}\text{C}$)						D (m)
	1998-1999	1999-2000	2000-2001	2001-2002	2002-2003	Average	
Active bouldery rock glaciers							
O1	-5.3/-1.0	-5.1/-0.5	-2.3/0.1	-5.9/-2.2	-3.4/0.3	-4.4/-0.6	
O2		-3.8/-0.1				-3.8/-0.1	
PN1		-3.7/-0.1	-2.1/-0.1			-3.7/0.0	2.8-2.9
PN5	-5.2/-1.7	-4.7/-1.4	-2.1/0.1	-5.3/-2.1	-3.2/-0.7	-4.1/-0.9	1.3-2.4
Active pebbly rock glaciers							
BNU		-2.0/0.4	-0.6/0.7	-2.0/0.0	-1.4/1.4	-1.5/0.6	2.2-2.6
BNL	-1.2/0.4	-1.2/0.9	-0.4/na	-1.8/0.0	-0.9/1.3	-1.1/0.6	2.1-2.3
NN12		-5.4/-0.5	-1.3/0.5	-5.7/na	-2.2/1.0	-3.6/0.3	2.2-2.4
Inactive bouldery rock glaciers							
O4	-5.0/0.6	-4.7/0.9	-2.1/2.0	-3.8/0.7	-3.1/2.2	-3.8/1.3	1.1-3.1
PS2	-4.6/0.9	-4.0/1.0				-4.3/1.0	
PS3	-3.1/ 0.6	-3.5/0.9	-1.5/1.0	-3.1/0.0	-2.6/1.6	-2.7/0.8	2.6-3.4
PS4	-2.2/-0.1	-1.9/0.4	-1.1/0.6	-1.9/0.0	-1.3/1.3	-1.7/0.5	8.8-9.2
NS2		-5.2/0.4	-2.6/1.5	-1.9/na	-3.2/2.2	-3.2/1.4	2.2-3.2
W2				-1.8/1.7	-2.5/2.0	-2.2/1.8	4.8-6.2
Inactive pebbly rock glaciers							
BN3			-0.6/1.0	-4.7/-1.5	-2.2/1.6	-2.5/0.4	2.1-2.7
BW	-3.4/-0.4	-6.3/-0.9	-1.0/0.7	-3.7/-0.8	-2.3/1.6	-3.4/0.1	2.3-5.3
NN8		-4.3/0.4	-0.9/1.8	-4.9/-0.9	-2.5/1.7	-3.1/0.8	4.8-8.6
Relict bouldery rock glaciers							
PN3	-0.8/1.0	-1.2/1.1	-0.1/0.9	-2.4/0.0	-0.7/1.9	-1.0/1.0	6.7-12
NS5	-0.6/1.8	-0.3/2.6	-0.0/2.5	-0.6/2.2	-0.1/3.3	-0.3/2.5	17-21
W1				-2.7/1.3	-0.7/2.6	-1.7/2.0	7.2-11
W3				-0.6/2.3	-0.3/2.4	-0.5/2.3	7.4-9.2
Relict pebbly rock glaciers							
BN4			-0.2/1.1	-3.1/0.0	-0.8/1.8	-1.3/1.0	

na = data not available.